EXPRESSION AND FUNCTION OF THE CHROMATIN REMODELING FACTOR ACF1 (BAZ1A) DURING MOUSE DEVELOPMENT

by

James Alexander Dowdle

A Dissertation

Presented to the Faculty of the Louis V. Gerstner, Jr.
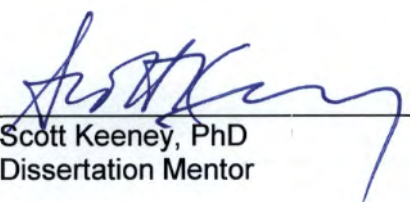
Graduate School of Biomedical Sciences,

Memorial Sloan-Kettering Cancer Center

in Partial Fulfillment of the Requirements for the Degree of

Doctor of Philosophy

New York, NY

April, 2012

_____   _____
Scott Keeney, PhD   Date 4/2/12
Dissertation Mentor

DEDICATION

This work is dedicated to my loving parents and grandparents who have never stood in the way of letting me be me and for selflessly ensuring and continuing to ensure that I have every opportunity to succeed. Also, in loving memory of my Grams who made the best damn Michigan the world has ever known.

A fellow scientist once reminded me that: "Science is boring, boring, boring, boring (breath), boring, boring, exciting! and that is why we keep doing what we do."

ABSTRACT

Acf1 was isolated almost 15 years ago from *Drosophila* embryo extracts as a subunit of several complexes that possess chromatin assembly activity. Acf1 binds to the ATPase Iswi (SNF2H in mammals) to form the ACF and CHRAC chromatin remodeling complexes, which can slide nucleosomes and assemble arrays of regularly spaced nucleosomes *in vitro*. Evidence from *Drosophila* and from human and mouse cell culture studies implicates *Acf1* in a wide range of cellular processes including transcriptional repression, heterochromatin formation and replication, and DNA damage checkpoints and repair. However, despite these studies, little is known about the *in vivo* function of *Acf1* in mammals.

This thesis is focused on elucidating the role of mouse *Baz1a*, which is the closest mammalian homolog of *Acf1* from *Drosophila*. The study began by characterizing the expression of *Baz1a*, which revealed high expression in the testis, and continued with analysis of unique splice variants and the subcellular localization of the protein product in this organ. Next, *Baz1a*-deficient mice were generated to investigate the role of this factor during development. In contrast to partially penetrant lethality of *Acf1* mutation in *Drosophila*, *Baz1a*-deficient mice are viable. Mice lacking BAZ1A show no obvious defects in B or T cell lineages, class switch recombination in cultured B cells, or meiotic recombination. Thus, BAZ1A is dispensable in vivo for the survival and differentiation of cells that require the repair of developmentally programmed DNA double-strand breaks (DSBs). However, $Baz1a^{-/-}$ male mice are sterile because of a severe defect in spermiogenesis that results in fewer and non-motile sperm with morphological defects, likely due to transcriptional perturbation that we observe in spermatocytes and round spermatids. Furthermore, we show that the ACF/CHRAC complexes form in the mouse and require BAZ1A for their stability and localization.

Thus, BAZ1A-containing chromatin remodelers play important roles in the development of mature spermatozoa.

ACKNOWLEDGMENTS

'First and foremost', being a phrase that likely begins this section in many a graduate student thesis, should signify that the person being acknowledged first deserves the greatest thanks and recognition. However, its overuse has added an element of frivolity to this intention. I mean to circumvent this by simply stating that Scott, you are the wind beneath my wings. Your patience and diplomacy are inspiring and admirable. Although the Keeney 'look' has made many a man question his own name, your attention to detail and insistence on clarity encouraged me to think in new and exciting ways. Admittedly, you were a bit pesky at times, especially while I was anticipating two-hybrid clones and germ-line transmission… However, you always kept tabs on me, even when I put tabs on everything. Thank you for insisting that I keep my eye on the ball, which is still the funniest unintentional pun, I have ever heard. You have fostered a lab environment where I felt safe taking a leap into the unknown without questioning that there would be something in place to catch me if I fell. You should feel confident that under your mentorship I have learned to think independently and will be successful in my next endeavor.

Maria, John and Iestyn: your helpful suggestions and quizzical nature ensured the success of my project from the beginning. I always looked forward to our meetings and couldn't imagine my graduate school experience without you. Thank you for your patience and wisdom.

A big thanks to Bao Vuong for performing the CSR experiments without hesitation and to Monika Mehta for her help with the co-IPs. I also need to thank Alex Flynt for teaching and assisting me with the piRNA northern blot and Eric Alonzo for help with the T cell assays. Dr. Dirk de Rooij assisted with the histology analysis and Dr. Steven Kistler provided the TNP antibodies and helpful suggestions for running the AU gels. None of this work would have been possible without the consistent and under-

TABLE OF CONTENTS

LIST OF FIGURES

LIST OF ABBREVIATIONS

ACF: ATP-dependent chromatin assembly and remodeling factor

AID: Activated cytidine deaminase

APH: Aphidicolin

ATP: Adenosine triphosphate

BAC: Bacterial artificial chromosome

BAZ: Bromodomain adjacent to zinc finger

BrdU: 5-bromo-2'-deoxyuridine

ChIP: Chromatin immunoprecipitation

CHRAC: chromatin accessibility complex

CSR: Class-switch recombination

DAPI: 4',6-diamidino-2-phenylindole

d.p.p.: Days post partum

DSB: DNA double-strand break

EF: Ear fibroblast

ESC: Embryonic stem cell

FACS: Fluorescence activated cell sorting

FISH: Fluorescence in situ hybridization

FRET: Fluorescence resonance energy transfer

GFP: Green fluorescent protein

HR: Homologous recombination

IF: Immunofluorescence

IL: Interleukin

IP: Immunoprecipitation

LPS: Lipopolysaccharide

MSCI: Meiotic sex chromosome inactivation

NHEJ: Nonhomologous end-joining

NURF: Nucleosome remodeling factor

PHD: Plant homeo domain

RAG: Recombinase activating gene

RNAi: RNA interference

RSF: Remodeling and spacing factor

SHL: Super helical location

TCA: Trichloracetic acid

TCR: T cell receptor

TP: Transition protein

TUNEL: Terminal deoxynucleotidyl transferase (TdT) dUTP nick end labeling

UTR: Untranslated region

V(D)J: Variable (diversity) joining gene segments

WAC: WSTF, Acf1, Cbp146 domain

WAL: WSTF Acf1-like

WSTF: William's syndrome transcription factor

INTRODUCTION

The eukaryotic cell is faced with a unique problem: how to package long stretches of DNA into a comparatively small nucleus. In humans, this equates to ~2 meters of DNA being packed into a nucleus with an average diameter of $5\mu m$. This is accomplished by packaging the genome into a periodic nucleoprotein complex known as chromatin. The basic repeating unit of chromatin is the nucleosome, an octamer with two copies of each of the core histones H2A, H2B, H3 and H4 around which 146 base pairs (bp) of DNA is spooled ~1.7 times and often held in place by a linker histone such as H1 (Luger et al., 1997). Typically, ~50 bp of DNA separate neighboring nucleosomes and regular spacing is thought to facilitate cooperative folding of nucleosomal arrays into the higher-order structures that comprise chromatin. Although chromatin solves the dilemma of how to package DNA into the nucleus, it also impedes DNA access to protein factors involved in essential cellular functions such as transcription, replication, recombination and repair. However, once thought to only provide a solution for efficient packaging, chromatin has been shown to play a regulatory function as well. The covalent modification of histone tails by most notably methylation, phosphorylation and acetylation and incorporation of histone variants can target factors and grant access to the underlying DNA sequence (Strahl and Allis, 2000). Histone-DNA contacts can also be disrupted to 'remodel' the chromatin and grant or block access to the genome. So-called 'chromatin remodeling factors' are multi-protein complexes that utilize the energy released during ATP-hydrolysis to assemble, reposition, restructure and disassemble nucleosomes. At the core of each of these complexes is an ATPase of the Swi2/Snf2 subfamily (Becker and Hörz, 2002; Erdel and Rippe, 2011; Flaus and Owen-Hughes, 2011; Lusser and Kadonaga, 2003). The focus of my research is on the role of *Baz1a* (an accessory subunit of the ACF/CHRAC remodeling complexes) in mammalian spermiogenesis.

1

I. The evolution of chromatin remodeling complexes

A shared component of every chromatin remodeling complex is an ATPase of the Snf2 family of helicases/translocases. The family is named after the archetypal member, Snf2 from *Saccharomyces cerevisiae,* where independent screens for factors contributing to the expression of the HO nuclease required for mating type switching (Nasmyth et al., 1987; Stern et al., 1984) and for factors affecting expression of *SUC2* by glucose repression (Neigeborn and Carlson, 1984) revealed its activity. These switch (SWI) and sucrose nonfermenting (SNF) screens pointed to the involvement of a gene encoding an ATPase, since named SNF2 (Abrams et al., 1986). Subsequent suppressor screens of *snf2* mutants revealed SWI/SNF independent Sin⁻ mutations that included mutations in histones and other chromatin components (Kruger et al., 1995) and suggested a function in chromatin structuring. Other family members share a homologous Snf2 ATPase domain consisting of two RecA-like folds and seven conserved sequence motifs that classify it as part of the Superfamily 2 (SF2) of helicases (Figure 1A). The Snf2 family can be further subdivided based on common protein motifs located outside of the ATPase domain, the four most well characterized subfamilies of which are SWI/SNF, ISWI, CHD and INO80 (Clapier and Cairns, 2009; Eisen et al., 1995; Flaus et al., 2006). Although they fall under the classification of 'helicase-like', Snf2 proteins are not *bona fide* helicases as they lack the ability to separate nucleic acid strands. They are more accurately termed DNA translocases as they apply ATP-dependent torsional strain to DNA to remodel nucleosomes (Bowman, 2010; Ryan and Owen-Hughes, 2011). Despite their common catalytic core, the families exhibit divergent remodeling activities owing to the variant domain composition of the ATPase itself or of accessory proteins, which can confer tissue or context specific functions.

The imitation switch or ISWI subfamily of ATPases are distinguished from SWI/SNF, INO80 and CHD subfamilies by the presence of HAND, SANT and SLIDE
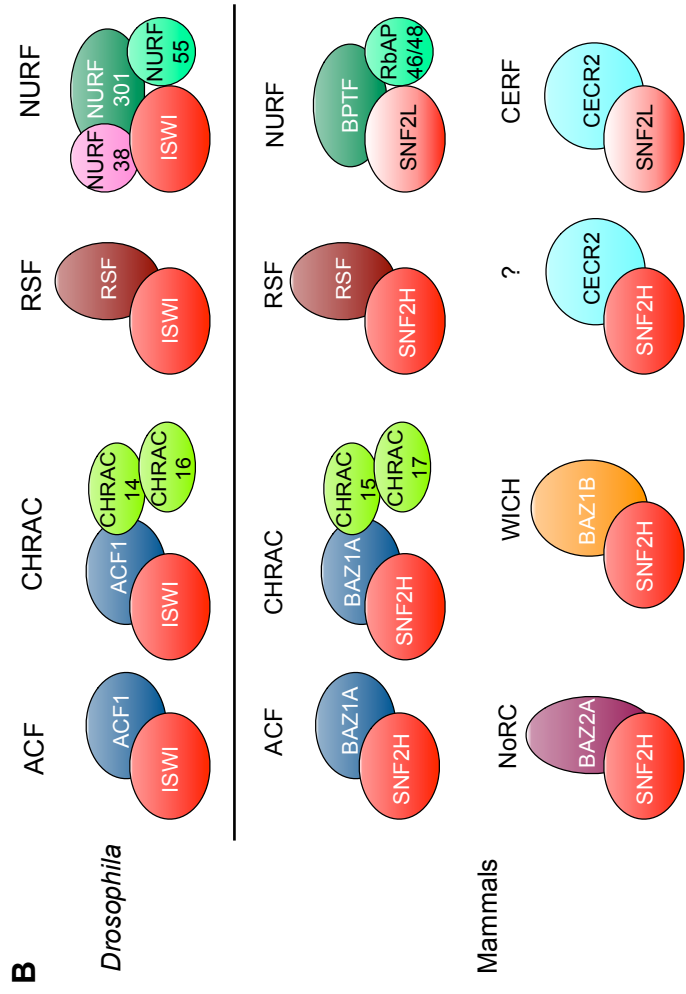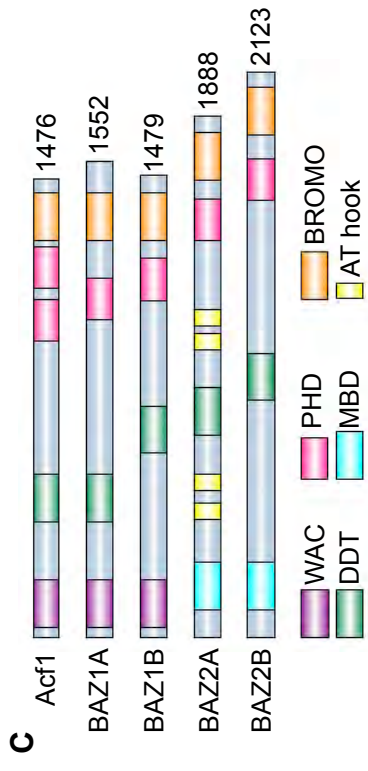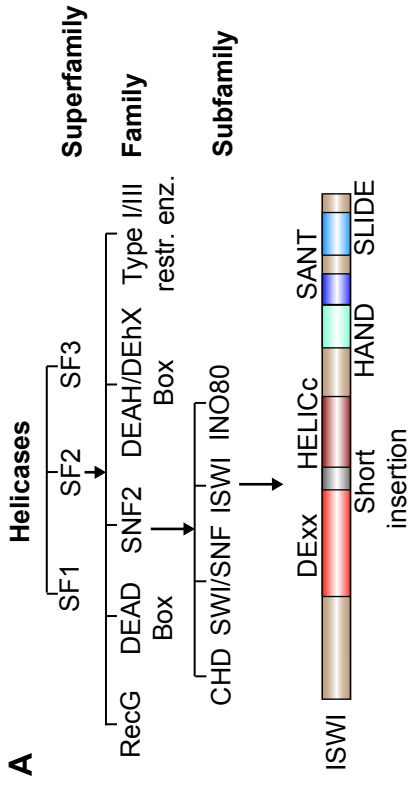
Figure 1. Summary of ISWI containing nucleosome remodeling factors.

(**A**) Schematic illustrating the hierarchical classification of the ISWI family of ATPases and the domain architecture of the ISWI proteins. The ATPase domain is split in two parts: DExx (red) and HELICc (brown). (**B**) Subunit compositions of known ISWI containing chromatin remodeling complexes from *Drosophila* and mammals. Like colors represent orthologous proteins. Adapted from Flaus et al., 2006; Yadon and Tsukiyama 2011. (**C**) Comparison of the domain architecture of Acf1 from *Drosophila* and the mouse BAZ/WAL family of proteins. Numbers at the right indicate the amino acid length of each peptide. Not to scale.

domains in the C-terminus of the protein which mediate interactions with nucleosomal DNA and the histone core (Boyer et al., 2004; Grune et al., 2003; Hota and Bartholomew, 2011) (Figure 1A). The ISWI group was originally identified in *Drosophila* and found at the core of four distinct chromatin remodeling complexes: NURF (nucleosome remodeling factor), RSF (remodeling and spacing factor), ACF (ATP-dependent chromatin assembly and remodeling factor) and CHRAC (chromatin accessibility complex) (Becker et al., 1994; Hanai et al., 2008; Ito et al., 1997; Tsukiyama et al., 1995; Tsukiyama and Wu, 1995).

There are two ISWI homologs in mammals, SNF2H and SNF2L. SNF2H is the catalytic core of six different complexes: RSF (LeRoy et al., 1998; Loyola et al., 2003), hACF (Bochar et al., 2000; LeRoy et al., 2000), hWICH (WSTF-ISWI chromatin remodeling complex) (Bozhenok et al., 2002), hCHRAC (Poot et al., 2000) and NoRC (nucleolar remodeling complex) (Strohner et al., 2001). Recently, SNF2H was also found in a complex with CECR2 in mouse testis but a name for the complex was not suggested (Thompson et al., 2012). SNF2L is the catalytic subunit of hNURF (Barak et al., 2003) and mCERF (CECR2-containing remodeling factor) (Banting et al., 2005). The subunit composition of the known ISWI complexes in various organisms is depicted schematically in Figure 1B.

This thesis will focus on the role of the ACF/CHRAC accessory subunit Acf1. In mammals, the closest homolog of *Drosophila Acf1* is also known as *Baz1a*, a member of the BAZ family of proteins with the name owing to the shared domain architecture of its members: a bromodomain adjacent to a zinc finger, typically a plant homeo domain (PHD) (Jones et al., 2000). It has also been termed the WAL protein family for WSTF-Acf1-like (Poot et al., 2000). BAZ1A and BAZ1B contain a WAC (WSTF, Acf1, Cbp146) domain in their N-terminus that has been suggested to be a heterochromatin-targeting domain (Tate et al., 1998). The other two family members, *Baz2a* and *Baz2b* lack this

4

domain (Figure 1C). There are also four other genes considered to be paralogs of *Acf1*: *Cecr2, Kat2a, Kat2b* and *Bptf,* all of which contain a DDT (<u>D</u>NA binding homeobox and <u>D</u>ifferent <u>T</u>ranscription factors) domain.

Aligning the amino acid sequences of BAZ1A and its paralogs from various species with the sequences of *Drosophila* Acf1 and the *Saccharomyces cerevisiae* homolog Itc1 reveals that Acf1 is more closely related to BAZ1A than to any of its other paralogs. Although Itc1 is closely related to BAZ1A, sequence divergence occurred prior to the duplication event that gave rise to the closely related BAZ1A and BAZ1B proteins (Figure 2).

II. Mechanisms of ATP-dependent nucleosome remodeling

The superhelical coiling of DNA around the histone octamer distorts the structure of DNA and is thus expected to occur at a high energy cost (Luger et al., 1997; Shore et al., 1981; Widom, 2001). Histone-DNA interactions occurring approximately every 10.4 bp create 14 relatively weak interaction clusters within a single nucleosome (Luger et al., 1997; Luger and Richmond, 1998). The sites at which the major and minor grooves of the DNA alternatively face the central core of the nucleosome are referred to as Super Helical Locations (SHLs). The major groove at the middle of the 146 bp DNA fragment aligns with the two-fold symmetry axis of the histone octamer—termed the dyad—and marks SHL0. As you move along the DNA away from the dyad, each major groove facing the histone core is denoted SHL±1, 2, etc. (negative in one direction and positive in the other) while each minor groove contact is named SHL±0.5, 1.5, etc. The term chromatin remodeling refers to the disruption of these contacts to shift the SHLs relative to the DNA.
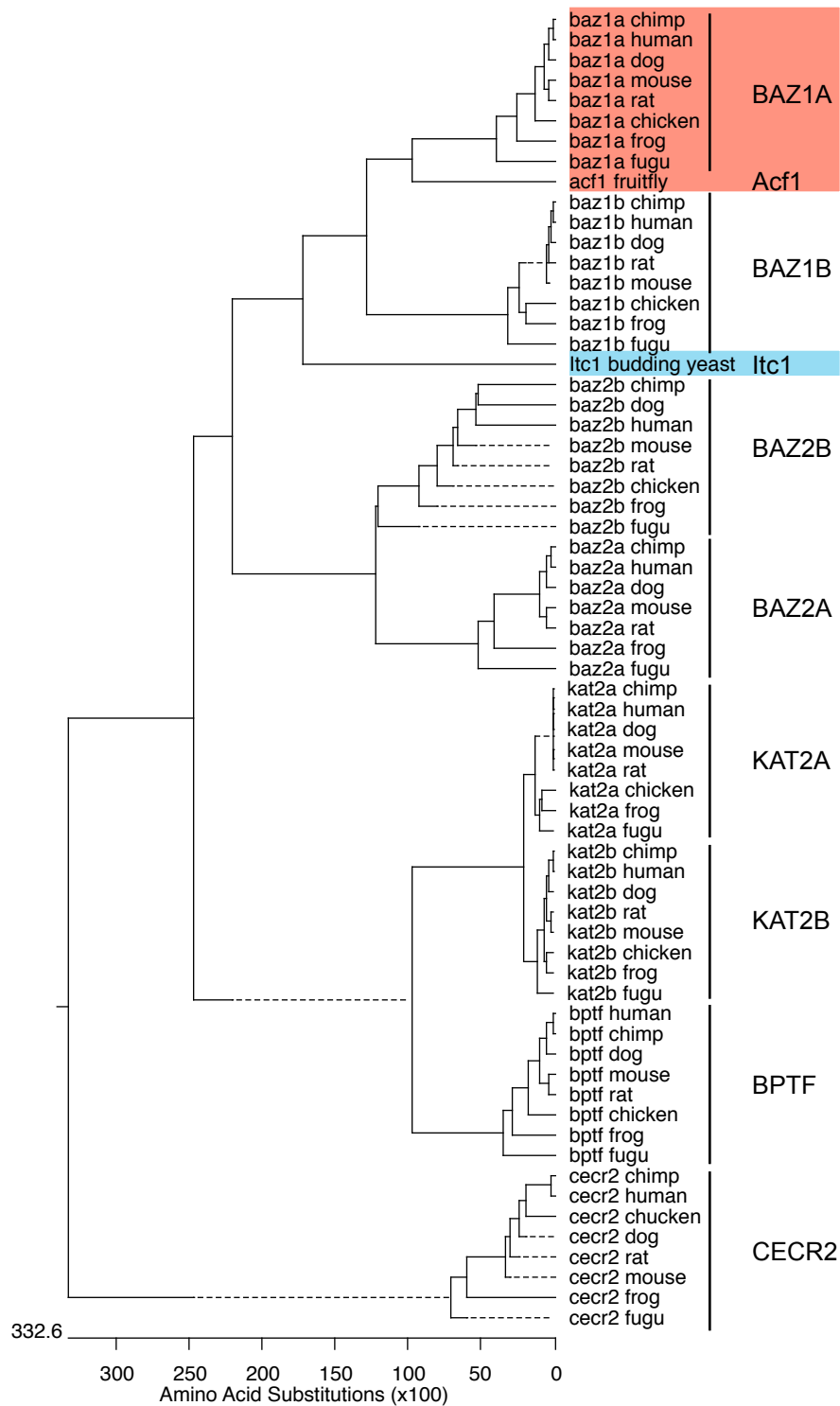
Figure 2. Phylogenetic comparison of BAZ1A paralogs. Peptide sequences of BAZ1A (red) and its 7 paralogs from primate (human and chimp), rodent (mouse and rat), bird (chicken), laurasiatheria (dog), fish (fugu) and amphibian (frog) were aligned with the BAZ1A homologs ACF1 from fruitfly and Itc1 (blue) from the budding yeast *Saccharomyces cerevisiae* by the Clustal V method and the tree constructed using MegAlign software. Dotted line, negative branch length.

The ACF/CHRAC complex has thus far only been shown to possess two of the four known chromatin remodeling activities, nucleosome sliding and assembly. There have been several models posited to explain how histone-DNA contacts are broken and reformed to effectively reposition the nucleosome. The energetically favorable twist diffusion model suggests that twisting of the linker DNA adjacent to the nucleosome would create a distortion that could propagate single base pairs of DNA around the nucleosome without extensive disruption of histone-DNA contacts. However, nicks in the DNA or physical barriers such as hairpins or biotin crosslinks that would prevent rotation do not inhibit remodeling arguing against this model (Aoyagi and Hayes, 2002; Langst and Becker, 2001; Strohner et al., 2005). Additional evidence that nucleosomes slide in increments of ~10 bp (Zofall et al., 2006) lent credence to the alternative, more energetically expensive loop propagation model that suggests a bulge of DNA propagates around the nucleosome, breaking and reforming local histone-DNA contacts to effectively reposition it.

However, several recent pieces of evidence support a third model. First, single-molecule studies revealed that histone-DNA contacts vary at the nucleosome dyad and entry/exit sites (Brower-Toland et al., 2002; Mihardja et al., 2006). This calls the loop propagation model into disfavor as a loop proposed to form at the entry/exit site would face an uphill battle as it progressed toward the increasing energetic barrier at the dyad. Secondly, innovative new experiments showed that unzipping of the DNA up to, but not past, the dyad did not alter the position of the histone octamer with respect to the DNA (Hall et al., 2009). Additionally, a histone octamer with a SIN mutation positioned near the dyad at SHL ±0.5 shifted more easily at elevated temperature compared to wild-type, explaining how this mutation suppressed the loss of a chromatin remodeling factor (Flaus et al., 2004; Muthurajan et al., 2004). Moreover, single stranded gaps in the DNA duplex only perturb nucleosome sliding when positioned at SHL2, supporting the idea

the ATPase acts primarily at this site (Saha et al., 2005; Schwanbeck et al., 2004). Together, these new details have brought about a model in which the ATPase engaged adjacent to the dyad at SHL2 disrupts the cluster of strong contacts around the dyad by introducing torsional strain in the DNA by the action of translocation, allowing the entire segment of DNA in contact with the histone core to swivel in concert to reposition the nucleosome (Bowman, 2010) (Figure 3A). It is tempting to speculate that the initial step in this process is facilitated by a non-histone component of chromatin, the high-mobility group protein B1 (HMGB1). ACF, which can be directed by an intrinsically curved DNA sequence element (Rippe et al., 2007) displayed enhanced binding to nucleosomal DNA in the presence of HMGB1, which is known to distort DNA (Bonaldi et al., 2002). Interestingly, another class of high-mobility group proteins, HMGN, were shown to potently repress chromatin remodeling by reducing the affinity of ACF for chromatin (Rattner et al., 2009) suggesting that the fine balance of non-histone chromatin components could serve as a modulator of remodeling.

The actions of transcription, replication, repair and recombination all necessitate another form of remodeling: nascent chromatin assembly on newly formed or transiently exposed DNA. ACF, as its name implies, was shown to possess this ability *in vitro* in the presence of the core histones, ATP, relaxed DNA and the histone chaperone NAP1 (Ito et al., 1997; Ito et al., 1999). The most recent model suggests that a histone chaperone rapidly deposits histones onto DNA to form a non-nucleosomal histone-DNA intermediate that can then be assembled into mature chromatin by ACF in an ATP-dependent process (Torigoe et al., 2011) (Figure 3B). An important aspect of chromatin assembly by ACF lies in the subsequent spacing of newly formed nucleosomes into periodic arrays, which is thought to promote chromatin compaction and effect gene silencing (Cairns, 2005; Gangaraju and Bartholomew, 2007). This is where modulation of the intrinsic ability of SNF2H to slide nucleosomes by the accessory subunit ACF1
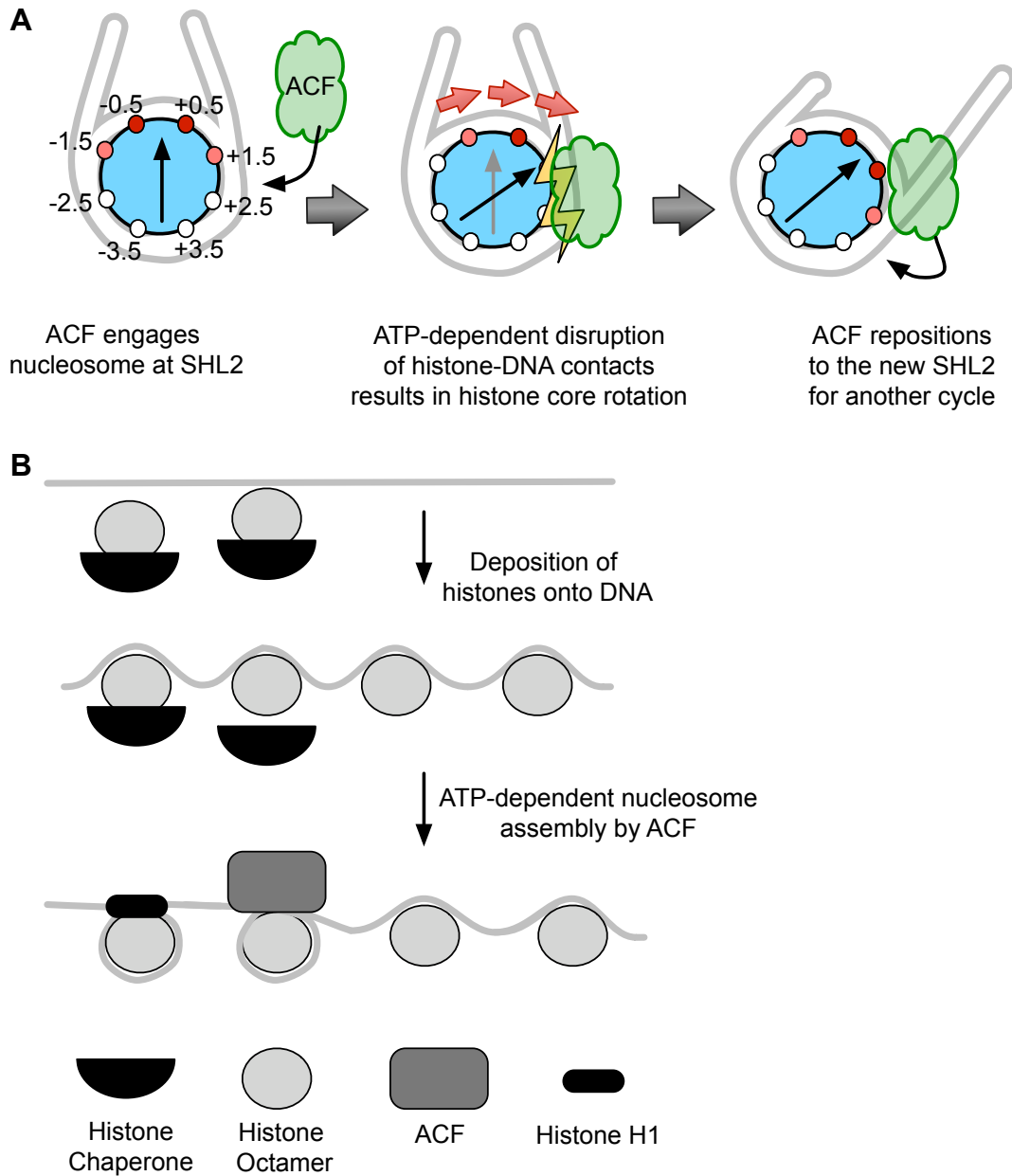
Figure 3. Models for ACF nucleosome assembly and sliding. (**A**) A model for nucleosome sliding based on swiveling of the histone core. ACF (green) engages the nucleosome (blue) at SHL2 and alters the structure of DNA (gray outline) to disrupt local histone-DNA contacts (yellow). These actions encourage the energetically important contacts around the dyad (black arrow) to shift toward the remodeler by a swiveling of the histone core within the outer wrapping of DNA, effectively sliding the nucleosome to new segment of DNA. SHL, super helical location. Adapted from Bowman, 2010. (**B**) A model for nucleosome assembly. Histones are deposited onto DNA with the help of chaperones to form a non-nucleosomal histone-DNA intermediate. ACF is then able to assemble this 'nascent' chromatin into 'mature' chromatin containing histone H1 in an ATP-dependent manner. Adapted from Torigoe et al., 2011.

affects a specific outcome that the ATPase alone cannot. It has been shown that this is directly related to the ability of ACF1 to center mononuclosomes on short stretches of DNA (Eberharter et al., 2001; Fyodorov et al., 2004; Ito et al., 1997). Coupled with the evidence that ACF acts as a dimer (Strohner et al., 2005), elegant fluorescence energy resonance transfer (FRET) experiments by the Narlikar group suggested that ACF acts as a length sensor, allowing the ATPase that engages a longer piece of linker DNA on one side of the nuclesome to hydrolyze ATP faster, preventing the subordinate ATPase engaging a shorter segment on the opposite side from firing. Succesive rounds of sampling and translcoation would then result in regular internucleosomal spacing (Blosser et al., 2009; Racki et al., 2009; Yang et al., 2006).

These single molecule FRET studies which were performed by labeling the histone H4 tail to which SNF2H binds also revealed two ATP hydrolysis dependent conformational changes, the first of which did not result in a change in FRET and the second which caused a continuous change that was consistent with the movement of DNA across the histone octamer (Blosser et al., 2009). This coupled with the evidence that the tail of histone H4 is required for the catalytic activity of ISWI motors (Clapier et al., 2001; Dang et al., 2006) led to a model for kinetic proof reading. The first ATPase cycle disrupts histone-DNA contacts creating a high-energy intermediate. ACF then senses structural cues from the H4 tail or length of the linker DNA for instance, rejecting the wrong substrate if cues do not lead to a stabilization of the high-energy intermediate. The correct template would stabilize the intermediate and a second ATPase cycle, perhaps catalyzed by the other dimer subunit, would result in translocation of the DNA on the histone octamer (Narlikar, 2010).

III. Functions of the ACF/CHRAC complex *in vivo*

Almost 15 years ago, 2 complexes (ACF and CHRAC) were independently isolated from *Drosophila* embryo extracts as possessing the ability to catalyze the deposition of histones into periodically spaced nucleosome arrays (Ito et al., 1997; Varga-Weisz et al., 1997). ACF was subsequently shown to consist of Acf1 and Iswi (Ito et al., 1999) while CHRAC is essentially ACF plus two small histone-fold proteins, CHRAC-14 and CHRAC-16 (Eberharter et al., 2001). The human counterparts of these complexes were subsequently isolated from HeLa cells, indicating their conservation (Bochar et al., 2000; LeRoy et al., 2000; Poot et al., 2000). Although ISWI/SNF2H possesses basal nucleosome assembly and sliding activity, Acf1 boosts these functions approximately 30 and 10 fold respectively and encourages centering of nucleosomes on a DNA fragment while Iswi alone directs the reverse reaction (Eberharter et al., 2001; Ito et al., 1999). The CHRAC proteins heterodimerize and directly bind to DNA and the N-terminus of Acf1 to further enhance performance of ACF (Hartlepp et al., 2005; Kukimoto et al., 2004). Although exhaustive biochemical studies have defined the *in vitro* functions of the ACF/CHRAC complexes, several groups have attempted to uncover a more physiological role for these chromatin remodelers. These studies have suggested roles in diverse cellular functions including replication of heterochromatin (Collins et al., 2002), nucleosome spacing and maintenance of repressive chromatin (Chioda et al., 2010; Fyodorov et al., 2004) transcriptional repression/activation (Ewing et al., 2007; Liu et al., 2008; Precht et al., 2010) DNA double-strand break repair (Lan et al., 2010) and the G2/M damage checkpoint (Sánchez-Molina et al., 2011).

1. Heterochromatin

The first evidence that *Baz1a* might function at heterochromatic DNA came with its identification in a gene trap screen in mouse embryonic stem (ES) cells (Tate et al., 1998). Random integration of a trap construct generated fusions between endogenous proteins and β-galactosidase and histochemical staining was used to assess sub-cellular localization. Expression of the reporter construct fused to *Baz1a* was only induced in differentiated ES cells and could be found at low levels diffusely staining the length of chromosome arms and with a strong concentration of staining at the centromeric heterochromatin.

A subsequent study reported BAZ1A and SNF2H co-localization with foci of incorporated bromodeoxyuridine (BrdU) that form during late stage replication in synchronized mouse fibroblasts (Collins et al., 2002). As these foci are thought to represent replicating heterochromatin, it was suggested that ACF might play a role in replicating heterochromatin. Depleting synchronized human or mouse cells of BAZ1A or SNF2H by RNAi reduced the number of BrdU positive cells over time. There is also an accumulation of cells in G2 when these proteins are depleted. These effects can be reversed by treating cells with 5-aza-2-deoxycytidine which inhibits DNA methylation, leading to decondensation of heterochromatin. Taken together, the authors conclude that DNA replication is impaired in later stages of S phase, when the heterochromatin is replicated. However, an alternative interpretation of many of these results is that replication takes place much faster and therefore S phase is shortened in the absence of ACF (Haushalter and Kadonaga, 2003).

Using purified *Drosophila* proteins, it was also shown that Acf1 enhances the ability of the HP1 heterochromatin proteins to bind methylated chromatin, suggesting it may play a role in the proper assemble of heterochromatin (Eskeland et al., 2007).

2. Development

The limited *in vivo* data we have for *Acf1* comes from the generation of nullizygous flies (Chioda et al., 2010; Fyodorov et al., 2004). The importance of *Acf1* in development is implied by the semi-lethal phenotype, with only 25% of animals surviving through the larval to pupal transition. This partial penetrance could indicate there are compensatory mechanisms in the absence of *Acf1*. Chromatin from mutant embryonic nuclei is less periodic and exhibits reduced average nucleosomal spacing, suggesting that the biochemical functions of Acf1 described *in vitro* occur *in vivo*. Repressive chromatin is also perturbed in the mutants as transgenes placed in pericentric heterochromatin fail to be silenced. Cultured neural fibroblasts from mutant flies exhibit a shortened S phase, which is potentially due to *Acf1* deletion removing the constraint of chromatin assembly on the replication process (Fyodorov et al., 2004). Further investigations in flies showed that Acf1 is mainly expressed in undifferentiated cells during embryogenesis and is required for the establishment of heterochromatin at the cellular blastoderm and in larvae. Moreover, constitutive overexpression of Acf1 is lethal while local, ectopic overexpression can lead to defects in cell fate determination (Chioda et al., 2010).

Iswi on the other hand is absolutely essential for fly development, as null mutations do not support life. Interestingly, the structure of the salivary gland polytene chromosomes from *Iswi* mutant larvae was altered. The autosomes appeared thinner than normal and the X chromosome from males was shorter and broader and much less condensed than normal (Deuring et al., 2000). *Snf2h* is also essential for mammalian development as mutant mouse embryos die during the periimplantation stage. Blastocyst outgrowth experiments revealed growth arrest and cell death of both the trophectoderm and inner cell mass in the absence of *Snf2h* (Stopka and Skoultchi, 2003).

Notably, mice lacking the *Baz1a* paralog *Baz1b/WSTF* (Williams syndrome transcription factor) display neonatal lethality due to severe cardiac defects (Yoshimura et al., 2009). However, BAZ1B is also a component of a SWI/SNF-like chromatin remodeling complex, WINAC. This report attributed the cardiac defects to the failure of a a defective WINAC complex to properly induce normal gene cascades crucial for development of the heart. In contrast, sensitivity of mouse embryonic fibroblasts derived from these mutant mice to DNA damaging agents was attributed to a failure to form the ISWI complex WICH (Yoshimura et al., 2009) as this complex is required for a proper DNA damage response mediated by the histone variant H2AX (Xiao et al., 2009a).

3. Transcription

Evidence that ACF activity might regulate transcription comes from cell culture studies in mouse, fly and human cells. Interpretation of these results is limited by the fact that all were performed in the context of reduced levels of Acf1/BAZ1A or Iswi/SNF2H by RNA interference (RNAi) and none of the studies performed proper control experiments using RNAi resistant complementation to rule out the possibility that the observed effect was not due to RNAi off-targeting. Moreover, there are no reports to date linking *Baz1a* to transcriptional control *in vivo.*

A study reducing levels of SNF2H in mouse T-cells using RNAi showed that SNF2H repressed expression of the cytokine interleukin-2 (IL-2) and induced expressed of IL-3 (Precht et al., 2010). SNF2H and BAZ1A bound the tested loci by Chromatin immunoprecipitation (ChIP), suggesting the regulation was direct. Depleting SNF2H resulted in reduced BAZ1A binding and protein levels, suggesting that BAZ1A interaction with SNF2H could be important for its targeting and stability. However, as mentioned above, SNF2H is found in multiple complexes. This raises the possibility that the opposing effects on the expression of different cytokines could be explained by different

SNF2H partners being required at the different loci, a point that was not addressed experimentally in this study.

BAZ1A was also found to regulate the expression of vitamin D3 receptor-regulated genes (Ewing et al., 2007). After first being identified as an interacting partner of the nuclear receptor corepressor protein (N-CoR), overexpression of BAZ1A in a human cell line showed enhanced repression of nuclear hormone receptor regulated genes. Conversely, reducing levels of BAZ1A by RNAi, relieved the transcriptional repression of these genes. ChIP experiments indicated that BAZ1A directly binds these target loci and that treatment of cells with vitamin D3 reduces occupancy (Ewing et al., 2007).

Additionally, it was reported that Acf1 and Iswi are required for repression of basal transcription of Wingless/Wnt (WG) target genes in *Drosophila* (Liu et al., 2008). Knock-down of either of these genes by RNAi in cultured fly cells resulted in derepression of WG targets. Interestingly, simultaneous depletion of both Acf1 and Iswi resulted in greater derepression than depletion of either factor alone and the distributions of these factors at WG targets by ChIP were distinct, possibly indicating distinct functions in transcriptional repression of WG target genes (Liu et al., 2008). However, one caveat to interpreting these data in a traditional epistasis sense is that levels of these factors were reduced but not eliminated in this study. In addition, to my knowledge, there are no other reports of ISWI-independent roles for Acf1.

SATB1 binds specific DNA sequences to tether large chromatin loop domains to matrix attachment regions in mouse thymocyte nuclei (Dickinson et al., 1992). Using mouse thymocyte extracts, purified human BAZ1A and SNF2H were shown to co-IP SATB1 (Yasui et al., 2002). Additionally, thymocytes from *Satb1*-deficient mice ectopically express *interleukin-2 receptor* α (*IL-2Rα*) as assessed by detection of hyper-acetylated histone H4 by ChIP in the promoter region of this gene, a mark that has been

correlated with active gene expression. It was also shown by ChIP that SATB1 recruits both mouse BAZ1A and SNF2H to this locus, implicating these chromatin remodeling factors in *IL-2Rα* repression. Interpretation of these results is limited by a lack of evidence for a direct interaction between mouse BAZ1A and SATB1 and that ectopic *IL-2Rα* expression was not measured directly but is inferred from H4 acetylation in the promoter.

4. DNA damage repair

Adding to the growing list of ACF/CHRAC functions, two recent reports describe its role in DNA double-strand break (DSB) repair by homologous recombination (HR) and non-homologous end joining (NHEJ) and the G2/M damage checkpoint (Lan et al., 2010; Sanchez-Molina et al., 2011). Roles for chromatin remodeling complexes in DSB repair have been reported previously but mainly for the large multi-protein complexes of the SWI/SNF and INO80 families of remodelers (Bao and Shen, 2007). It was recently reported that the ISWI family complex WICH, consisting of BAZ1B and SNF2H, plays a role in the DNA damage response (Xiao et al., 2009a). BAZ1B was reported to contain a novel kinase domain that constitutively phosphorylates tyrosine 142 on H2AX. Following induction of DNA damage, this mark must be removed prior to phosphorylation of serine 139 (referred to as γ-H2AX) by the ATM/ATR kinases, which recruits a host DNA response proteins. The two studies described below expand the list of ISWI complexes with reported roles in the DNA damage response.

ACF/CHRAC and the Repair of DNA Double-Strand Breaks
Screening for chromatin remodeling factors that localize to sites of laser induced DNA double-strand breaks (DSBs) in human cells using BrdU as a photsensitizer, Lan et al.

identified BAZ1A and SNF2H (Lan et al., 2010) by tagging them with green fluorescent protein (GFP) and observing co-localization with phosphorylated histone H2AX (γ-H2AX), a marker of DSBs. Recruitment was not observed following treatment of cells with UVC, which does not generate DSBs but instead forms bulky photo-adducts like pyrimidine dimers. However, neither BAZ1A nor SNF2H formed foci following X-ray irradiation, which will also generate DSBs. The authors reconcile this discrepancy in recruitment to DSBs induced by different sources of damage by suggesting that the laser-induced DSBs are more concentrated at a specific location making the recruitment of proteins easier to visualize.

To observe the recruitment of a smaller number of protein molecules to sites of DSBs, they generated U2OS cells (human osteosarcoma cell line) stably expressing a ~200 copy transgene array of a plasmid containing I-Sce1 restriction sites adjacent to a Tet-responsive element. A plasmid encoding cherry fused to a Tet-response element binding protein (TetR) with an estrogen receptor hormone-binding domain was electroporated into these cells to locate the array. A plasmid expressing the I-Sce1 endonuclease and GFP-tagged BAZ1A or SNF2H were then electroporated in and tamoxifen was added to translocate the cherry-TetR binding construct into the nucleus. BAZ1A and SNF2H localized to break-sites ~30% of the time while two known DSB targeted proteins (KU70/80) were recruited ~90% of the time.

Reducing levels of BAZ1A or SNF2H by RNAi sensitized U2OS cells to increasing doses of methyl methane sulfonate (MMS), bleomycin, camptothecin and X-rays but not UVC as assessed by measuring the percentage of surviving cells. Again, UVC is known to create bulky adducts in the DNA while the other agents all result in DSBs directly or indirectly by conversion of single-strand breaks into DSBs by passage of the replication machinery or by inhibiting topoisomerases. As great as a 10-fold difference in the surviving fraction of control versus knock-down was observed in cells

17

treated with MMS while as little as a 2-fold effect was seen following X-ray irradiation. In addition, following bleomycin treatment, U2OS cells with reduced levels of BAZ1A or SNF2H had ~3 times longer mean tail moments in a comet tail assay compared to control. Moreover, 4 times as many cells with reduced levels of BAZ1A, SNF2H or Ku80 have persistent γ-H2AX foci following treatment with X-rays compared to controls.

To test for a role in repair by NHEJ, an assay in human H1299 cells (human non-small cell lung carcinoma cell line derived from the lymph node) was performed by stably integrating a DNA fragment with two I-Sce1 restriction sites flanking a thymidine kinase (TK) gene separating a GFP cassette from upstream promoter sequences. Cleavage at the two sites followed by NHEJ results in excision of the TK gene, enabling expression of GFP from the upstream promoter. Reducing levels of BAZ1A, SNF2H or KU80 reduced the number of GFP positive cells 2-fold compared to control, interpreted as a defect in NHEJ efficiency.

To assess a role in repair by HR, an assay that involves cleavage of I-Sce1 sites to induce HR between two incomplete EGFP genes was used to measure the efficiency of repair. HeLa cells with reduced levels of BAZ1A or SNF2H showed reduced frequencies of GFP positive cells by ~5-fold and ~20-fold respectively. This suggests that BAZ1A enhances a basal activity of SNF2H to aid in the repair of DSBs by HR.

Co-expression of GFP-tagged KU70/80 in U2OS cells showed that these proteins are not recruited to laser-induced stripes of DSBs when BAZ1A levels are reduced but the same effect was not seen when SNF2H was reduced, suggesting BAZ1A specifically and uniquely is required for the recruitment of the KU proteins. To test for a direct interaction, HEK293 cells (human embryonic kidney cells) stably expressing FLAG-KU80 were used and interactions with BAZ1A, SNF2H, CHRAC17 and CHRAC15 were detected and enhanced following treatment with bleomycin. These data seems to conflict with the above result that BAZ1A is recruited to 30% of I-Sce1

breaks while KU80 is recruited to 90%. This could be explained if BAZ1A localization is transient and KU localization is persistent.

To test a requirement for CHRAC15/17 in repair, the same NHEJ and HR assays described above were used. Reducing either protein reduced the fraction of GFP positive cells ~2-fold in the NHEJ assay and ~5- and 2.5-fold respectively in the HR assay. These results suggest that the ACF/CHRAC complexes may play a role in DSB repair in cultured human cells.

This report is intriguing as it is easy to imagine that chromatin remodeling would be required at sites of breaks to grant access to DNA-binding repair proteins and assemble histone octamers onto newly synthesized DNA. However, the use of different cancerous cell lines complicates the interpretation as each assay was performed in the background of a different spectrum of mutations. Also, like the other cell culture studies described above, the lack of proper 'rescue' experiments to control for the possibility of RNAi off-target effects limits the interpretation of the results. Moreover, the observed effect of reducing the ACF/CHRAC complex components was often only on the order of a few fold depending on the assay, suggesting that if ACF/CHRAC does play a role during DSB repair these complexes are not absolutely required for repair, counter to the suggestion of the title of the study.

ACF/CHRAC and The G2/M Damage Checkpoint in Cultured Human Cells
Another group, also using human cells and RNAi, report a role for BAZ1A in the G2/M damage checkpoint (Sánchez-Molina et al., 2011). Reducing levels of BAZ1A or SNF2H in HeLa cells reduced proliferation ~1.6-fold after 72 hours compared to control cells. An ~1.5-fold increase in the number of apoptotic cells was also observed in Hela or U2OS cells with reduced levels of BAZ1A or SNF2H as measured by Annexin V staining. In addition, following induction of replication stress by aphidicolin (APH) treatment, there

was a 2-fold increase in the number of chromosomal breaks at fragile sites in metaphase spreads from cells with reduced levels of BAZ1A compared to untreated cells. Cell survival was also 30% less in BAZ1A knock-down cells treated with APH compared to control cells.

To assess a role in the G2/M checkpoint, cells were treated with APH and replication was monitored by FACS. In control cells, ~65% of cells arrested at the G2/M checkpoint, which was decreased to 42% when the levels of BAZ1A were reduced. Moreover, staining for histone H3 phosphorylated at serine 10 (H3S10ph), a marker of mitotic cells, showed a 5-fold decrease in the number of positively staining control cells following APH treatment while the population of mitotic cells with reduced levels of BAZ1A remained the same following treatment, suggesting BAZ1A is required for proper checkpoint activation.

Checkpoint activation was also assessed following the induction of DSBs following X-ray irradiation or exposure to UVC. By again measuring H3S10ph by FACS, either damaging agent reduced the number of mitotic cells by 50% in control 1 hr after treatment compared to only a 30% reduction in cells with reduced levels of BAZ1A, suggesting its depletion compromises the G2/M checkpoint.

In addition, BAZ1A depleted cells failed to induce γ-H2AX or CHK2 phosphorylation (a marker of checkpoint activation) following exposure to X-rays or UVC radiation as measured by quantitative western blots using the Li-cor system. Like the previous study, the observed effects on checkpoint activation were quantitatively subtle in the absence of BAZ1A, suggesting that BAZ1A is not absolutely required or that levels of protein were not sufficiently reduced by RNAi to fully reveal the requirment . Again, controls that would exclude the possibility that the observed effect was due to off-target effects of the RNAi were not included in this study, limiting the interpretation of the results.

IV. Spermatogenesis and chromatin dynamics

Spermatogenesis refers to the unique developmental program that begins with mitotically dividing, pluripotent spermatogonia at the basal lamina of the seminiferous epithelium and ends with mature spermatozoa (sperm) being released into the lumen (spermiation). Following the meiotic divisions, the last stage of spermatogenesis (spermiogenesis) produces dramatic changes that alter the basic composition of a typical somatic cell to produce what is essentially a nucleus with a tail. The Golgi apparatus will coalesce and stretch over one end of the nucleus to produce the acrosomal cap, which contains digestive enzymes to aid in penetration of the outer membrane of the ovum during fertilization. At the other end of the nucleus, one of the centrioles will elongate to produce the flagellar tail structure that confers locomotion to the sperm. The energy to power the whip-like beating of the tail is produced by the mitochondria, which migrate and collect in the tail's midpiece just below the sperm head during spermiogenesis. The majority of the cytoplasm will be shed to form a residual body, which is phagocytosed by the Sertoli cells. Sertoli cells are a somatic population of cells with large cytoplasmic projections that provide an organized structure to the tubule and nurture the germ cells during spermatogenesis by secreting various factors. They will also aid in the forward progression of the germ cells from the basal to the luminal compartments of the tubule as they develop.

Spermatogenesis also results in a dramatic makeover of the genetic material. Spermatogonia that receive signals to differentiate will undergo one round of replication followed by two rounds of divisions to produce haploid sperm. Prior to the first, reductional division, 100's of DNA double-strand breaks per primary spermatocyte nucleus form and repair to shuffle the maternal and paternal chromosomes to generate physical linkages between homologous chromosomes required for their proper segregation during the end of meiosis I. Meiosis II is a equational division that occurs in

secondary spermatocytes, separating sister chromatids into two round spermatids, which will elongate and condense to form mature sperm.

With a nuclear volume ~5% that of the average somatic cell and tasked with protecting and delivering the paternal genome during fertilization, a mature sperm must employ a new strategy to package its genetic cargo. As spermatocytes progress in the developmental program up to the elongated spermatid stage, somatic histones are almost completely replaced by histone variants, some of which are testis-specific. Then, in the final stages of spermiogenesis, histones are replaced by the small, basic, transition nuclear proteins (TPs) and finally by the protamines to allow for a highly compacted, almost crystalline arrangement of the DNA within the sperm head (Figure 4). Our knowledge of the importance of these chromatin dynamics in sperm development comes from studies in mice in which various histone variants, the transition proteins or protamines and other components were deleted by gene-targeting. Understanding how aberrations in the repackaging of the sperm DNA affect their development could provide clues for the role of chromatin remodeling during this process and so the relevant findings are summarized below.
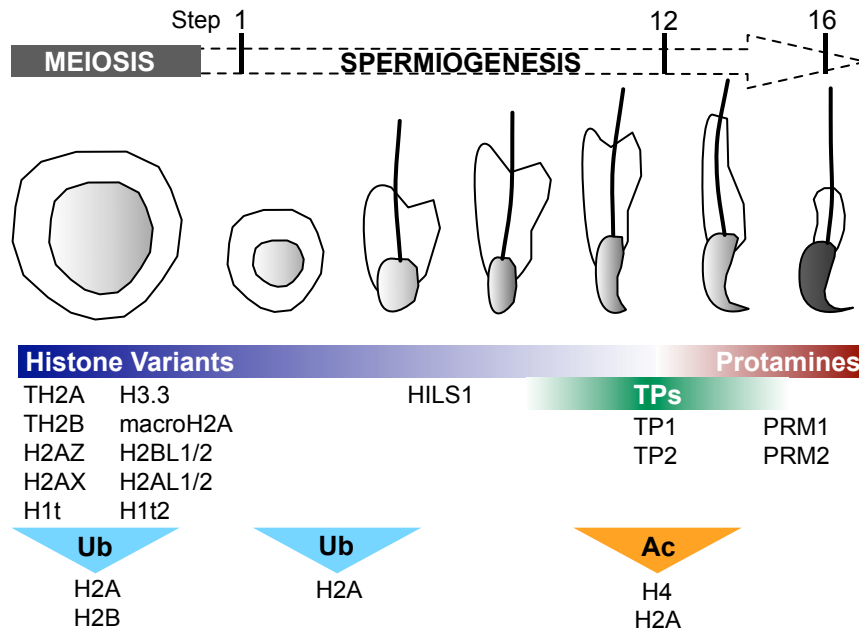
Figure 4. Chromatin dynamics during spermatogenesis. Schematic showing the changes in chromatin composition and post-translational modifications as spermatogenesis progresses from primary spermatocytes (meiosis) to mature sperm (step16). Histone variants, transition proteins (TPs) and protamines (PRMs) are listed below the stage when they are incorporated. Triangles indicate the approximate timing of indicated covalent modifications. Ub, ubiquitination; Ac, acetylation. Adapted from Govin et al., 2004; Gaucher et al., 2010. See text for additional references.

1. The role of histone variants

With the exception of histone H4, there are several nonallelic isoforms of each of the conventional histones commonly referred to as histone variants (Malik and Henikoff, 2003). While the bulk of conventional histones are synthesized and incorporated in a replication-coupled manner, histone variants can be synthesized and assembled throughout the cell cycle. They are sometimes referred to as replacement histones as they can be essential for maintenance of the nucleosome in non-dividing, long-lived cells where eventual degradation of the conventional histones necessitates replacement in the absence of replication (Frank et al., 2003).

During spermatogenesis, the majority of conventional histones will be replaced by variants and are thought to loosen the chromatin, as structure-function analysis has shown that many form nucleosomes that are less stable compared to their conventional counterparts (Gaucher et al., 2010). Although some of these variants are ubiquitously expressed, a large number of them (notably all known H2B variants) are testis-specific and all have varying temporal expression patterns during spermatogenesis.

There are three known testis-specific variants of the linker histone H1: H1T, H1T2 and HILS1. H1T is expressed during mid-pachytene in primary spermatocytes and can be detected until the elongated spermatid stage (Drabent et al., 1996). H1T has been approximated to constitute up to 55% of the total linker histone population during this time and yet mice lacking this variant display no phenotype (Drabent et al., 2000; Fantz et al., 2001; Lin et al., 2000). Interestingly, chromatosomes containing H1T have been shown to have a less compact structure than those containing other H1 subtypes (De Lucia et al., 1994; Khadake and Rao, 1995), suggesting it may be involved in loosening chromatin. Conversely, male mice lacking the round and elongated spermatid expressed H1T2 are sterile due to the production of morphologically abnormal sperm with severely reduced motility. Lastly, the more recently discovered Hils1 (H1-like protein

in spermatids 1) variant was found to be expressed much later in spermatogenesis compared to the other H1 variants, at a time when elongating spermatids are condensing to form mature sperm (Yan et al., 2003).

There are several non-testis specific H3 variants expressed during spermatogenesis. CENP-A is a centromere specific variant important for recruitment of other proteins to the centromere and kinetochores (Smith, 2002). Intriguingly, CENP-A is retained in mature sperm and has been suggested to mark the centromere during the protamine-to-histone exchange that occurs during fertilization (Palmer et al., 1990). The H3.3 variant is present in germ cells prior to meiosis and replaces the majority of canonical H3 as spermatogenesis progresses (Akhmanova et al., 1995). H3.3 is also enriched in the specialized subnuclear domain known as the sex body that contains the transcriptionally silenced X and Y chromosomes (Bramlage et al., 1997; van der Heijden et al., 2007). Homozygous disruption of H3.3 causes partial neonatal lethality with surviving animals displaying male subfertility but without any appreciable sperm malformation (Couldrey et al., 1999).

A testis-specific H2B variant, TH2B, is expressed early in primary spermatocytes and persists until the round and elongating spermatid stage (Meistrich et al., 1985; van Roijen et al., 1998). Two other testis H2B variants, H2BL1 and H2BL2 localize to pericentric heterochromatin (Govin et al., 2007).

Numerous ubiquitous and testis-specific H2A variants are expressed during spermatogenesis. Testis-specific TH2A is expressed and incorporated into the chromatin of pachytene spermatocytes (Meistrich et al., 1985; Rao et al., 1983). Recently, the mouse orthologs of human testis-specific H2ABbd (H2AL1 and H2AL2) were reported (Govin et al., 2007). H2ABbd affects nucleosome stability and so may contribute to a loosening of the chromatin (Gonzalez-Romero et al., 2008). The other two H2A variants expressed during spermatogenesis are macroH2A1.2 and H2AX. Both are components

of the heterochromatinized sex body (Handel, 2004; Hoyer-Fender et al., 2000) but H2AX is required for sex-body formation as H2AX null mice are sterile due to abortive spermatogenesis (Celeste et al., 2002). More specifically, macroH2A1.2 co-localizes with the heterochromatin protein HP1β at the pseudo-autosomal region (PAR) of the paired X and Y and plays a role in stabilizing X-Y synapsis (Turner et al., 2001). Importantly, ACF was unable to remodel nucleosomes containing the macroH2A variant *in vitro* (Doyen et al., 2006), adding to the complexity of remodeling control mechanisms. Lastly, H2AZ is also expressed in primary spermatocytes but is specifically excluded from the sex body. Instead, it becomes enriched in the post-meiotic sex chromatin of round spermatids, suggesting it may play a role in the maintenance of X-Y silencing that is known to extend into this stage (Greaves et al., 2006). In contrast to macroH2A, H2AZ stimulates the activity of ISWI containing chromatin remodelers *in vitro* (Goldman et al., 2010).

2. Testis-specific histone post-translational modifications

Histones are awash with sites that have the potential for covalent modification, namely acetylation, methylation, phosphorylation, glycosylation and ubiquitination. These epigenetic marks can serve as docking sites for other proteins with domains that can specifically recognize and bind these marks thus altering the structure and function of particular chromatin domains (Strahl and Allis, 2000). Acetylation and ubiquitination, the two most studied modifications during spermatogenesis are discussed.

Prior to the almost complete swap of histones for protamines in elongating spermatids, the histones are hyperacetylated (Govin et al., 2004). Usually associated with replication-dependent histone incorporation or transcriptional activation, this widespread acetylation occurs in the absence of either and is tightly linked to the timing of histone removal. Indeed, the disappearance of hyper-acetylated H4 as elongating

26

spermatids condense occurs in a parallel spatio-temporal pattern as that of genome compaction (Hazzouri et al., 2000). This idea is supported by the observation that histones are under-acetylated in fish species that do not undergo histone replacement during spermiogenesis (Kennedy and Davies, 1980, 1981). It has also been shown *in vitro* that acetylated histones are more easily displaced by protamines (Oliva et al., 1987; Oliva and Mezquita, 1986), although the exact role of histone acetylation is still unknown.

Ubiquination entails the covalent addition of a 76 amino acid peptide, ubiquitin, to an acceptor site of a substrate and is mediated by a multi-step enzymatic reaction to activate, conjugate and ligate the modifying group. Although polyubiquitin chains usually mark a substrate for degradation by the proteasome, recent studies have shown that monoubiquitination can serve in other capacities. Ubiquitinated H2A (uH2A) is enriched in the sex body of early pachytene spermatocytes and then more diffusely on the chromatin in mid-pachytene. Its levels then decrease at the round spermatid stage only to increase again in elongating spermatids (Baarends et al., 1999). H2B is known to be ubiquitinated by RAD6, an ubiquitin-conjugating enzyme, in *S. cerevisiae.* When the ubiquitin targeted lysine-123 of H2B is replaced by arginine, thus preventing ubiquitination, this strain experiences an early block in meiosis (Robzyk et al., 2000). HR6B is the mammalian ortholog of RAD6 and is highly expressed in the testis. Disruption of the *Hr6b* gene in mouse results in male sterility, with an arrest at the round-to-elongating spermatid stage (Roest et al., 1996). These mutants display a damaged synaptonemal complex, an increase in cross-over frequency and a de-repression of X-chromosome silencing (Baarends et al., 2007; Baarends et al., 2003; Mulugeta Achame et al., 2010), suggesting this modification plays a role in creating a repressive chromatin state.

3. Transition nuclear proteins and protamines

Following the turnover of conventional histones to variants, the majority of them will be completely replaced by an array of testis-specific, low molecular weight basic proteins to facilitate a higher level of genome compaction as sperm finish elongating and condensing into their mature form. This process occurs in a stepwise manner, first with incorporation of the transition nuclear proteins (TPs) of intermediate basicity and subsequently with the highly basic protamines (Ward and Coffey, 1991).

The transition from histones to protamines occurs directly in fish and birds (Oliva and Dixon, 1991) but is facilitated by an intermediate, the TPs in mammals. There are two TPs in rodents, TP1 and TP2 (Platz et al., 1977). Both are very basic owing to their high lysine and arginine content (Grimes et al., 1975; Kistler et al., 1975). TP1 is highly conserved (Kremling et al., 1989) while TP2 is not (Alfonso and Kistler, 1993). The gene encoding TP2, *Tnp2*, is in the same locus as *protamine 1* (*Prm1*) and *protamine2* (*Prm2*) suggesting they may have arisen by gene duplication (Engel et al., 1992). *Tnp1*, in contrast, is on a separate chromosome. Both genes are transcribed in step 7 spermatids and their mRNAs are stored as cytoplasmic ribonucleoproteins for 3 to 7 days prior to translation (Mali et al., 1989). Surprisingly, single knockout mice of either TP did not significantly impact fertility, although both gave reduced litter sizes (Yu et al., 2000; Zhao et al., 2001). *Tnp2* null mice on a pure 129/Sv inbred background are sterile, however, indicating the interplay of a genetic modifier (Adham et al., 2001). Also, *Tnp1* and *Tnp2* double mutant mice are sterile, indicating that they are necessary for proper sperm chromatin dynamics in the mouse (Shirley et al., 2004).

The protamines are highly basic sperm nuclear proteins with high arginine and cysteine composition, which create a net positive charge and facilitate the formation of inter and intra-protamine disulphide bonds respectively (Balhorn et al., 2000). Protamine 1 (Prm1) is translated as a mature protein while protamine 2 (Prm2) is translated in a

long precursor form that is proteolytically cleaved to its smaller, mature form (Aoki and Carrell, 2003). The pre-protamine 2 (pPrm2) intermediate is phosphorylated by the kinase CAMK4 as a prerequisite to cleavage. CAMK4 deletion results in male sterility with prolonged retention of TP2 (Wu et al., 2000), indicating that removal of the transition proteins is in part mediated by the protamines. Deletion of either protamine renders mice infertile due to fewer sperm and non-motile sperm with morphological abnormalities, demonstrating that they are essential for proper sperm development (Cho et al., 2001). Transcription of both protamines is regulated by cyclic adenosine monophosphate (cAMP) response elements (CRE) in their promoter regions, which serve as binding sites for the transcription activator CREM. CREM is considered the 'master-regulator' of spermiogenesis as it controls the transcription of many essential genes including the TPs. Mice lacking CREM experience a complete block in spermiogenesis at the round-spermatid stage (Blendy et al., 1996; Nantel et al., 1996), demonstrating its role in the induction of the spermiogenic program. Like the transition proteins, the protamine mRNAs expressed in step 7-9 spermatids are stored as translationally repressed ribonucleoproteins (Balhorn et al., 1984; Kleene et al., 1984). The 3' untranslated region (3' UTR) is both necessary and sufficient to mediate this repression (Braun, 1990; Braun et al., 1989). Transgenic mice lacking this control region of protamine 1 prematurely translate Prm1, which causes precocious condensation of DNA, abnormal sperm head morphologies and incomplete processing of pPrm2, resulting in sterility (Lee et al., 1995).

SCOPE OF THESIS

The central focus of my thesis is to understand the *in vivo* function of *Baz1a*; namely, if its well characterized *in vitro* functions and known high testis expression (Jones et al., 2000) interplay with the unique chromatin remodeling events that take place during spermatogenesis in that organ. The story begins with the discovery of multiple, mainly testis-specific alternative transcripts of *Baz1a*. Next, to ask about its role in development, I generated mice deficient for *Baz1a*. In contrast to partially penetrant lethality of *Acf1* mutation in *Drosophila*, *Baz1a*-deficient mice are viable. Mice lacking BAZ1A show no obvious defects in B- or T-cell lineages, class switch recombination in cultured B cells, or meiotic recombination. Thus, BAZ1A is dispensable *in vivo* for the development of cells that require the repair of developmentally programmed DNA double-strand breaks. However, *Baz1a*$^{-/-}$ male mice are sterile because of a severe defect in spermiogenesis that results in fewer and non-motile sperm with morphological defects, likely due to transcriptional perturbation observed in spermatocytes and round spermatids. Furthermore, the ACF/CHRAC complexes form in the mouse and require BAZ1A for their stability and localization. Thus, BAZ1A-containing chromatin remodelers play important roles in the development of mature spermatozoa.

MATERIALS AND METHODS

Generation of Baz1a conditional targeting construct

A schematic of the targeting strategy is shown in Figure 2.1A. Bacterial artificial chromosome (BAC) DNA (RP23-235B6) containing the *Baz1a* genomic locus was used to PCR amplify long (~2 kb) and short (~5 kb) arms of homology with *Spe*I and *Hind*III and *Not*I and *Hind*III sites respectively at their ends, which were cloned into the PL253 plasmid at *Spe*I and *Not*I. The *E. coli* strain containing the same BAC was electroporated with the pRed/ET recombineering plasmid (Gene Bridges) and PL253 containing the homology arms linearized with *Hind*III to clone a partial genomic *Baz1a* sequence (~12 kb) containing exons 5-7 into PL253 by homologous recombination upstream of thymidine kinase (TK) under the control of the *Mc1* promoter for selection against random integration. Next, short arms of homology were PCR amplified from intronic sequence between exons 5 and 6 with a 3' EcoRI site added to the left arm and a 5' *Bam*HI site added to the right arm and were ligated onto pPL452 linearized with EcoRI and BamHI. The recombineering strain EL350 were used to add this construct which contains a neomycin-resistance cassette (NEO) under the control of the *pgk* promoter flanked by FRT sites and with a single lo*x*P site on the 3' end into the inton upstream of exon 6 of the partial *Baz1a* locus cloned into pPL253. Traditional cloning was then used to add a second *lox*P site into a unique *Avr*II site located in the intron downsteam of exon 6. The targeting construct was linearized with *Sal*I prior to electroporation.

Generation of Baz1a-deficient mice

The targeting construct was electroporated into albino C57Bl/6J, CY2.4 embryonic stem (ES) cells by the Rockefeller University Gene-Targeting Facility and G418-resistant clones were screened for successful homologous recombination by

Southern blot analysis of *Bam*HI and *Eco*RI digested ES cell DNA using external probes (Figure 5.1). The BamHI fragment was detected using probe S2, a 290 bp fragment, which was amplified from genomic DNA using primers ShortProbe2for (5'-TCTTCTGGTATAGAGGGCTGAC) and ShortProbe2rev (5'-AGCCAGAGAGCAACAGAAAC). The EcoRV fragment was detected using probe L2, a 361 bp fragment, which was amplified from genomic DNA using primers LongProbe2for (5'-AAGTGTGGAGGTTGGCTCATAC) and LongProbe2rev (5'-CTGCTTACTAGCAATGCTGTC). Two targeted ES cell clones (#73 and #83) were injected into blastocyts and implanted into pseudopregnant females by the MSKCC Transgenic Mouse Core Facility. Clone #73 went germline to generate chimeras with 1 floxed and 1 wild-type *Baz1a* allele.

To delete *Baz1a, Baz1a^flox* mice were crossed to a FVB/NJ transgenic line expressing Cre recombinase under the control of the *Stra8* promoter (Sadate-Ngatchou et al., 2008). Males heterozygous for the deletion in their germline were fertile and bred to generate mice fully nullizygous for *Baz1a* (*Baz1a^-/-*). All of the mice described in this study were subsequently maintained on C57Bl/6JxFVB/NJ mixed genetic background by mating brothers and sisters. To minimize variability from strain background, experimental animals were compared to controls from the same litter or from the same matings involving closely related parents. Adult mice between 2-6 months of age were used in all experiments unless otherwise noted.

Genotyping was performed by PCR on 1 μL tail tip DNA which was extracted using 200 μL DirectPCR lysis reagent (Viagen #101-T) and 1 μL proteinase K (Qiagen #19133) at 55°C overnight at 400 rpm in a Thermomixer R (Eppendorf) followed by inactivation at 85°C for 1 hr. PCR conditions were as follows: 1 minute at 95°C, then 33
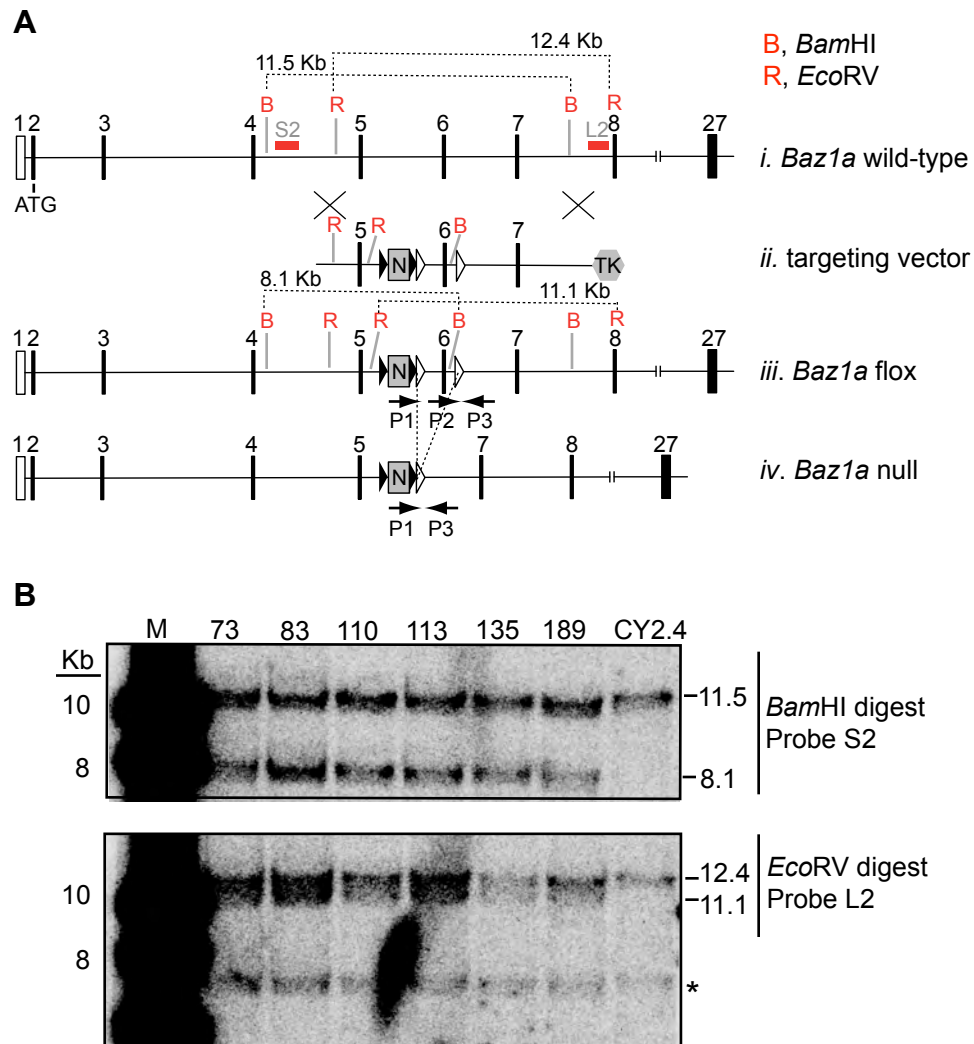
Figure 5. Targeted disruption of the mouse *Baz1a* locus. (**A**) Schematic representation of the strategy used to generate a conditional allele of *Baz1a*. (*i*) Partial *Baz1a* genomic locus. (*ii*) Map of the targeting vector. (*iii*) Targeted conditional allele. (*iv*) Null allele following Cre-mediated recombination of the *loxP* sites (open triangles) flanking exon 6. Red boxes, Southern blot probes; Black triangles, FRT sites; N, *pgk-neo*; TK, *hsv*-thymidine kinase; P2 and P3, primers used to amplify wild-type and flox allele; P1 and P3, primers used to amplify the null allele. Not to scale. (**B**) Southern blots confirming successful gene targeting in six CY2.4 ES cell clones, designated by the numbers above each lane. The top panel shows a *Bam*HI digest of genomic DNA with probe S2 and the bottom panel, an *Eco*RV digest with probe L2. The expected digest fragment sizes are indicated at the right in Kb. M, marker; CY2.4, untargeted ES cell DNA serves as a negative control. Asterisk indicates a cross-hybridizing band.

cycles of 20 s at 95°C, 30 s at 55°C, and 45 s at 72°C, followed by a final extension for 3 minutes at 72°C. The $Baz1a^{flox}$ allele was detected with primers P2 (5'-AAACAGGTGGAGAACTTGG) and P3 (5'-CACAGGCATATGCTACCTAGG), which amplify fragments of 245 bp for the wild-type allele and 411 bp for the mutant (Figure 2.1B). Recombination of loxP sites by Cre recombinase was confirmed using primers P1 (5'-TTCCTCGTGCTTTACGGTATCG), P2 and P3, which amplify fragments of 245 bp for the wild-type allele and 331 bp for the null allele (Figure 2.1B). Electrophoresis of PCR products was performed using 1.5% agarose (Fisher #BP160-500) in 1X TAE at 120 V.

All animal work was performed in compliance with relevant regulatory standards and was approved by the MSKCC Institutional Animal Care and Use Committee.

Mouse ear-fibroblast generation and immortalization

Wild-type and $Baz1a^{-/-}$ mice were anesthetized using isofluorane and ears were sanitized with ethanol wipes prior to cutting off the dorsal tip of both and placing them in a tube with 1 mL DMEM media. Ear tips were transferred to sterile 10 cm dishes and rinsed with 2 mL PBS with kanamycin (100 μg/mL). Tips were transferred to fresh dishes using flame-sterilized forceps and 300 μL of DMEM with collagenase D/dispase (4 mg/mL) that had been filter sterilized using a 0.22 μ syringe filter was added to each. Ear tips were minced into small pieces using a flame sterilized razor blade and transferred with liquid to 1.5 mL tubes and incubated in a thermomixer R (Eppendorf) at 600 rpm at 37°C for 2 hr. Following the incubation, 1.5 mL DMEM with 10% fetal bovine serum and 5X antibiotic/antimycotic (Gemini Bioproducts) was added. Working in a sterile tissue-culture hood, the pieces and liquid were transferred to a single well of a 24-well dish and incubated overnight at 37°C with 5% CO_2. Tissue was dissociated by pipetting up and down ~30X with a P1000. Cells were passed through a 40 μm cell strainer and collected

into a 50 mL conical tube and pelleted at 1000 rpm for 5 min. The pellets were resuspended with 3 mL DMEM with 10% fetal bovine serum and 5X antibiotic/antimycotic and plated in a single well of a 6-well dish and incubated at 37°C with 5% CO_2. After 2 days, the media was changed with the amount of antibiotic/antimycotic reduced to 2X.

For simian virus 40 (SV40) transformation, 10 cm dishes containing subconfluent early-passage ear fibroblasts (EFs) were each transfected with 5 μg of the p129-SV40 plasmid (kind gift from Janet Mertz, University of Wisconsin) using FuGENE 6 (Roche) transfection reagent according to the manufacturer's instructions. Immortalized cells were selected for by passaging the cells 10 times.

RNA expression analysis

For the reverse-transcriptase PCR (RT-PCR) analysis of *Baz1a* alternative splicing, RNA from adult mouse organs and juvenile mouse testes was isolated using TRIzol (Invitrogen) according to the manufacturer's instructions and cDNA was produced using SuperScript III First-Strand Synthesis System (Invitrogen) with oligo-dT as primers. *Baz1a* transcripts were amplified using primers spanning different exons as depicted in Figure 1.1A. PCR conditions were as follows: 1 minute at 95°C, then 40 cycles of 20 s at 95°C, 30 s at 55°C, and 1 minute at 72°C, followed by a final extension for 3 minutes at 72°C. The exon 13 skip was detected using primers P4 (5'-TAAAGCAGTGGAGTAAACCCAG) and P5 (5'-GTGGCTTCTCTCTCTTTACG). The exon 15 extension was detected using primers P6 (5'-CCAGAAATTATCCATTTTGGCAGG) and P5 (5'-GTGGCTTCTCTCTCTTTACG). The inclusion of a cassette exon between exons 22 and 23 was detected using primers P7

(5'-GCTGATAGCAAGCCTGTGTCTTC) and P8 (5'-TGCAACGTGCGTTCAGTATGGACTTAG).

For quantitative real time PCR (qRT-PCR), RNA was extracted from FACS sorted populations of either spermatocytes or spermatids using TRIzol (Invitrogen) according to the manufacturer's instructions and cDNA produced as above. To separate different cells using FACS, testes from adult mice were processed as described elsewhere (Bastos et al., 2005). Briefly, cells were liberated from testes by enzymatic treatment with collagenase, trypsin and DNaseI and the resulting cell suspension was stained with Hoechst 33342 (Sigma) and sorted using a MoFlo cytometer (Dako) based on DNA content and chromatin complexity. Sorts were performed by the MSKCC Flow Cytometry core facility. The purity of enriched populations was confirmed on squash preparations of sorted cells based on cellular morphology (round spermatids) or immunofluorescence (IF) for SYCP3 (primary spermatocytes) (data not shown). The amplifications were performed using a LightCycler 480 II (Roche) under the following conditions: 5 minutes at 95°C, then 60 cycles of 10 s at 95°C, 20 s at 55°C, and 30 s at 72°C. Primers used for CREM target gene and repetitive element analysis by qRT-PCR were as described (Yabuta et al., 2011). Each primer pair was used to generate an amplicon from the cDNA that was gel purified following traditional PCR. Each amplicon was then serially diluted by a factor of 10 to create a dilution series ranging from 10^{-2} to 10^{-6} to generate a standard curve by qPCR specific for each primer pair against which the relative expression of each unknown was measured.

The pachytene piRNA northern was performed using MIWI-bound RNA isolated from an immunoprecipitation (IP) of testis lysate. Testes were lysed in 1 mL RIPA buffer (50 mM Tris-HCl, pH 7.4; 150 mM NaCl; 1% NP40; 0.25% sodium deoxycholate), and homogenized with a plastic pestle prior to to pelleting cellular debris at 15,000 rpm for 10 minutes. Supernatants were incubated with 10 µL anti-MIWI antibody (Cell Signalling #

2079) overnight at 4°C and bound with 50 μL protein-G agarose. Beads were washed 3X5 minutes with 1 mL RIPA buffer before RNA was extracted using TRIzol (Invitrogen) according to the manufacturer's instructions. RNAs were separated on a denaturing 8% polyacrylamide gel at 300 V and transferred to hybond-N membrane (Amersham) by semi-dry transfer in 0.5% TBE for 1 hr at 300 mA. The blot was cross-linked at 1200 μJ and blocked with hybridization buffer (5X SSC, 1 mM EDTA, 2X Denhardt's, 1% SDS, 2% dextran sulfate, 30 μg/mL ssDNA) at room-temperature for 10 minutes and then at 42°C for 20 minutes and probed overnight at 42°C with a γdATP [^{32}P] labeled mixture of oligonucleotides directed against pachytene piRNAs: piR-1,2,3, which were described elsewhere (Girard et al., 2006). The blot was washed 4X30 minutes with 2XSSC, 0.1%SDS at 42°C followed by exposure to a phosphoimaging screen overnight.

For microarray gene expression profiling, RNA was extracted using TRIzol (Invitrogen) according to the manufacturer's instructions from FACS sorted pachytene/diplotene spermatocytes and spermatids (sorting as described above). RNA samples were labeled and hybridized to the MouseWG-6 v2.0 Expression BeadChip (Illumina) microarray by the MSKCC Genomics Core Laboratory. Data analysis was performed using Partek Genomics Suite software (version 6.5).

Histology and Cytology

For histology, testes or epididymides from adult mice were fixed overnight in 4% paraformaldehyde (PFA) or Bouin's fixative. Tissue was embedded in paraffin and 5 μm sections were cut and mounted on slides for staining with hematoxylin and eosin (H&E) or periodic acid Schiff (PAS) by the MSKCC Molecular Cytology Core Facility.

Sperm were isolated from the epididymis by mincing this organ in PBS and allowing the sperm to swim or diffuse out. Sperm were counted by hemocytometer and a

drop of suspension was added to a 4% PFA coated slide and allowed to air-dry prior to rinsing with PBS for viewing by bright field microscopy.

Immunofluorescence on paraffin sections was performed by the MSKCC Molecular Cytology Core Facility using the Ventana Medical Systems Discovery XT automated stainer. Surface spread spermatogenic cells were prepared as described elsewhere (Peters et al., 1997) as were squashes (Page et al., 1998). Sections and/or spreads and/or squashes were incubated with blocking buffer (1x PBS with 0.2% gelatin from cold-water fish skin, 0.05% TWEEN-20, 0.2% BSA) at room-temperature with gentle agitation for 30 min and stained with the following antibodies diluted in blocking buffer: anti-BAZ1A (Sigma # HPA002730), 1:100 dilution; anti-SNF2H (Novus # H00008467), 1:100 dilution; anti-HP1γ (Millipore # MAB3450), 1:100 dilution; anti-HP1β (Millipore # MAB3448), 1:100 dilution; anti-H3K9me3 (Abcam # ab8898), 1:1000 dilution; anti-CHRAC17 (Novus # NB100-61082) 1:100 dilution; anti-acetylH4 (Millipore # 06-866) 1:100 dilution; anti-γH2AX (Millipore #05-636) 1:100 dilution; anti-MLH1 (BD Parmingen #51-1327GR) 1:50 dilution; antiDMC1 (Santa Cruz # sc-22768) 1:100 dilution; anti-SYCP3 (Santa Cruz # sc-74569), 1:50 dilution. Slides were incubated with primary antibody at 4°C overnight followed by 3x5 minute washes in blocking buffer with gentle agitation, incubation with the appropriate AlexaFluor secondary antibody (Invitrogen) diluted 1:100, washed 3x again and mounted with coverslips using vectashield containing 4',6-diamidino-2-phenylindole (DAPI).

Terminal deoxynucleotidyl transferase (TdT) dUTP nick end labeling (TUNEL) was perfomed by the MSKCC Molecular Cytology Core Facility on 4% PFA fixed testis sections as described elsewhere (Gavrieli et al., 1992).

Fluorescence *in situ* hybridization (FISH) was performed on squashed spermatogenic cells using BAC probes directed against the X and Y chromosomes and chromosome 19 by the MSKCC Molecular Cytogentics Core Facility. Probes were

38

labeled using a nick end translation kit (Abbott Molecular) and hybridized following the manufacturers instructions.

Electron Microscopy (EM)

Testes from adult mice were fixed overnight in 2.5% glutaraldehyde and 2% PFA in 0.075 M sodium cacodylate buffer (pH 7.5). Tissues were then post-fixed in 1% osmium tetroxide, dehydrated, embedded in resin and ultra-thin sections cut and stained with 2% uranyl acetate and Reynolds lead citrate and mounted on copper grids by the MSKCC Electron Microscopy Core Facility for evaluation using a JEOL1230 transmission electron microscope.

SDS-PAGE and western blots

For IP-western and co-IP, a single testis per IP from an adult mouse was homogenized in hypotonic lysis buffer (20 mM HEPES-NaOH, pH 7.5; 5 mM KCl) using a plastic pestle, lysed by freeze/thawing 3X in liquid nitrogen and 37°C water bath for 30 s each and treated with 25 units of benzonase (Novagen) at 4°C for 1 hr. The level of NaCl was increased to 500 mM using 5 M NaCl to increase protein solubility and then reduced to 150 mM by adding dH_2O. Lysates were incubated with antibody overnight and incubated with protein-G beads (Roche) for 1 hr. Beads were washed 3X with PBS and boiled in 2X Laemmli buffer prior to separation on 3-8% Tris-acetate polyacrylamide gels (Invitrogen) at 150 V. Proteins were transferred to PVDF by wet-transfer in Tris-glycine at 100 V for 1 hr at 4°C. Membranes were blocked with 5% non-fat milk in TBS-T (1X TBS with 0.1% TWEEN-20) at room-temperature for 1 hr and incubated with antibodies (as listed above but diluted 1:1000 in block) overnight at 4°C, washed 3X5 minutes with

TBS-T, and subsequently detected with HRP-congugated secondary antibodies (diluted 1:10,000 in block) for 1 hr at room-temperature followed by exposure to film.

For multi-tissue western, ~100 mg pieces of a panel of adult mouse organs were flash frozen in liquid nitrogen and homogenized in RIPA buffer by first mincing with scissors and then grinding with a plastic pestle. Lysates were treated with 25 units of benzonase (Novagen) at 4°C for 1 hr and sonicated alternating 30 sec on high setting, 30 sec off for 15 min using a water bath sonicator at 4°C (Diagenode Bioruptor). Protein concentrations were measured using the Bio-Rad protein assay and 8.5μg of each lysate was added to an equal volume of 2X Laemmli buffer and boiled prior to separation on 3-8% Tris-acetate gels (Invitrogen) and transferred to PVDF by wet-transfer in Tris-glycine as described above. The membrane was stained with Ponceau-S to evaluate protein loading prior to incubation with antibodies.

For cell culture extracts, the various cell lines were grown to confluency in DMEM + 10% fetal calf serum on 10 cm plates, scraped and pelleted by centrifugation and processed like the tissue samples except 25 μg of each extract was used. Additional antibodies: anti-BAZ1B antibody (Sigma # W3516), diluted 1:1000; anti-actin [ac-15] (Abcam # ab6276), diluted 1:2500.

For cellular fractionation, testes were dissociated enzymatically by incubating with 4 mg collagenase in 10 mL Gey's balanced salt solution (GBSS) in a thermomixer R (Eppendorf) at 32°C at 450 rpm for 15 min and mechanically by pipetting up and down using a transfer pipette. The resulting single cell suspension was fractionated as described elsewhere (Mendez and Stillman, 2000). Samples were run on 4-12% Bis-Tris gels (Invitrogen) and transferred to PVDF by wet-transfer in Tris-glycine as described above. The following antibodies were used for western analysis: anti-MacroH2A1.2 (kind gift from John Pehrson, University of Pennsylvania), diluted 1:1000; anti-Hils1 (kind gift

40

from Martin Matzuk, Baylor College of Medicine), diluted 1:2000; anti-H2A.Bbd (Millipore # 06-1319), diluted 1:1000; anti-H2AZ (Millipore # 07-594), diluted 1:2000; anti-H3.3 (Abcam # ab62642), diluted 1:1000; anti-Tubulin (Santa Cruz # sc-5286), diluted 1:5000.

Acid-Urea PAGE analysis of sperm basic nuclear proteins

For acid-urea analysis of sperm basic nuclear proteins, testes were dissociated and nuclei were isolated as described above for the cellular fractionation. Nuclei were then sonicated alternating 30 sec on high setting, 30 sec off for 15 min using a water bath sonicator at 4°C (Diagenode Bioruptor) and sonication resistant nuclei were pelleted at 6000 x g for 5 minutes and the supernatant was saved as the sonication sensitive fraction. Hydrochloric acid (500 mM) soluble proteins were isolated from each population of nuclei and precipitated with 4% and then 20% trichloracetic acid. Insoluble pellets were washed with 500 μL acetone and dried by speed-vac. Pellets were boiled in 100 μL loading buffer (5.5 M urea, 5% acetic acid, 20% β mercaptoethanol) and separated on a 2.5 M urea, 0.9% acetic acid, 15% polyacrylamide gel (which was pre-run overnight in reverse polarity at 150 V) in reverse polarity at 150 V in 5% acetic acid and stained with Coomassie and destained with 50% methanol, 10% acetic acid.

B cell purification and in vitro class-switch stimulation

The following experiment was performed by Bao Q. Vuong, a senior post-doc in Jayanta Chadhuri's Lab at MSKCC: mouse splenic B cells were purified using negative selection with anti-CD43 magnetic beads (Miltenyi Biotec) and stimulated with LPS to induce CSR to IgG3 or anti-CD40+IL4 at a density of 10^6 cells/mL in B cell media (RPMI 1640, 15% fetal calf serum, 2 mM L-glutamine, 100 IU/mL penicillin, 100 μg/mL streptomycin, 60 μM beta-mercaptoethanol). Activated B cells were re-fed at 48 hours with fresh stimulation media and analyzed by flow cytometry at 96 hours post-stimulation on a FACSAria flow

cytometer (BD Biosciences). Antibodies used for flow cytometry were purchased from BD Biosciences: anti-IgG1-APC (#550874) and anti-IgG3-FITC (#553403). Reagent concentrations used in the stimulation were 10 mg/mL LPS (Sigma # L4130), 1 mg/mL anti-CD40 (eBiosciences #16-0402-86), and 12.5 mg/mL IL4 (R&D Systems #404-ML-050).

FACS analysis of CD4/CD8 T cell populations

Single-cell suspensions of mouse thymocytes and splenocytes were generated by dissecting these organs and grinding each between the frosted-portion of glass slides into 5 mL Bruff's media with 5% fetal bovine serum. Cells were pelleted at 1500 rpm for 5 minutes. To the splenocytes, 1 mL red blood cell lysis buffer (Sigma) was added and incubated at room-temperature for 10 minutes. Splenocytes were pelleted and resuspended in 5 mL Bruff's media. Both cell suspensions were counted by hemacytometer and plated at 10^6 cells/well in a 96-well plate. Each well was incubated with normal mouse serum and 75 μg Fc receptor-blocking antibody (Miltenyi Biotec) at 4°C for 20 minutes before being stained at 4°C for 30 minutes with 50 μL/ well of monoclonal antibody conjugates. Cells were stained using the following antibodies purchased from BD Biosciences: anti-CD4-Pacific Blue (#558107) and anti-CD8-FITC (#561968) and analyzed using a FACSAria flow cytometer (BD Biosciences).

CHAPTER I. THE EXPRESSION AND LOCALIZATION OF BAZ1A.

I. Summary

The *in vivo* mRNA expression and protein expression and localization of BAZ1A reported in this chapter correlates well with previous studies but also revealed testis-specific alternative transcripts and an interesting spatiotemporal subcellular localization of the protein during spermatogenesis.

II. Background

BAZ1A has been extensively studied for over a decade. However, to this date, the major focus has been its *in vitro* biochemical function. Although these studies have been useful in elucidating the mechanisms by which *Baz1a* potentially acts to remodel nucleosomes, little about its *in vivo* function in mammals has been uncovered. *Baz1a* message is known to be high in human testis compared to other tissues (Jones et al., 2000); however, there has been no detailed characterization of gene or protein expression in the mouse prior to this study.

As detailed in the introduction, cell culture experiments have implicated *Baz1a* in transcription and replication control and therefore BAZ1A might be expected to localize to the nucleus, which is supported by reports of BAZ1A targeting to heterochromatin (Tate et al., 1998). Moreover, it is a logical assumption that chromatin remodeling might be an essential process in every tissue and that expression of *Baz1a* would therefore be ubiquitous. However, as detailed in chapter 2, *Baz1a*$^{-/-}$ mice develop normally but are male sterile, demonstrating that the increased expression in the testis is consistent with essential BAZ1A functions in this organ.

III. Results

1. Expression and alternative splicing of *Baz1a* in the mouse.

Baz1a expression was detected by PCR on a panel of mouse tissue cDNA libraries generated by reverse transcribing RNA extracted from various dissected organs (Figure 1.1B). As expected, message was detected in every tissue, indicating that *Baz1a* is ubiquitously expressed. However, using primers spanning different exons, amplification revealed band sizes by agarose gel electrophoresis not predicted by the *Baz1a* transcripts reported in genome databases. Figure 1.1A depicts the portion of the *Baz1a* genomic locus where alternative transcripts were detected. Primers binding exons 12 and 14 (red arrows) amplified a product of the expected ~800 bp but another band ~100 bp smaller was also detected to varying degrees in different tissues (Figure 1.1B, top panel). Sequencing showed that this amplicon lacked the exon 13 sequence (data not shown). Alternative splicing skips this exon to produce a transcript that is the dominant species in the testis and kidney while only faintly detected in other tissues (Figure 1.1B, top panel). Sequencing of the *Baz1a* cDNA revealed several other alternative transcripts (data not shown), including alternative 3' splice acceptor site usage in splicing exon 14 to 15 that results in a 14 bp extension of the 5' end of exon 15, and the inclusion of a cassette exon located in the intron between consensus exons 22 and 23. Using a forward primer that binds the unique exon 15 sequence extension and a universal reverse primer (blue arrows), an amplicon of the expected size was detected in every tissue examined, suggesting that this alternative transcript is ubiquitous (Figure 1.1B, middle panel). This amplicon cannot provide quantitative information about the level of this splice variant in different tissues, however. Primers spanning exons 22 and 23 (purple arrows) amplified a product of the expected ~600 bp but also revealed a fainter band ~100 bp larger in both kidney and testis, suggesting this alternative transcript does
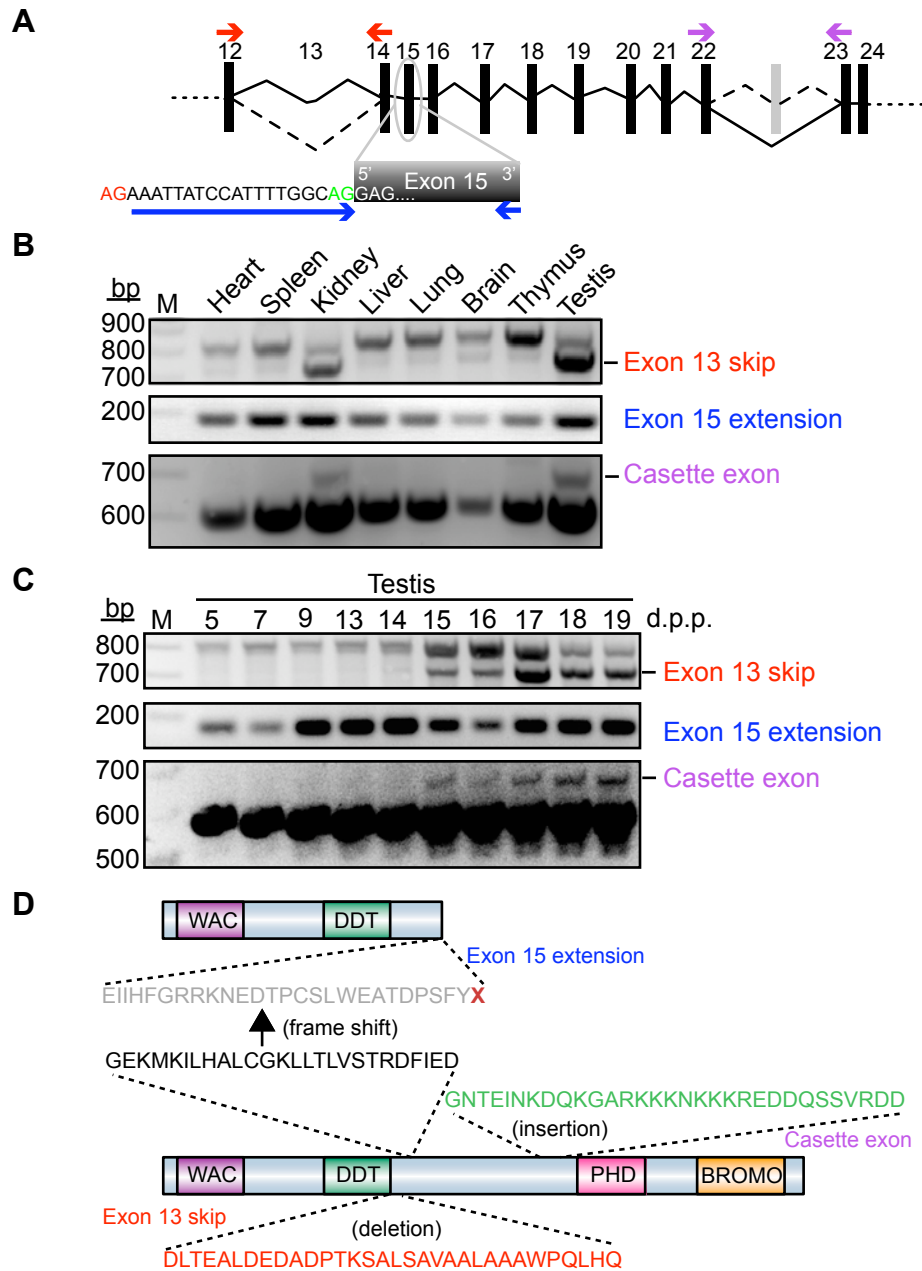
Figure 1.1. Expression and alternative splicing of *Baz1a*. (**A**) Schematic of the portion of the *Baz1a* genomic locus where alternative splice events were detected. Colored arrows represent primers used for RT-PCR in (**B**). The exon 15 alternative transcript is extended on the 5' end due to use of an alternative 3' splice acceptor site ('AG', red) versus the canonical splice site ('AG', green). Dashed line, alternative splice; black box, exon; gray box, casette exon. Not to scale. (**B-C**) RT-PCR of alternative transcripts from a panel of mouse tissues (**B**) or from testis collected at various days post-partum (d.p.p.) (**C**). M, marker. (**D**) Schematic summarizing how the alternative splice events would translate to changes in the BAZ1A peptide sequence. The exon 15 extension leads to a frame shift, altering the peptide sequence (from black to gray text) and would introduce a premature termination codon (dark red 'X'), leading to a truncated protein product lacking the PHD finger and bromodomain.

45

not represent the major transcript population in these tissues (Figure 1.1B, bottom panel).

To examine expression of these alternative transcripts during a time course of testis development, the same analysis was performed on RNA extracted from a panel of juvenile testis dissected beginning at five days post partum (d.p.p.), before the first wave of spermatogenesis initiates, until 19 d.p.p., when the first wave has reached the end of meiosis I. Transcripts that skip exon 13 and/or include the cassette exon between exons 22 and 23 were first detected at 15 d.p.p. (Figure 1.1C, top and bottom panels), corresponding to the time when the first spermatocytes should have reached the mid-pachytene stage of prophase I of meiosis (Goetz et al., 1984). The transcript containing an extended exon 15 was detected at all time points (Figure 1.1B, middle panel).

How these changes in the constitutive *Baz1a* transcript translate to changes at the peptide level were determined by sequencing of the alternative transcripts and are depicted in Figure 1.1D. The domain architecture of the BAZ1A protein as described in the introduction is shown with the approximate location of the amino acid sequence alterations. Skipping of exon 13 occurs in-frame and would result in a 32 residue deletion in a portion of the protein that lies just downstream of the DDT domain. Inclusion of the cassette exon also occurs in-frame and would insert a lysine-rich, 31 amino acid sequence just upstream of the PHD finger. Conversely, the alternative 3' splice acceptor site usage that extends the 5' end of exon 15 shifts the reading frame to change the sequence of a stretch of 26 amino acids and introduce a premature termination codon that, if translated, would produce a truncated protein product lacking the PHD finger and bromodomain.

2. Tissue-specific expression of BAZ1A.

To investigate whether ubiquitous expression of *Baz1a* message translated to a detectable protein product in every tissue, a commercially available polyclonal antibody directed against a central 135 amino acid epitope of human BAZ1A was used for immunoblotting of protein extracts from a panel of mouse tissues (Figure 1.2A). The epitope to which this reagent is directed shares 85% amino acid sequence identity with mouse BAZ1A and its specificity was verified on extracts from cultured cells (Figure 1.2B, top panel, last lane) and tissue from *Baz1a* nullizygous mice (described in chapter 2).

Electrophoretic separation of equal amounts (as determined by Bradford protein assay) of nuclear-enriched (by low speed centrifugation) mouse tissue extracts followed by immunoblotting showed that BAZ1A is highly expressed in the testis but was not detectable in the other tissues examined with the amounts of protein that could be feasibly loaded (Figure 1.2A, top panel). Two closely migrating bands appear at the expected molecular weight of ~178 kDa while a third, faster-migrating band is detected at ~130 kDa. The ~178 kDa doublet could reflect the translation of one or more of the alternative transcripts, which are not predicted to alter the molecular weight by more than two or three kDa but could also be indicative of a population of protein with a post-translational modification that retards migration. The third band does not correspond to an expected molecular weight of any of the splice isoforms but could represent the protein product of an unknown alternative transcript or, more simply, represent a degradation product. It should be noted that the putative truncation product derived from the exon 15 extension described above would delete the epitope detected by the antibody and therefore would not be detectable in this analysis.
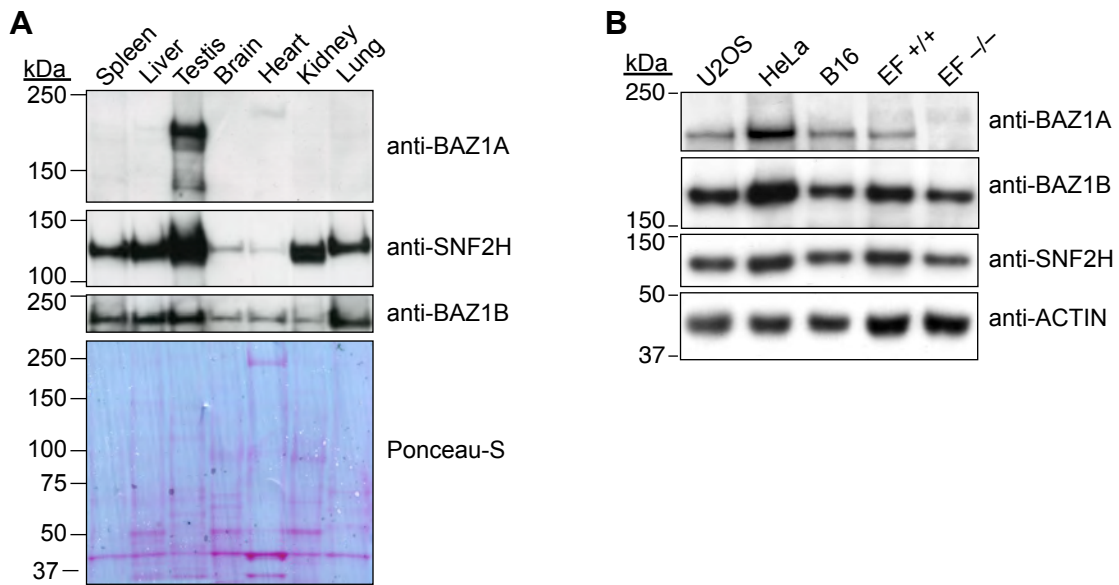
Figure 1.2. BAZ1A is highly expressed in the testis. (**A, B**) Equal amounts of whole cell extracts from a panel of mouse tissues (8.5μg) (**A**) or cultured human (U2OS and HeLa) and mouse (B16 and ear fibroblasts (EF)) cells (25μg) (**B**) were immunoblotted with anti-BAZ1A, SNF2H and BAZ1B antibodies. Approximate molecular weights: BAZ1A = 178 kDa, SNF2H = 122 kDa and BAZ1B = 171 kDa. Ponceau-S staining of the membrane serves as a loading control for (A) and anti-Actin (~42 kDa) for (B). +/+, wild-type; -/-, *Baz1a*-nullizygous.

Conversely, immunoblotting showed that expression of the other ACF complex component SNF2H and the closely related BAZ1A paralog BAZ1B were readily detectable in every tissue examined, albeit at varying levels (Figure 1.2A, middle panels). SNF2H levels were also highest in the testis but showed strong expression in most of the other tissues examined with the exception of brain and heart, where it was only faintly detected. BAZ1B displayed a more uniform expression but like SNF2H, was also expressed at lower levels in the brain and heart and additionally the kidney when compared to other tissues. Ponceau-S staining of the membrane is shown as a control for the relatively equal loading of material as the use of any one protein as a measure of this could be biased by the diverse cellularity of these different tissues.

Since numerous studies of BAZ1A were performed in cultured human and mouse cells, I investigated the levels of detectable protein by immunoblot from equally loaded protein extracts derived from a panel of human and mouse cells. The human lines, U2OS and HeLa are cancerous cells derived from an osteosarcoma and cervical cancer respectively and were used in the studies describing roles for BAZ1A in DNA damage repair. For mouse, the B16 melanoma line and SV-40 immortalized ear fibroblasts (EFs) that I generated were used. BAZ1A, SNF2H and BAZ1B were detected in both human and mouse lines and levels were more or less uniform with slightly higher levels of BAZ1A and BAZ1B detected in HeLa cells when compared to the uniform levels of the actin loading control (Figure 1.2B). The discrepancy between the lack of detectable BAZ1A in most organ extracts versus cultured cells is likely a simple matter of the limit of detection as three-times more concentrated extracts from cultured cells could be loaded compared to whole tissue extracts but may also reflect BAZ1A levels in non-dividing tissue versus actively-dividing cultured cells.

3. Subcellular localization of BAZ1A in the testis.

Since BAZ1A is highly expressed in the testis, I examined its expression and localization in the various cell populations of the testis, which include germline cells at various stages in the spermatogenic program and somatic cells that serve to nurture the germ cells and provide other functions such as structuring the seminiferous tubules. This characterization was performed by indirect immunofluorescence on histological sections of testis with an anti-BAZ1A antibody. Because spermatogenesis progresses in semi-synchronous waves along a stretch of seminiferous tubule, sectioning the testis will bisect tubules in various states as the wave progresses. Sections of individual tubules can then be classified into 12 distinct stages based on their cellularity at the time that a snap-shot was effectively taken during wave progression (as schematized in Figure 1.3A) by way of fixing and sectioning the tissue.

A timeline for BAZ1A expression was established by examining the cells present in tubules at various epithelial stages (Figure 1.3B). BAZ1A is not detected in primary spermatocytes in the leptotene stage of prophase I of meiosis (Figure 1.3B *i,* inset) but is detected in cells slightly further along in the developmental timeline: pachytene spermatocytes, where it can be seen preferentially localizing to the densely 4',6-diamidino-2-phenylindole (DAPI) stained pericentromeric DNA, which is known to contain AT-rich heterochromatin (Figure 1.3B *ii,* inset). Targeting to the heterochromatin was supported by co-localization of BAZ1A signal with HP1β, a marker of heterochromatin (Figure 1.3B *i-iv*). Interestingly, BAZ1A was also detected in a large subnuclear domain exclusive of HP1β in mid-pachynema. At a slightly later stage of development, HP1β was then itself detected in a large domain exclusive of BAZ1A in diplotene spermatocytes (Figure 1.3B *ii* and *iii*, insets) and is likely indicative of localization to the sex body, the transcriptionally inactive domain of the X and Y chromosomes of which it is a known component (Turner et al., 2001) that is present in

50
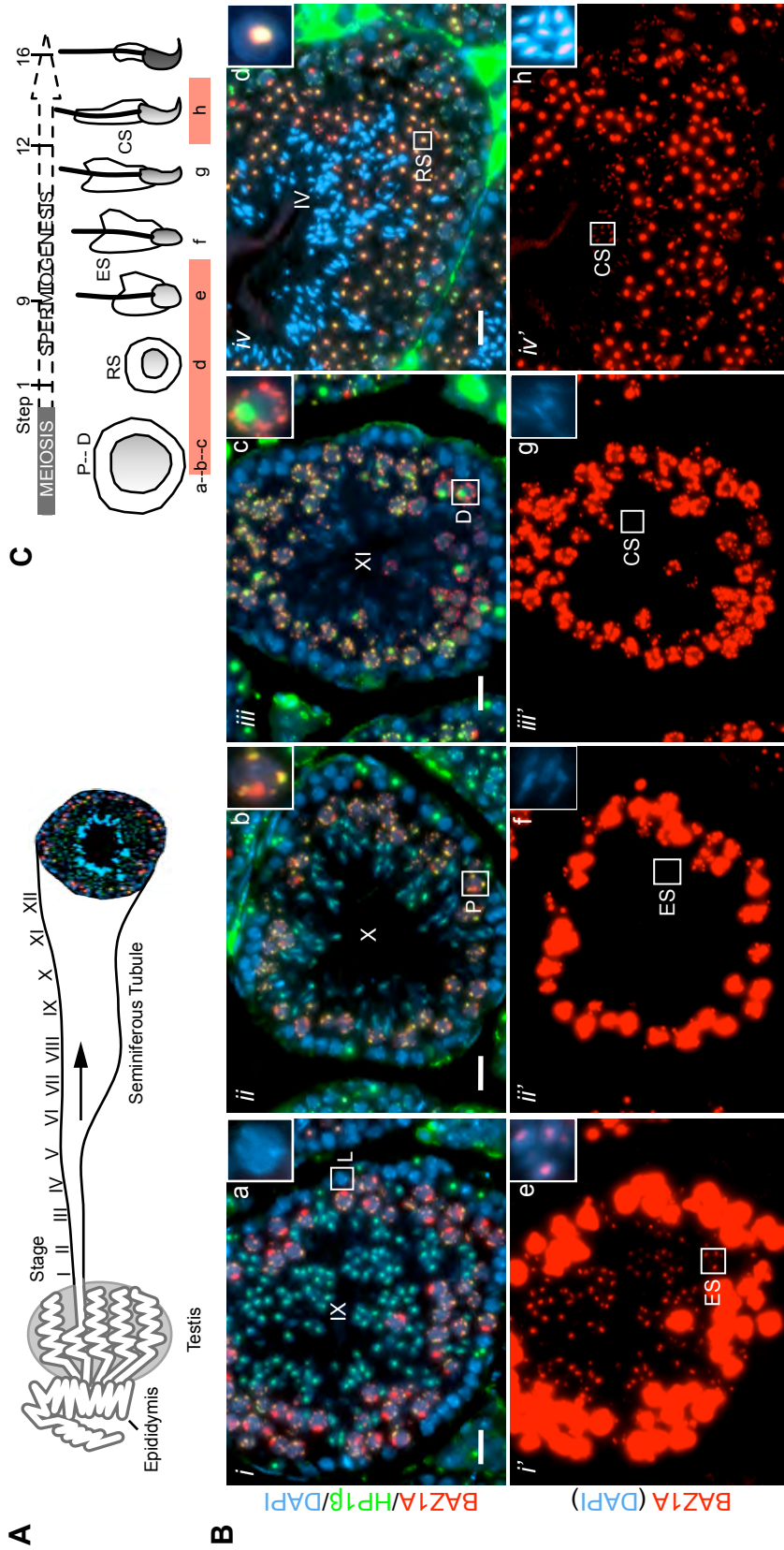
Figure 1.3. Expression and localization of BAZ1A during spermatogenesis. (A) Simple schematic illustrating anatomy of the testis. A single seminiferous tubule is enlarged with an example of a fluorescent-stained cross-section at the end. Arrow indicates the direction of the semi-synchronous wave of spermatogenesis on mouse testis sections. **(B)** Immunofluorescence on mouse testis sections. (*i-iv*) Sections were co-stained with BAZ1A and HP1β antibodies. Tubule stage is indicated in uppercase roman numerals. (*i'-iv'*) Same image as above with increased exposure of the BAZ1A (red) channel alone. Insets show magnification of the indicated cell. DAPI was included in the insets in the bottom panel to indicate nuclear shape. Lower-case letters to the left of the inset correspond to the letters below the schematic summarizing BAZ1A expression during spermatogenesis in **(C)**, with the red highlight indicating in which cell types BAZ1A was detected. L, leptotene spermatocyte; P, pachytene spermatocyte; D, diplotene spermatocyte; RS, round spermatid; ES, elongating spermatid; CS, condensing spermatid; bar = 20 μm.

51

these cells. BAZ1A is also found enriched at the heterochromatic chromocenter characteristic of round spermatids (Figiure 1.3B *iv,* inset). Because BAZ1A signal was so strong in primary spermatocytes, detection in other cells necessitated increasing the exposure and is more easily observed without the DAPI and HP1β channels (Figure 1.3B *i'-iv'*). Under these conditions, BAZ1A could also be detected in the elongating spermatids found in stage IX tubules (Figure 1.3B *i',* inset) but not in the step ~11-13 spermatids found in stage X-XI (Figure 1.3B *ii'* and *iii'*, insets). BAZ1A expression was then detected again in step ~14-15 spermatids (Figure 1.3B *iv',* inset). Figure 1.3C summarizes which cells in this developmental program BAZ1A was detected: mid-pachytene spermatocytes until ~ step 9 elongating spermatids when levels drop below detection only to be detected again in condensing, ~ step 14-15 spermatids.

4. Subnuclear and chromatin localization of BAZ1A in male germ cells.

To assess whether the large domain of BAZ1A staining seen in primary spermatocytes was indeed the sex body, I co-stained sections with antibodies against BAZ1A and γH2AX, a component of the sex body (Figure 1.4A). In a stage II-III tubule, when primary spermatocytes are in the early pachytene stage, BAZ1A cannot be detected but γH2AX stains a large domain marking the already formed sex body (arrows) and can also be seen in a stretch along the nuclei of elongating spermatids, likely do to a non-specific cross-reaction of the antibody with the acrosomal cap (Figure 1.4A *i'*). BAZ1A detection is absent from zygotene spermatocytes and the somatic Sertoli cells (Figure 1.4A *i'*). However, in a stage VIII tubule where spermatocytes have progressed to mid-pachytene, BAZ1A can be seen accumulating at distinct, DAPI-dense, heterochromatic foci and co-localizing in a large domain with γH2AX (arrows). Round spermatids are also present at this stage and anti-γH2AX antibody is again seen cross-reacting with the

B

SNF2H/BAZ1A/DAPI

A

BAZ1A/γH2AX/DAPI
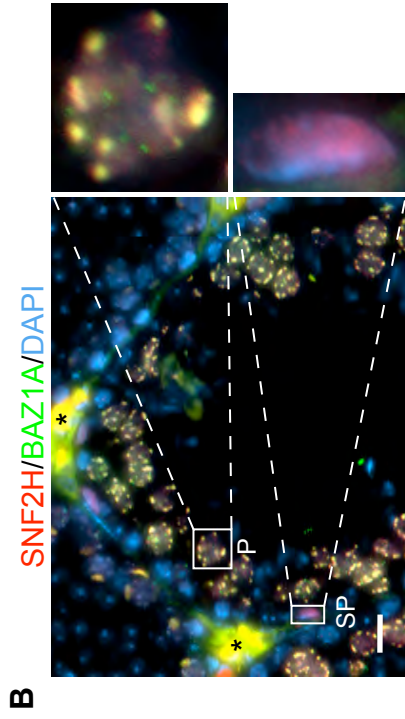
Figure 1.4. BAZ1A is detected in the sex-body and co-localizes with SNF2H. (A) Immunofluorescence of testis sections with BAZ1A and γH2AX antibodies. (*i-iii*) Testis sections at various substages (indicated by uppercase roman numerals). Bar = 20 μm. (*i'-iii'*) Magnification of area indicated in left panel. Bar = 10 μm. Arrows point to the sexbody. ES, elongating spermatid; RS, round spermatid; Z, zygotene spermatocyte; EP, early pachytene spermatocyte; S, Sertoli cell; P, pachytene spermatocyte; L, leptotene spermatocyte; M, peritubular myoid cell; D, diplotene spermatocyte. **(B)** Immunofluorescence of testis sections with BAZ1A and SNF2H antibodies. Magnification of the indicated cells are shown. SP, spermatogonia; *autofluorescent red blood cells; bar = 20 μm.

53
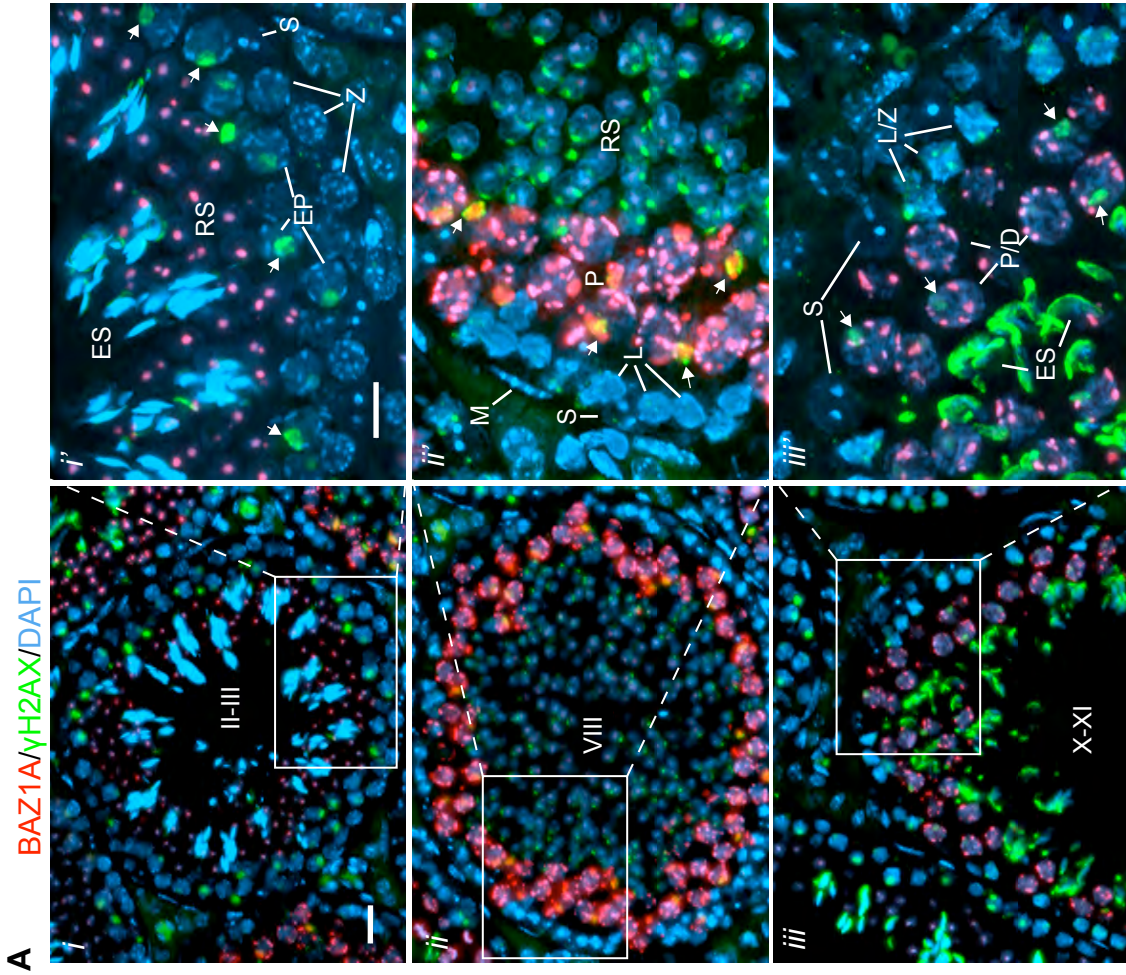
acrosomal granule that has begun forming in these cells (Figure 1.4A *ii'*). BAZ1A cannot be detected in leptotene spermatocytes in this tubule section or the somatic peritubular myoid cells surrounding the seminiferous tubules (Figure 1.4A *ii'*), but is detected in the chromocenter of the round spermatids when the exposure is increased as was shown above (data not shown). Interestingly, when primary spermatocytes have reached diplonema in a stage X-XI tubule, γH2AX is still detected in the sex body while BAZ1A no longer is (arrows), highlighting a dynamic localization pattern that localizes BAZ1A to the sex body after it has already formed and then disfavors its accumulation there just before the end of meiosis I. This pattern cannot be simply explained by a decrease in expression as BAZ1A is still readily detected co-localizing with DAPI-dense heterochromatic foci in these same cells (Figure 1.4A *iii'*). As shown above, BAZ1A is not detectable in leptotene/zygotene spermatocytes where γH2AX displays a punctate pattern, which is consistent with the known role of γH2AX in the repair of DNA double-strand breaks that form at this stage to initiate meiotic recombination (Figure 1.4A *iii'*). Once again, anti-γH2AX antibody can also be detected on the acrosomal cap that has stretched further over the step 10-11 elongating spermatids in this stage X-XI tubule, again, probably due to cross-reaction (Figure 1.4A *iii'*).

To ask whether BAZ1A co-localized with its other ACF complex component SNF2H, testis sections were co-stained with antibodies against both of these proteins. Indeed, there is almost a complete overlap in BAZ1A and SNF2H as indicated by the yellow signal that results from the overlapping red and green channels on the pericentromeric heterochromatin in pachytene spermatocytes (Figure 1.4B, top magnification), suggesting that the ACF complex forms in these cells. Interestingly, SNF2H was also detected in spermatogonia in the absence of BAZ1A (Figure 1.4B, bottom magnification).

Independent confirmation of the temporal expression and localization of BAZ1A in primary spermatocytes was performed by immunostaining squash preparations of nuclei from these cells, a technique which leaves nuclei partially extracted. In this experiment, cells were staged by staining for the axial element component SYCP3 and analyzing formation of the synaptonemal complex that defines the four cytological stages of prophase I. Consistent with the histological staining patterns, BAZ1A is largely absent in leptotene and zygotene nuclei. It is first detected in mid-to-late pachynema localizing to the sex body (arrows) and beginning to accumulate at heterochromatic foci (Figure 1.5A). It is then seen highly enriched at heterochromatic foci in diplotene cells and diffusely on the chromatin but no longer enriched in the sex body (arrows in Figure 1.5A). Spread preparations of spermatocyte nuclei, which are more extensively extracted and therefore mainly report on chromatin-bound proteins, showed a similar staining pattern, with BAZ1A accumulating in a more punctate fashion in the sex body (arrows) and diffusely on the chromatin during late pachynema. Consistent with the squash nuclei stains, BAZ1A can then be seen excluded from the sex body (arrows), in effect outlining the boundaries of this domain with high levels of diffuse BAZ1A staining on autosomal chromatin and exclusive absence from the sex chromatin (Figure 1.5B).

IV. Discussion

Characterization of *Baz1a* mRNA and protein expression in the mouse revealed interesting tissue and cell-type specific patterns as well as specific temporal expression. These results foreshadow the previously unrealized *in vivo* roles for this chromatin remodeling factor in the mouse described in the following chapter.
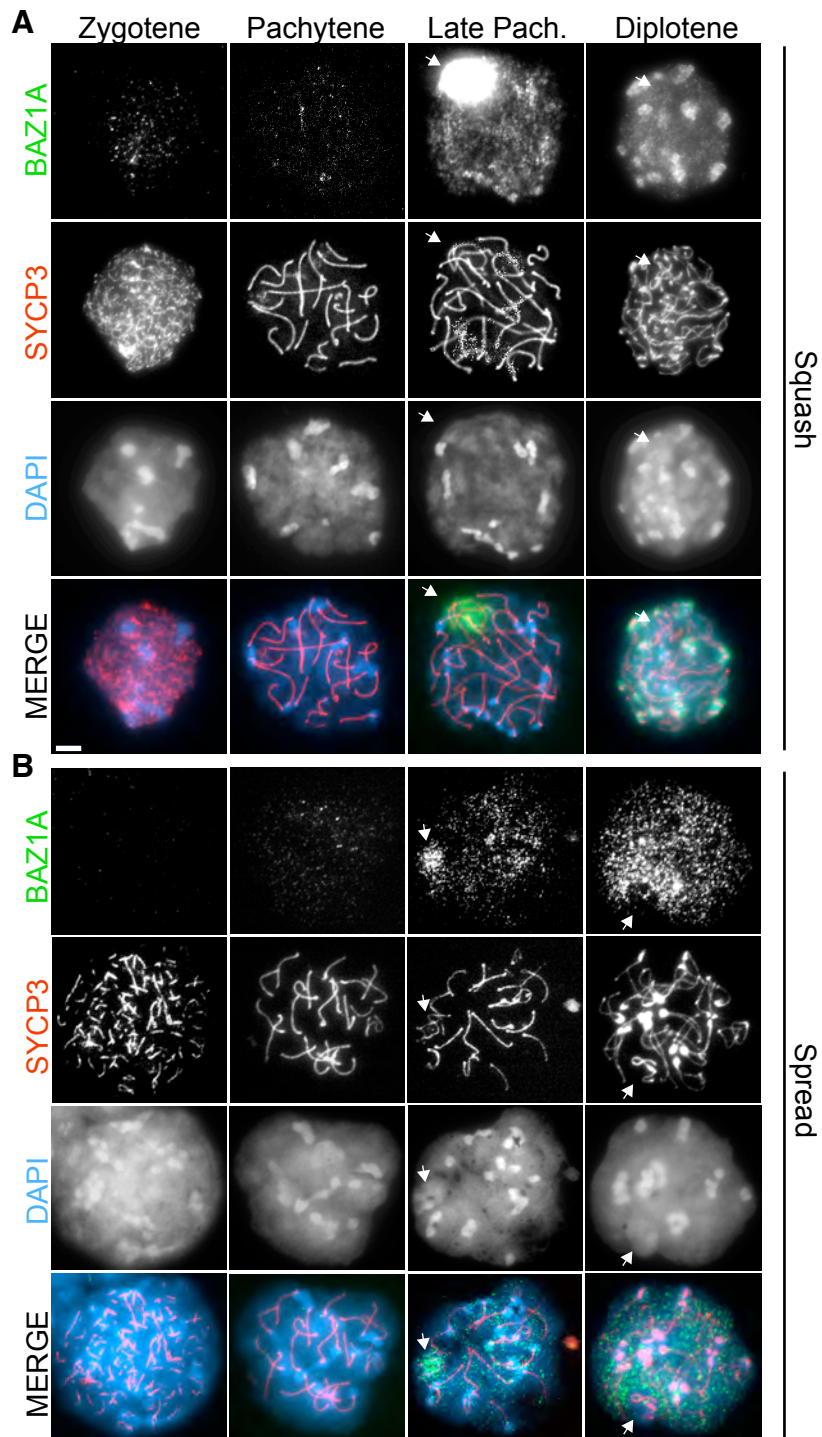
Figure 1.5. BAZ1A subnuclear and chromatin localization. (**A**-**B**) Immunofluorescence for BAZ1A on squashed spermatocyte nuclei (**A**) and spread spermatocyte nuclei (**B**) at different stages of prophase I of meiosis as indicated by accumulation of the synaptonemal complex component SYCP3. Arrows point to the sexbody. Bar = 5 µm.

1. Are the BAZ1A splice isoforms biologically relevant?

High levels of alternative splicing is found in tissues in which extensive developmental programs are known to occur, including the thymus where T-cells develop and differentiate and the testis, where spermatogenesis is ongoing (Elliott and Grellscheid, 2006); however, rarely have distinct functional roles for splice isoforms been reported. A notable exception is the recent report of a transgenic mouse expressing only one of the two major splice isoforms of SPO11—the topoisomerase-like protein that generates DSBs to induce meiotic recombination—that displays a dramatic defect in recombination of the X and Y chromosomes, resulting in sterility for the majority of mutant males (Kauppi et al., 2011).

Alternative splicing may be productive, adding to the diversity of protein products in the testis; however, it is equally plausible that splicing errors are for some reason inherently more frequent in the testis, leading to the production of irrelevant alternative transcripts. Some interesting experimental evidence relating to this phenomenon was the observation that levels of the otherwise ubiquitously expressed splicing repressor hnRNPA1 are reduced from meiosis onwards during spermatogenesis (Kamma et al., 1995), suggesting this may be one factor contributing to the increased alternative splicing observed in the testis.

Sequencing revealed three alternative splice events in the *Baz1a* transcript, one of which comprised the majority of detected message in the testis and kidney and one which appeared ubiquitous. There does not appear to be an obvious anatomical connection between the kidney and testis that might explain why higher levels of alternative transcripts are exclusive to these organs as they are not known to share any biological process. However, it could simply be a coincidence due to down-regulation of a mutual factor involved in splicing in these organs.

Potentially also coincidental, it is interesting that these splice events are first detected when the first primary spermatocytes should have reached the middle of pachynema, the same stage at which BAZ1A protein was also first detected. If the alternative transcripts are more stable or preferentially translated, this could explain the correlation with protein expression. However, it is equally possible that translational controls restrict BAZ1A protein expression to this particular stage and that protein levels are not coupled with the production of alternative transcripts.

Translation of splice variants lacking exon 13 would delete a stretch of amino acids adjacent to the DDT domain, which is a putative DNA binding domain (Doerks et al., 2001). The deleted peptide sequence is predicted to have a net negative charge of five owing to the presence of six acidic residues in this sequence. It is tempting to speculate that a deletion like this adjacent to this domain might alter or modulate its function, potentially increasing the domains binding affinity to nucleic acids by deleting this local negative charge.

Inclusion of the cassette exon downstream of exon 22 would insert a highly basic peptide sequence adjacent to the histone binding PHD-finger domain of BAZ1A. If this alternative transcript is translated into a stable protein, this local charge increase might potentially reduce the affinity of the PHD-finger for positively charged histones.

The third alternative splicing event (5' extension of exon 15) was ubiquitous and the only one to shift the reading frame, which would potentially result in the production of a truncated protein lacking the PHD-finger domain and acetyl-lysine binding bromodomain. Since this isoform would still contain the SNF2H interacting region (Collins et al., 2002), it could compete for binding with the full-length protein, possibly sequestering SNF2H into non-functional complexes or complexes with altered function or prevent the formation of other SNF2H containing complexes. One potential way to test these predictions would be to express the splice isoforms in cultured cells in which

58

endogenous *Baz1a* has been deleted and assay for changes in ACF or CHRAC dependent functions such as such as nucleosome spacing. Another strategy would be to purify ACF/CHRAC complexes containing the different splice isoforms to assay for a change in their chromatin remodeling abilities using *in vitro* assays*.*

2. BAZ1A expression varies widely despite reported roles in ubiquitous cellular processes.

It seems logical to predict that if BAZ1A is involved in the numerous cellular processes in which it has been implicated that protein levels would be relatively equal in cells from different tissues. In contrast, BAZ1A is highly expressed in the testis and almost undetectable in other organs. However, BAZ1A was readily detected in extracts of cultured cells and so it is detectable in tissues other than the testis albeit at much lower levels. This discrepancy could indicate that BAZ1A is not required in other tissues due to compensatory mechanisms, potentially provided by its numerous paralogs. Indeed, the closely related paralog BAZ1B was detected at much more uniform levels in an array of tissues. This idea is also supported by the fact that in flies where *Acf1* paralogs have not been detected, *Acf1* deletion is semi-lethal suggesting weaker compensatory mechanisms might exist in this species. Another possibility is that BAZ1A levels do not correlate with function and that the protein is present and functional at undetectable levels in other tissues. However, as reported in chapter 2, *Baz1a* deletion does not have an effect on the development of any organ other than the testis and so even if it is expressed at undetectable levels, it would appear to be dispensable.

3. Do BAZ1A expression and localization patterns in the testis predict function?

Focusing on the subcellular localization of BAZ1A in the testis revealed an intriguing spatiotemporal expression pattern. It is first detectable at the mid-pachytene stage and

can be seen preferentially accumulating at heterochromatic foci. This timing coincides with a stage of meiosis during which the majority of DSBs that form to initiate recombination have been repaired and homologous chromosomes have fully synapsed along the length of their axes. It also coincides with the stage of spermatogenesis in which canonical histones begin to be replaced by histone variants. The heterochromatin targeting was not completely unexpected, as this has been previously reported in cultured cells (Tate et al., 1998); however, it has also been reported that BAZ1A may aid in the formation of heterochromatin and subsequently facilitate replication through heterochromatic DNA (Collins et al., 2002). If this heterochromatin localization points to a function of BAZ1A in spermatocytes, a role during replication can be ruled out as this process has long since ceased at this stage of spermatogenesis. Moreover, DAPI-dense heterochromatic foci are visible in cells prior to BAZ1A detection and so it seems unlikely that it is necessary for proper heterochromatin formation, which was indeed unpertubed in *Baz1a*$^{-/-}$ spermatocytes (see chapter 2).

Localization to the sex body showed a very specific temporal pattern, appearing after formation of this subnuclear domain and disappearing prior to the end of meiosis. As the sex body is a transcriptionally inactive domain of the X and Y chromosomes, it is tempting to speculate that BAZ1A might play a role in this process as it has been previously shown to be involved in transcriptional silencing in other cellular contexts (Ewing et al., 2007; Liu et al., 2008; Yasui et al., 2002). Nevertheless, expression profiling of *Baz1a* mutant spermatocytes did not indicate sex chromosome reactivation, arguing against a role for *Baz1a* in their silencing (see chapter 2). Interestingly, The timing of BAZ1A localization to the sex body coincides with removal of the histone H3 variant H3.1 and its replacement by H3.3 (van der Heijden et al., 2007), although a gross disruption in the loading of H3.3 onto chromatin was not observed in the absence of *Baz1a* (see chapter 2).

Intriguingly, BAZ1A detection ceases as spermatids begin to elongate, coincident with replacement of the histones by the transition proteins and then reappears when spermatids have almost fully condensed into mature sperm at a time when the protamines replace the transition proteins. These parallel events but might also indicate that BAZ1A is somehow involved in these remodeling events. However, as detailed in chapter 2, an investigation of spermatogenesis in $Baz1a^{-/-}$ mice did not indicate a gross defect during the histone to protamine exchange.

Lastly, BAZ1A was found to co-localize with SNF2H in spermatocytes, suggesting that BAZ1A is functioning in the context of the ACF complex. This is the first evidence that this complex may form in the mouse although this was predicted from its conservation in both flies and humans (Ito et al., 1997; LeRoy et al., 2000). SNF2H could also be detected without BAZ1A in spermatogonia, suggesting it may serve multiple roles during spermatogenesis. Indeed, SNF2H was recently detected bound to the BAZ1A paralog CECR2 in spermatogonia. Mice lacking $Cecr2$ display reduced male fertility (Thompson et al., 2012). CECR2 expression was mainly restricted to spermatogonia, suggesting that mutually exclusive expression of accessory subunits might modulate SNF2H by forming distinct complexes at different stages of spermatogenesis.

CHAPTER 2. ACF/CHRAC COMPLEXES ARE REQUIRED FOR PROPER SPERMIOGENESIS.

I. Summary

To investigate the *in vivo* function of *Baz1a*, I used gene-targeting to generate a mutant conditional allele that would prevent production of the protein product during mouse development. As reported in this chapter, *Baz1a* was not required for embryonic development. However, homozygous mutant males were sterile due to a severe defect in spermiogenesis that results in fewer and non-motile sperm with morphological defects. For the most part, the unique changes in chromatin structure that occur during spermatogenesis appeared normal in the mutants although a slight reduction in the levels of mature PRM2 was observed. Strikingly, expression profiling revealed a wide-spread transcriptional perturbation in spermatocytes and round-spermatids that likely causes the observed defects.

II. Background

The BAZ1A protein expression and localization analysis presented in the previous chapter suggests that mammals might have evolved with tissue-specific requirements for this chromatin remodeling factor. The majority of *Acf1* mutant flies do not make it past the larval to pupal transition, suggesting a strong requirement during the development of this organism (Chioda et al., 2010; Fyodorov et al., 2004). However, the presence of numerous *Baz1a* paralogs in mice that are not detected in flies raises the possibility that deletion of this factor during mouse development may result in different consequences.

II. Results

1. Targeted disruption of the *Baz1a* locus.

I reasoned that *Baz1a* might be essential for development given its reported role in so many diverse cellular processes and semi-lethality in mutant flies. So, I chose to use a conditional knock-out strategy to generate a null allele. The mouse *Baz1a* gene, located on chromosome 12, comprises 27 exons. *LoxP* sites were inserted on either side of exon 6 (Figure 2.1); deleting this exon creates a frame-shift and introduces a premature termination codon 25 nucleotides downstream. If this transcript were translated, it would produce a truncated protein product containing the N-terminal WAC domain but lacking the SNF2H interacting region, DDT, PHD and bromo- domains. This construct was introduced into ES cells and successful targeting was confirmed by Southern blot (Figure 5). To delete *Baz1a*, *Baz1a^flox^* mice were crossed to a transgenic line expressing Cre recombinase under the control of the *Stra8* promoter (Sadate-Ngatchou et al., 2008), which is specifically expressed in the male germline. Recombination of *loxP* sites was confirmed by PCR on tail DNA (Figure 2.1B). Males heterozygous for the deletion in their germline were fertile and were bred to generate mice fully nullizygous (null) for *Baz1a* (*Baz1a^-/-^*). Immunoprecipitation (IP) of whole testis extracts with an anti-BAZ1A antibody followed by immunoblot (Figure 2.1C) and immunostaining (Figure 2.1D) of testis sections from *Baz1a^-/-^* mice indicated absence of detectable protein; this and other evidence discussed below (Figure 2.5) suggests this is a null allele.

2. *Baz1a*-deficient mice are viable but display male sterility.

Contrary to the initial expectation, *Baz1a^-/-^* mice were viable and the proportions of wild-type (95/363, 26%), heterozygous (186/363, 51%) and nullizygous (82/363, 23%) offspring did not deviate significantly from the expected Mendelian pattern of inheritance.

63
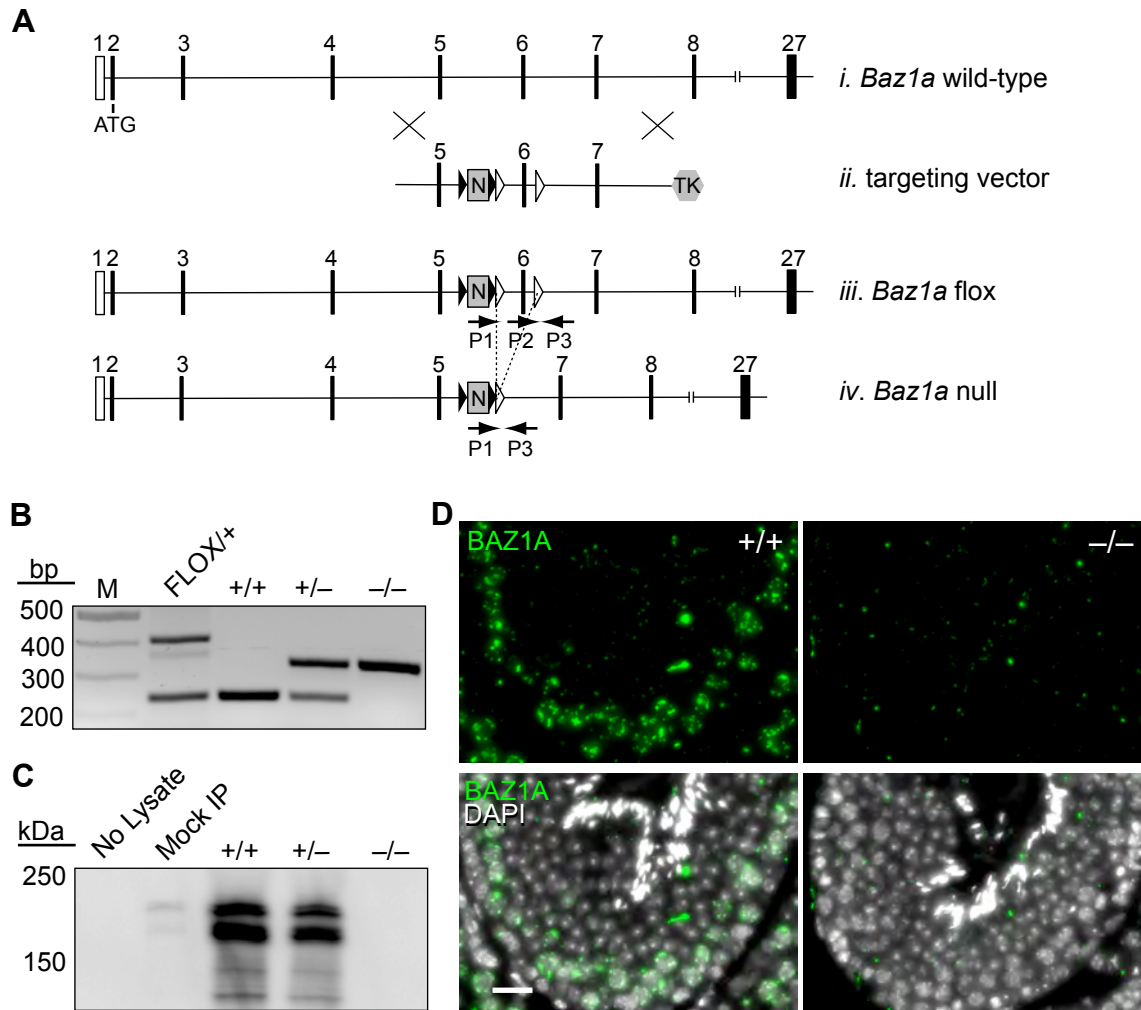
Figure 2.1. Generation of *Baz1a*-deficient mice. (**A**) Schematic representation of the strategy used to generate a conditional allele of *Baz1a.* (*i*) Partial *Baz1a* genomic locus. (*ii*) Map of the targeting vector. (*iii*) Targeted conditional allele. (*iv*) Null allele following Cre-mediated recombination of the *loxP* sites (open triangles) flanking exon 6. Black triangles, FRT sites; N, *pgk-neo*; TK, *hsv*-thymidine kinase; P2 and P3, primers used to amplify wild-type and flox allele; P1 and P3, primers used to amplify the null allele. Not to scale. (**B**) PCR genotyping of tail DNA from the wild-type (+/+), floxed (FLOX) and null (–/–) alleles. M, marker. (**C**) Immunoblotting of BAZ1A immuno-precipitated from whole testis lysates from wild-type (+/+), heterozygous (+/–) and homozygous (–/–) mutant mice. Mock IP, no antibody; No Lysate, IP from lysis buffer alone. (**D**) Immunofluorescence with anti-BAZ1A antibody on testis sections from wild-type and mutant mice. Bar = 20 μm.

Homozygous null females were fertile (n=4; average litter size= 8.8±1.9) and a gross histo-pathological examination of all major organs revealed no abnormalities (data not shown) with the exception of the testis, which is presented in more depth later. To assess male fertility, 15 homozygous null males were bred with wild-type females for 8 weeks and failed to produce a single pup despite the presence of plugs, which indicated that copulation was unaffected.

3. Spermiogenesis is severely impaired in the absence of *Baz1a*

To further investigate the infertility phenotype of *Baz1a*$^{-/-}$ males, a histo-pathological analysis was performed. Sperm from the epididymides of mutant mice displayed an array of aberrant head morphologies, a pathology termed teratospermia (Figure 2.2A). Epididymal sperm also had numerous tail abnormalities (Figure 2.2B) including a frequently observed narrowing of the annulus (arrows in *ii* & *v*), which is an electron-dense ring-domain that separates the principal piece of the tail from the midpiece. Sperm were also observed with: heads folded back against the tail (*iii*), two tails (*iv*), midpieces folded back against the tail (*v*), and coiling of the tail around the head (*vi*). There was a 5-fold reduction in total sperm (termed oligospermia) and an almost complete absence of motile sperm (termed asthenospermia) (Figure 2.2C and D), with the exception of a few twitching movements that did not support forward progression (data not shown). Sections of mutant caput epididymides showed a complete absence of mature sperm in the lumen of tubules in this organ in contrast to wild-type, which displayed lumens packed with mature sperm (Figure 2.2E and F). High magnification images of sections of cauda epididymides revealed a collection of debris and degenerating, mostly round cells that likely sloughed from the testis in the mutant while, in contrast, darkly stained sperm heads with their characteristic hook and tangles of lightly stained tails were visible in the wild-type organ (Figure 2.2G and H).
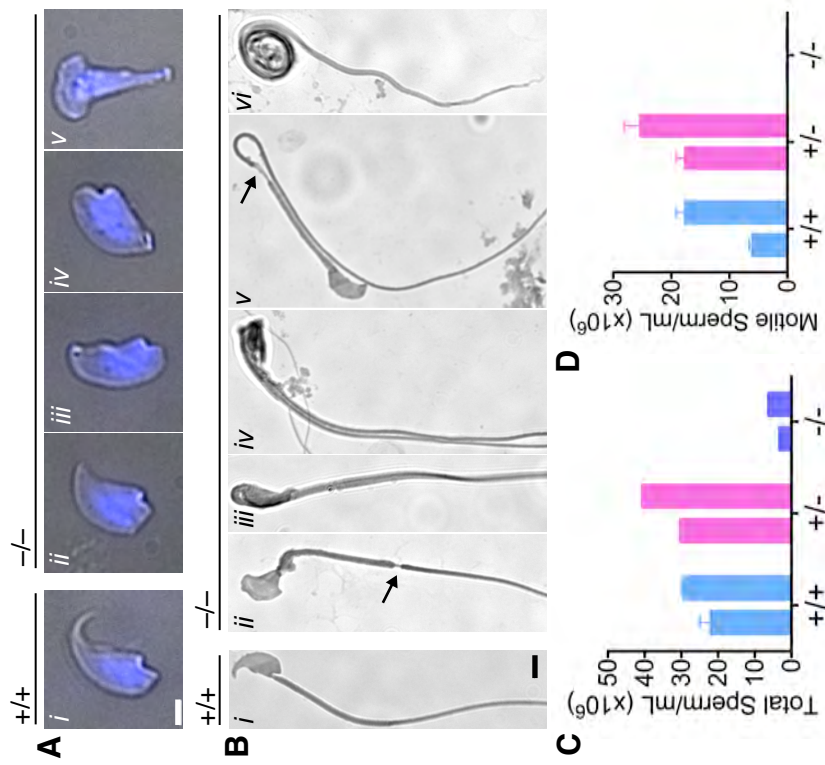
Figure 2.2. *Baz1a* mutant sperm are reduced in number and display a wide range of morphological defects. (**A**) Bright field microscopy of wild-type (*i*) or mutant (*ii-v*) sperm heads overlaid with DAPI fluorescence (blue). Bar = 2 μm. (**B**) Bright field microscopy of wild-type (*i*) or mutant (*ii-vi*) sperm with tails attached. Arrows point to a narrowing between the mid- and principal piece. Bar = 5 μm. (**C-D**) Total (**C**) and motile (**D**) epididymal sperm counts from 2 mice of each genotype (individual bars) counted in triplicate. Bars, mean ± s.d. (**E-H**) Hematoxylin and eosin stained sections of wild-type (**E&G**) and mutant (**F&H**) caput (**E&F**) and cauda (**G&H**) epididymides. Bar = 20 μm.

66

One aberration observed in mutant testis was the high frequency of multi-nucleate cells (arrows in Figure 2.3A-*i*), on average, two per mutant seminiferous tubule section (Figure 2.3B). The presence of multi-nucleate cells was confirmed by electron microscopy on testis sections where both bi-nucleate round spermatids (Figure 2.3E) and bi-nucleate elongating spermatids, often with a single acrosome stretching over both nuclei (arrows in Figure 2.3F) were detected. Larger-than-average *Baz1a*$^{-/-}$ round spermatids (identified by their darkly staining chromocenter and developing acrosome) were also occasionally observed (magnification in Figure 2.3A-*i*); such large round spermatids have been shown to correlate to a diploid rather than the normal haploid DNA content (de Boer et al., 1986). Fluorescence in situ hybridization with X, Y and chromosome 19 probes on squash preparations of mutant round spermatid nuclei (Figure 2.3 A *ii-iv*) supported this interpretation as a larger nucleus (arrow, judged to be a round spermatid based on its prominent chromocenter) was found to contain 2 autosome signals and both X and Y signals while smaller nuclei contained only 1 autosome signal and either an X or Y signal. However, it should be noted that cells found to be diploid in the FISH analysis was extremely rare compared to the number of larger than average round spermatids observed in testis sections. One possibility is that these cells are more prone to lyse during the squash preparation of nuclei, reducing the number of detectable cells. It is also possible that the majority of larger round spermatids observed in mutant testis sections are in fact not diploid, however. Taken together, these observations indicate that in the absence of *Baz1a*, the highly ordered sperm developmental program is thrown off course, resulting in a range of aberrations.

Testis sections from *Baz1a*$^{-/-}$ mice also displayed a modest but significant (P<0.0001, t-test) increase in the average number of apoptotic cells per tubule and a three-fold increase in the percentage of mutant tubule sections with one or more apoptotic cells (Figure 2.4A-D). Interestingly, this increased apoptosis did not appear

Figure 2.3. Spermatogenesis is abnormal in the absence of *Baz1a.* (**A**-*i*,**C**&**D**) Periodic acid-Schiff and hematoxylin stained sections of wild-type (**C**) and mutant (**A**&**D**) testis. (**A**) (*i.*) Multi-nucleate round spermatids (white arrows) and large, diploid round spermatid (magnified region, black arrow). (*ii-iv.*) Fluorescent *in situ* hybridization on squash preparations of round-spermatids with chromosome X (red), Y (green) and 19 (red) probes. White arrow points to diploid cell. Bar = 5 µm. (**B**) Quantification of the number of multi-nucleate cells per tubule in wild-type versus mutant testis (**P<0.0001, t-test) Bars, mean ± s.d. (**C**&**D**) Stage IX seminiferous tubules showing a spermiation failure in the mutant. (**E**&**F**) Transmission electron microscopy of mutant testis sections showing a multi-nucleate round spermatid (**E**) and elongating spermatids (**F**). Arrows point to the boundaries of where acrosome stretching has reached. N, nucleus; V, vacuole; bar = 2 µm.

Figure 2.4. Increased apoptosis in *Baz1a* mutant testis.
(**A**&**B**) TUNEL staining of wild-type (**A**) and mutant (**B**) testis
sections. Bar = 20 μm. (**C**&**D**) Quantification of TUNEL
positive cells per tubule (**C**) (**P<0.0001, t-test) and percent-
age of tubules with ≥ 1 TUNEL positive cell per tubule (**D**)
(**P<0.0001, Fisher's exact test) from wild-type and mutant
mice. Bars, mean± s.d.

restricted to any particular cell-type and is unlikely to account for the dramatic decrease in mature spermatozoa or the morphological defects present in the mutant.

4. *Baz1a* is dispensable for gross chromatin dynamics associated with spermatogenesis.

Since *Baz1a* is a chromatin-remodeling factor, I hypothesized that it may play a direct role in the dramatic chromatin makeover that occurs during spermatogenesis and, if absent, cause a disruption that could explain the observed failure in spermiogenesis. To test this, I looked at one of the initial steps: the exchange of somatic histones for testis-specific histone variants. Cellular fractionation of whole testis from wild-type and *Baz1a*$^{-/-}$ mice followed by immunoblotting for various histone variants indicated that those examined were expressed and present in the enriched, chromatin-bound fraction (Figure 2.5A). Although the improper loading of other untested histone variants cannot be ruled out, these findings indicate that *Baz1a*-deficiency does not cause a global disruption in this process.

Following incorporation of histone variants, the N-terminal lysines of histone H4 are hyper-acetylated, which is thought to make the chromatin more accessible to aid in the histone-to-protamine exchange that follows (Awe and Renkawitz-Pohl, 2010; Hazzouri et al., 2000; Oliva et al., 1987). Immunostaining of wild-type and mutant testis sections revealed a strong signal in the lumen-proximal elongating spermatids from both genotypes, suggesting that this pattern of hyper-acetylation was also unperturbed in the mutant (Figure 2.5B).

Next, I looked at the expression of the transition proteins (TP1 and 2) and protamines (PRM1 and 2), which are loaded onto chromatin following histone removal to allow for the tight compaction of chromatin in the mature sperm. These highly basic proteins were extracted using hydrochloric acid from sonication sensitive and resistant
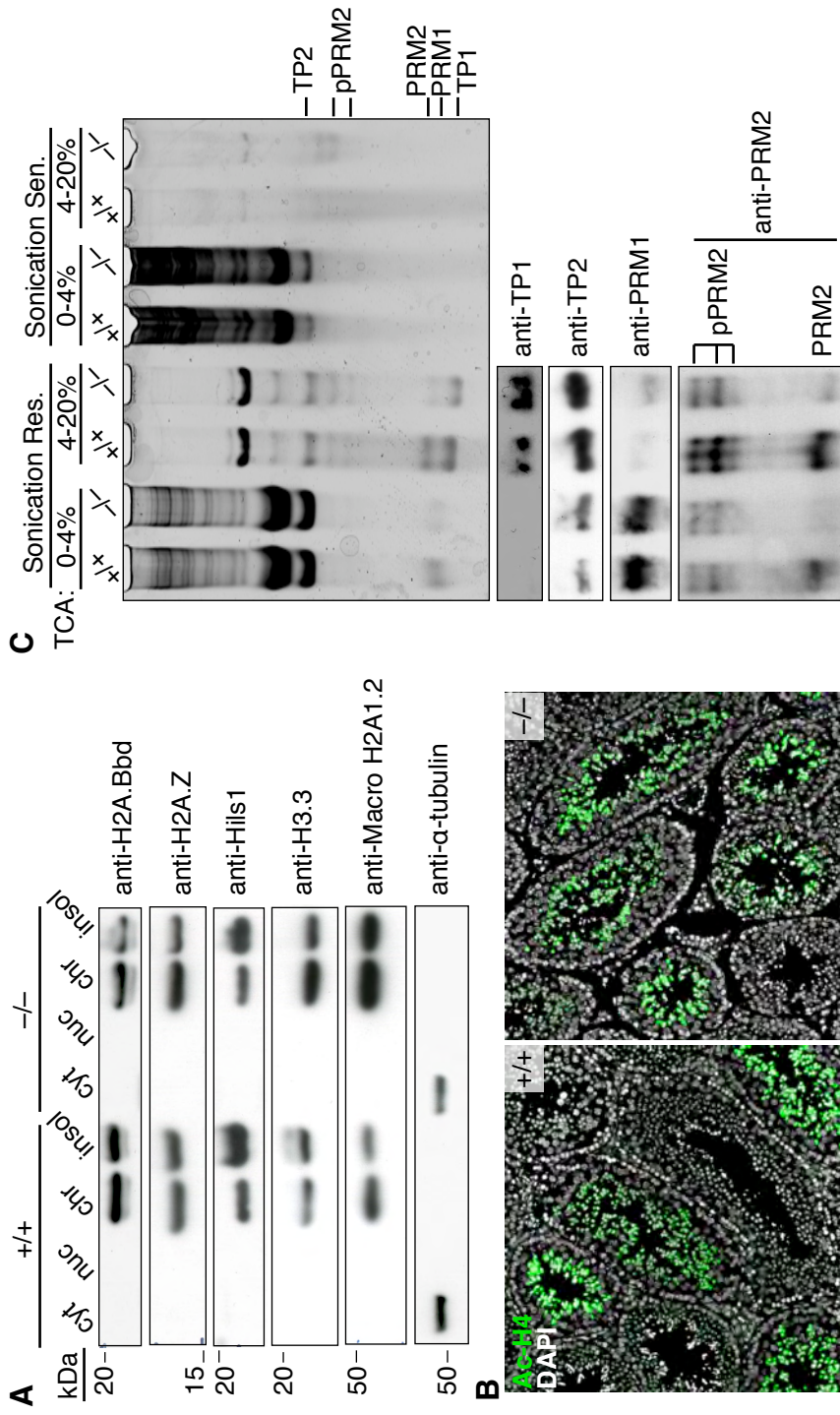
Figure 2.5. *Baz1a* is not essential for spermatogenesis associated chromatin dynamics. (A) Testes from wild-type and mutant mice were fractionated into cytoplasmic (cyt), nucleoplasmic (nuc), chromatin bound (chr) and insoluble (insol) enriched extracts and were immunoblotted for a panel of testis-specific histone variants. α-tubulin serves as a cytoplasmic marker. (**B**) Immunofluorescence on testis sections from wild-type and mutant mice with anti-acetyl histone H4 (Ac-H4) antibody. Bar = 50 μm. (**C**) Hydrochloric acid extracted proteins from sonication resistant (Res.) and sensitive (Sen.) spermatids were precipitated with 4% and then 20% trichloroacetic acid (TCA), separated by acid/urea PAGE and stained with Coomassie (top panel). A duplicate gel was used for western blotting with antibodies against transition protein 1 (TP1), transition protein 2 (TP2), protamine 1 (PRM1) and protamine 2 (PRM2) (bottom panels). pPRM2, pre-protamine 2.

71

spermatids. Because of their extreme compaction, late stage spermatids are immune to disruption by sonication. Following precipitation with trichloroacetic acid (TCA), fractions were separated by acid-urea polyacrylamide gel electrophoresis. Coomassie staining revealed bands from the sonication resistant spermatids corresponding to the expected migration of all four of these proteins and the higher molecular weight precursors of PRM2 (pPRM2), which are proteolytically cleaved to yield the mature form (Figure 2.5C, top panel). PRM1 is less soluble in TCA and is therefore detected in the 0-4% cut while the other proteins are detected in the 4-20% TCA cut. These bands are almost undetectable in the sonication sensitive extracts, providing further evidence for their identity as these proteins are only expected to be present in sonication resistant, late stage spermatids. Immunoblotting confirmed the identity of the bands and revealed a decrease in the levels of mature PRM2 from mutant sonication resistant spermatids when compared to wild-type (Figure 2.5C, bottom panels). As pPRM2 levels seemed unperturbed in the mutant, it is possible that there is a defect in the processing of pPRM2 that leads to observed decrease of its mature form. Alternatively, this reduction may be a secondary consequence of a loss of developing spermatids specifically at the step of PRM2 cleavage (step 13-15).

5. The ACF/CHRAC complexes require *Baz1a* for their formation and localization.

The expression analysis provided evidence to suggest that the ACF complex forms in mouse (Figure 1.4B). Therefore, localization of the other component of the complex, SNF2H was investigated in the absence of BAZ1A. As shown in Figure 2.6B, SNF2H, which normally localizes to the DAPI-dense pericentromeric heterochromatin in primary spermatocytes, is now found diffusely throughout the nucleus, further confirming the mutant is defective for *Baz1a* function. Similarly, one of the small histone-fold protein components of the CHRAC complex, CHRAC17, also fails to accumulate at DAPI-dense

regions (Figure 2.6C). Various commercial antibodies directed against CHRAC15 failed to detect a signal (data not shown); however, like CHRAC17, it too has been shown to bind BAZ1A and so a similar result is to be expected. These results were confirmed by co-IP experiments from whole testis extracts. CHRAC17 is able to co-IP SNF2H in the presence but not absence of BAZ1A or antibody (mock) (Figure 2.6D). CHRAC17 was not detected in a SNF2H IP, which is consistent with the idea that CHRAC15/17 bind directly to BAZ1A in the CHRAC complex (Hartlepp et al., 2005). Together, these results suggest a targeting function for BAZ1A, perhaps mediated by the heterochromatin targeting WAC domain (Fyodorov and Kadonaga, 2002).

6. Heterochromatin formation appears normal in the absence of BAZ1A.

As *Baz1a* was previously shown to play a role in the formation of heterochromatin in flies (Eskeland et al., 2007; Chioda et al., 2010), I asked whether heterochromatin formation during spermatogenesis was disrupted in its absence. There was not an appreciable difference in the levels of staining of the heterochromatin markers HP1β, HP1γ or H3K9Me3 in primary spermatocytes in the absence of BAZ1A, suggesting that this protein is likely dispensable for heterochromatin formation in mice (Figure 2.7).

7. *Baz1a* depletion leads to a widespread transcriptional disruption in spermatids.

The protein expression and localization analysis presented in the previous chapter revealed that BAZ1A is first detected at the pachytene stage of spermatogenesis (Figure 1.3B). Intriguingly, this correlates with the expression of a class of testis-specific micro-RNAs with unknown function: the MIWI bound pachytene-piRNAs. It stands to reason that the temporal expression of this class of small RNAs could suggest a role in the regulation of genes required during the spermiogenic program and, if misregulated in the absence of *Baz1a*, lead to the observed phenotype. MIWI bound RNA was recovered by
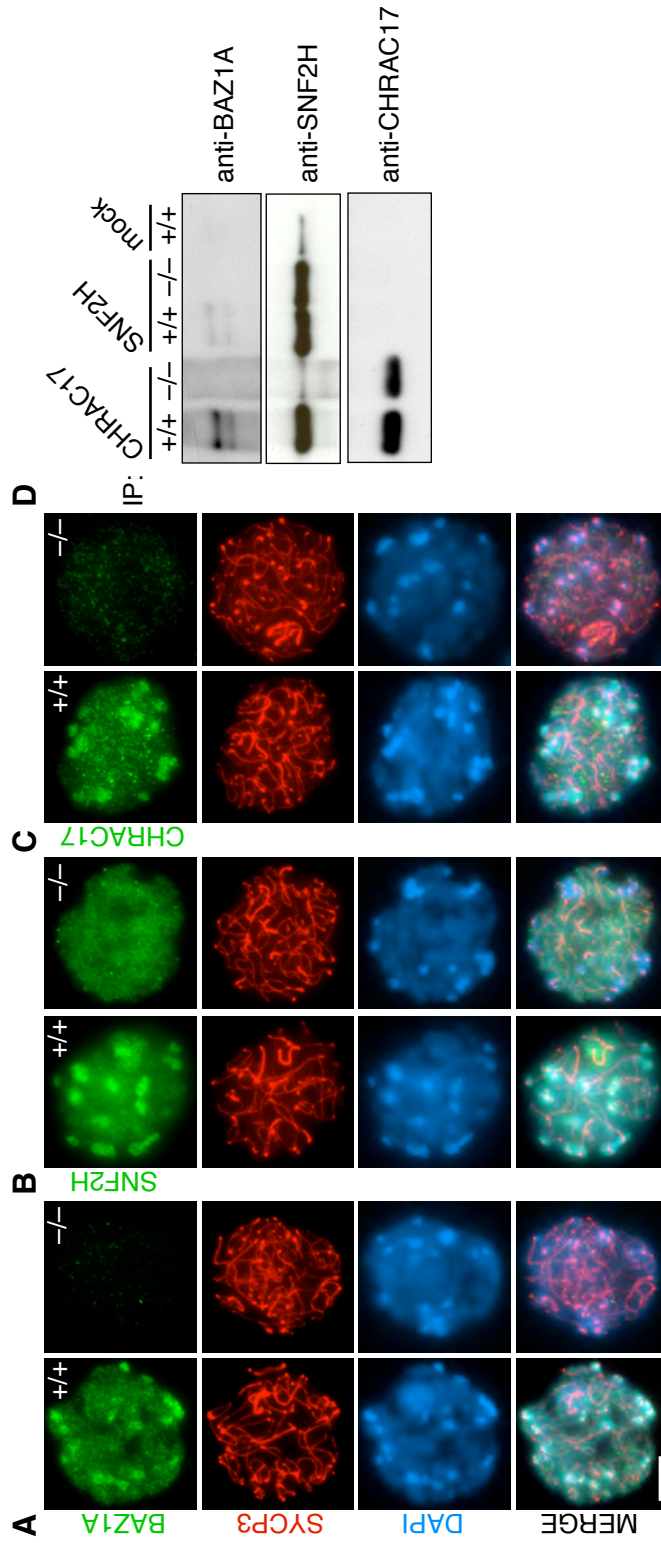
Figure 2.6. CHRAC components mislocalize in the absence of BAZ1A. (**A-D**) Immunoflurescence on squash preparations of pachytene/diplotene spermatocyte nuclei from wild-type and mutant using antibodies against BAZ1A (**A**), SNF2H (**B**), and CHRAC17 (**C**). Bar = 10 μm. (**D**) CHRAC17 and SNF2H were immunoprecipitated (IP) from wild-type and mutant whole testis lysates and immunoblotted for co-IP with BAZ1A, SNF2H and CHRAC17. Mock IP, no antibody.
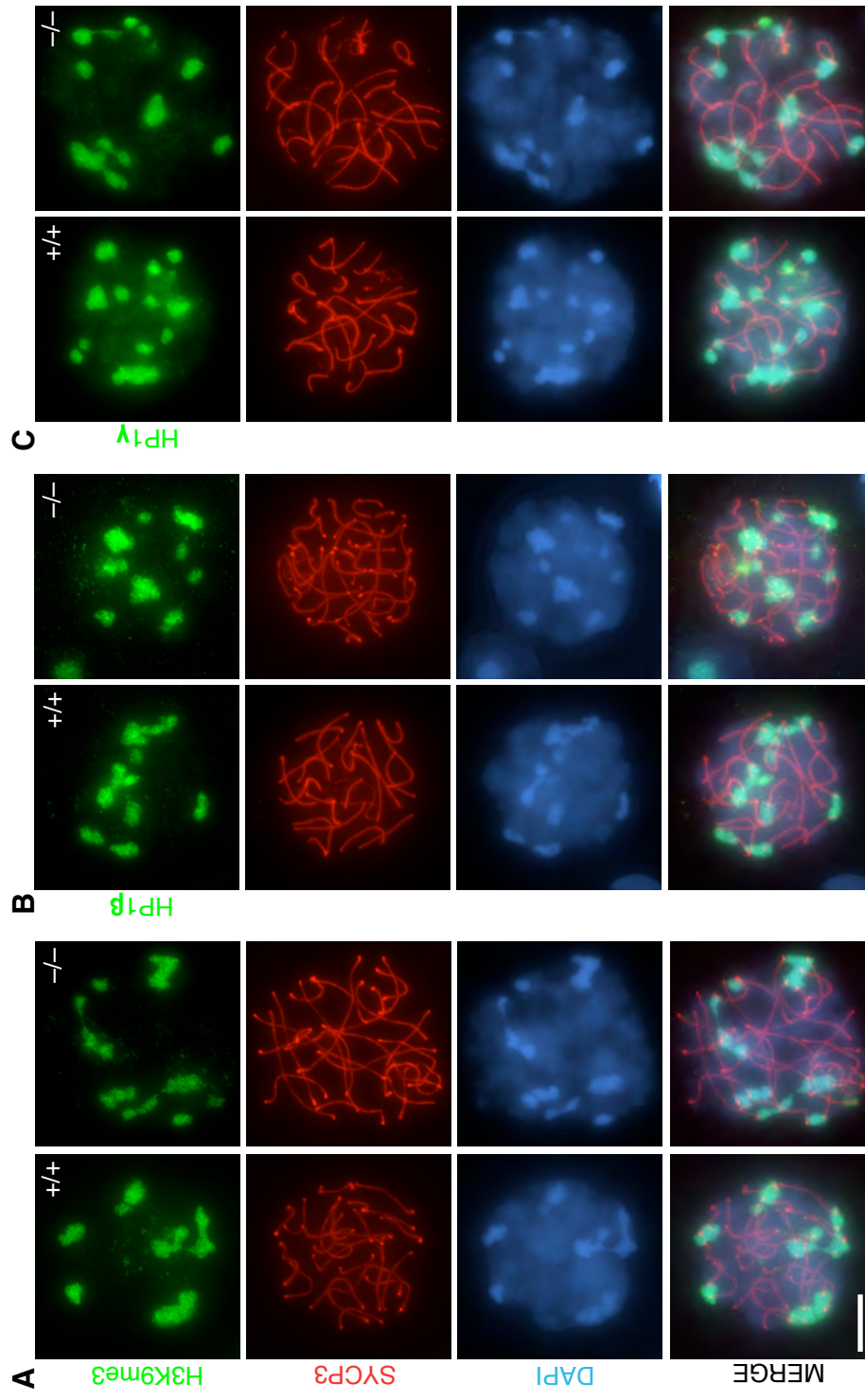
Figure 2.7. Heterochromatin formation appears normal in the absence of _Baz1a_. (A-C) Immunofluorescence on squash preparations of pachytene/diplotene spermatocyte nuclei from wild-type and mutant with antibodies against the heterochromatin markers H3K9me3 (**A**), HP1β (**B**) and HP1γ (**C**). Bar = 10 μm.

IP from wild-type and mutant testis and probed by northern blot using a mixed probe directed against three pachytene piRNAs: piR-1, -2 and -3, which revealed no appreciable difference in their levels (Figure 2.8A), suggesting their expression and subsequent loading onto MIWI is grossly normal in the absence of *Baz1a*.

The localization of BAZ1A to pericentromeric heterochromatin in spermatocytes and spermatids (Figure 1.3B), suggests that it might play a role in suppressing transcription of repetitive elements located in these and other regions as spermatogenic defects have been observed in mutants with a failure to suppress transcription of these elements (Carmell et al., 2007; Yabuta et al., 2011). However, quantitative real time PCR (qPCR) analysis of cDNA libraries generated from FACS sorted spermatids showed that expression of several repetitive elements was unchanged or decreased in the mutant compared to wild-type (Figure 2.8B).

As there is precedent for *Baz1a* as a transcriptional regulator in other organisms (Ewing et al., 2007; Liu et al., 2008) I wondered whether transcriptional misregulation could be responsible for the spermiogenesis defect in the mutant. To test this hypothesis, transcription profiling was used to compare the primary spermatocyte and round spermatid populations in triplicate from wild-type and mutant. RNA was isolated from highly enriched cell populations that had been collected by FACS from dissociated testis and used for microarray analysis. Following quantile normalization of the data, a one-way ANOVA analysis with a false discovery rate of 0.05 comparing mutant versus wild-type spermatocytes revealed 55 genes that were differentially expressed at least 1.5 fold (23 up, 22 down) while only 22 genes were changed at least 2 fold (14 up, 8 down). Conversely, when spermatids were compared, 395 genes were differentially expressed at least 1.5 fold (259 up, 136 down) and 188 at least 2 fold (147 up, 41 down) (Figure 2.9 A-C). Of the 22 genes altered 2-fold or more in the spermatocyte populations, 21 overlapped with those genes altered 2-fold or more in spermatids.
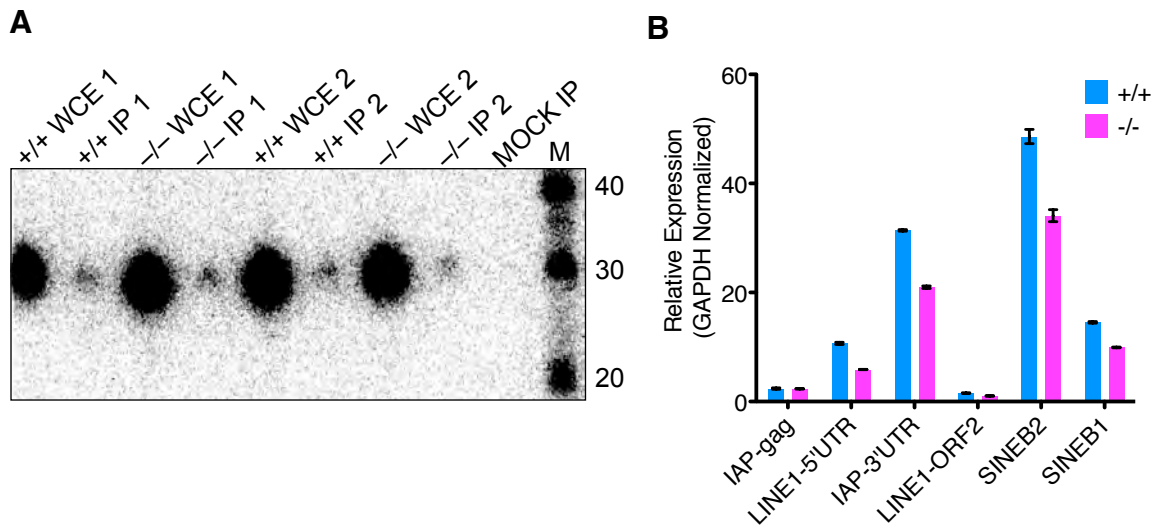
Figure 2.8. Normal expression of pachytene piRNAs and repetitive elements in *Baz1a*-**deficient spermatids.** (**A**) Northern blot of MIWI-bound RNA following IP and detection with a mixed probe of the pachytene-piRNAs piR-1, 2 and 3. WCE, whole cell extract; IP, immunoprecipitation; M, marker; mock IP, no antibody. (**B**) Quantitative real time PCR analysis of different repetitive elements from wild-type and mutant spermatids in triplicate. Bars, mean ± s.d.
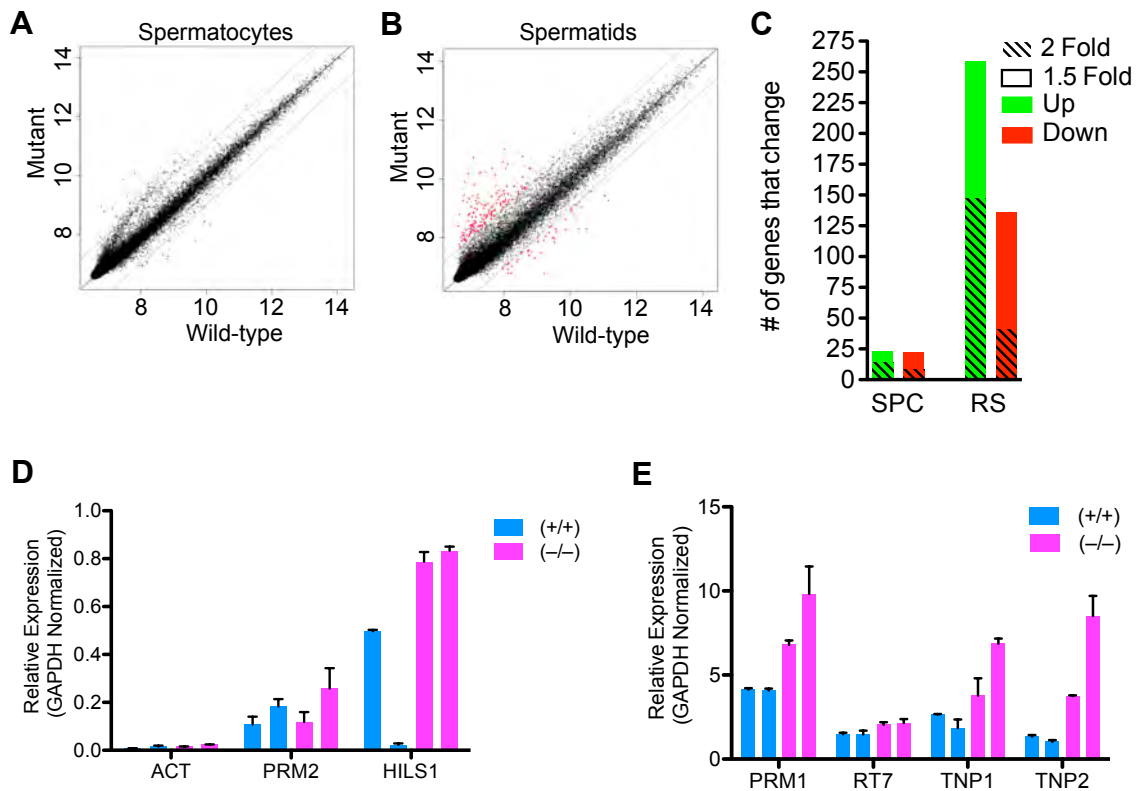
Figure 2.9. Wide-spread transcriptional perturbations in *Baz1a*-deficient sperma-tids. (**A**-**B**) Expression of individual genes on the microarray from wild-type versus mutant spermatocytes (**A**) and spermatids (**B**). Dotted gray lines indicate 2-fold differ-ences. Red dots represent genes with statistically significant differences (P<0.05) of at least 2-fold. (**C**) Summary of genes significantly up-regulated (green) or down-regulated (red) 1.5- (solid bar) and 2-fold (diagonal stripes) in mutant versus wild-type spermatocytes (SPC) and round spermatids (RS). (**D&E**) Quantitative real time PCR analysis of *Act, Prm2, Hils1* (**D**) and *Prm1, Rt7, Tnp1* and *Tnp2* (**E**) from wild-type versus mutant spermatocytes from two independent mice (individual bars) in triplicate. Bars, mean ± s.d.

Interestingly, although not significantly different by the standard 0.05 P value cut-off, a 2.55-fold increase in the expression of *Act* (activator of CREM in the testis) was observed in mutant versus wild-type spermatocytes (P=0.08). This was accompanied by the increase in CREM target genes in mutant spermatocytes, including *Tnp2* (2.16-fold, P=0.052), *Tnp1* (2.2-fold, P=0.078) and *Prm1* (1.54-fold, P=0.14). *Prm2* was not represented on the array and so could not be queried. Notably, it has been reported that premature translation of *Prm1* causes precocious condensation of spermatid DNA, resulting in a phenotype similar to *Baz1a*^{-/-} mutant mice (Lee et al., 1995). The testis-specific linker histone variant *Hils1* was also found to be up-regulated 3.42-fold (P=0.04) in spermatocytes. *Hils1* has been suggested to participate in sperm nuclear condensation and shows delayed expression compared to the other histone variants (Yan et al., 2002) and so it too might lead to precocious DNA compaction if prematurely expressed in spermatocytes.

To further investigate the possible differential expression of these CREM target genes, qPCR analysis using primers for *Act, Hils1,* the protamines and transition proteins and another CREM target, *Rt7,* was performed on cDNA libraries generated from FACS sorted primary spermatocytes from two independent mice of each genotype. Expression of *Act* was almost undetectable in spermatocytes from both wild-type and mutant cells, discounting the possibility that mis-regulation of this activator of CREM leads to the change in expression of CREM target genes. One CREM target that did not exhibit differential expression in the array data, *Rt7,* was also unchanged in this analysis (Figure 2.9E), indicating that there was not a global disruption in CREM target gene regulation. *Prm2* levels were also unchanged in mutant spermatocytes (Figure 2.9D); however, *Prm1, Hils1, Tnp1* and *Tnp2* all appeared elevated in the mutant, although there was some mouse-to-mouse variation in this trend (Figure 2.9D&E). These data

provide further evidence that precocious expression of these factors in primary spermatocytes may contribute to defective spermiogenesis in the mutant.

Another interesting feature of the data from the expression array was a preponderance of the most highly up-regulated genes in mutant spermatids to be either multicopy genes or reside near or in genomic loci containing other multicopy gene families (Figure 2.10). Indeed, 50% of the 46 genes up-regulated 3-fold or more in mutant spermatids fell into this category. It is also worth mentioning that the fourth most highly up-regulated gene, *Cdkn1c*, is a known imprinted locus, although this may simply be coincidental as expression of other imprinted loci was unaffected (data not shown).

Taken together, these data suggest that as spermatocytes develop into spermatids, *Baz1a* directly or indirectly regulates a transcriptional program required for proper sperm formation or acts to suppress the transcription of factors that may antagonize this developmental program.

Symbol	Gene	Note	Chr.	Fold
Rragd	Ras-related GTP binding D		4	3.01
Sulf2	sulfatase 2	near MC locus	2	3.05
Kcnma1	potassium large conductance calcium-activated channel, subfamily M, alpha member 1		14	3.07
Exosc8	exosome component 8		3	3.12
C2	complement component 2 (within H-2S)	near MC locus	17	3.14
Bzw2	basic leucine zipper and W2 domains 2	next to MC gene	12	3.16
Zfp637	zinc finger protein 637		6	3.19
Irf1	interferon regulatory factor 1	in MC locus	11	3.21
Kcnma1	potassium large conductance calcium-activated channel, subfamily M, alpha member 1		14	3.25
LOC100043357	hypothetical protein		?	3.38
Lhx1	LIM homeobox protein 1		11	3.39
Plcb2	phospholipase C, beta 2		2	3.42
LOC625758	similar to M199.5	in MC locus	6	3.43
Fxyd2	FXYD domain-containing ion transport regulator 2		9	3.44
LOC100046690	hypothetical protein		?	3.45
Cd14	CD14 antigen	near MC gene	18	3.52
Pnlip	pancreatic lipase	multicopy	19	3.57
LOC382102	(unannotated)		?	3.64
LOC619842	gm12633		4	3.70
Lum	lumican		10	3.88
Lpin3	lipin 3		2	3.96
Steap1	six transmembrane epithelial antigen of the prostate 1		5	4.09
Car4	carbonic anhydrase 4		11	4.15
Rhou	ras homolog gene family, member U	next to rRNA cluster	8	4.30
Slc22a1	solute carrier family 22 (organic cation transporter), member 1	multicopy	17	4.41
Ces3	carboxylesterase 3	multicopy	8	4.42
Bpil1/Bpifb2	bactericidal/permeability-increasing protein-like 1	multicopy	2	4.61
Spdef	SAM pointed domain containing ets transcription factor	in MC locus	17	4.78
Tpo	thyroid peroxidase		12	4.95
Flg	filaggrin	multicopy	3	5.02
1520401A03Rik	RIKEN cDNA 1520401A03 gene	in MC locus	17	5.20
Evpl	envoplakin	next to MC gene	11	5.21
Olfr303	olfactory receptor 303	in MC locus	7	5.29
Igfbp7	insulin-like growth factor binding protein 7		5	5.29
Epha6	Eph receptor A6	near MC locus	16	5.64
Epgn	epithelial mitogen	in MC locus	5	6.15
Klk1b24	kallikrein 1-related peptidase b24	multicopy	7	6.31
Klk1b21	kallikrein 1-related peptidase b21	multicopy	7	6.48
Cldn5	claudin 5		16	6.54
Pcdh17	protocadherin 17		14	6.96
LOC639715	similar to calpain large subunit (LOC639715)		?	7.60
Abcb4	ATP-binding cassette, sub-family B (MDR/TAP), member 4	multicopy	5	7.65
Cdkn1c	cyclin-dependent kinase inhibitor 1C (P57)	imprinted	7	7.98
Sp5	trans-acting transcription factor 5		2	8.44
Klk1b27	kallikrein 1-related peptidase b27	multicopy	17	9.53
2610016A17Rik	misc. RNA	in MC locus	19	12.52

Figure 2.10. Multicopy genes are upregulated in *Baz1a* mutant spermatids. A preponderance of genes upregulated 3-fold or more in mutant spermatids were multicopy (blue) or reside near other multicopy genes (orange). A known imprinted gene is also indicated (pink). MC, multicopy; Chr, chromosomal location; Fold, fold increase in mutant spermatids versus wild-type.

III. Discussion

The generation of *Baz1a*^{-/-} mice revealed that this chromatin remodeling factor is dispensable for embryonic development. However, as the protein expression and localization analysis presented in the previous chapter suggested, it is required in the testis during spermatogenesis, resulting in male sterility when absent. Interestingly, *Baz1a* was recently reported to be down-regulated in human testis tissue displaying round spermatid maturation arrest isolated from infertile men with azoospermia (Steilmann et al., 2010), suggesting that decreased levels of BAZ1A may also lead to human male sterility.

1. *Baz1a*^{-/-} mice are viable!?

It was presumed that the deletion of *Baz1a,* with its plethora of reported *in vitro* functions, roles in cultured cells and requirement for full viability in the fly, would not support life. In contrast, *Baz1a* mutant mice were viable and displayed no gross developmental defects with the exception of the testis. One possibility of course is that ACF/CHRAC does indeed generate arrays of regularly spaced nucleosomes *in vivo* and aids in the creation of and replication through heterochromatin, etc. but that mild perturbations in these processes in the absence of BAZ1A are not deleterious to cellular and organismal viability. Since aberrations in these processes were not assayed directly in the mutant, future investigations mapping nucleosome positions in the mutant could test this hypothesis directly. Another possibility is that mammals have evolved compensatory mechanisms that exist to a lesser degree in the fly. Indeed, the protein expression analysis presented in chapter 1 revealed ubiquitous expression of at least one *Baz1a* paralog, *Baz1b* in the mouse*.*

2. *Baz1a* is required for proper sperm development.

The observation that breeding of homozygous mutant males to wild-type females was unproductive sparked an examination of spermatogenesis, which revealed dramatic defects. To begin, epididymal sperm counts were much lower in the mutants. One obvious factor that could have contributed to this reduction is apoptosis. Unexpectedly, the increase in apoptosis observed in mutant testis sections was not specific to any one cell-type. In fact, cells like leptotene and zygotene spermatocytes in which BAZ1A expression is not detected were as frequently apoptotic in the mutant as round spermatids in which BAZ1A is readily detectable. The analysis is complicated by the fact that spermatogenesis occurs in a syncytium, resulting in the sharing of cytoplasmic factors. Cells undergoing apoptosis release factors that can induce a similar fate in adjacent cells and might explain why apoptotic rows of similar cell types were occasionally seen. Moreover, mutant round spermatids were frequently observed containing vacuoles (data not shown)—which can be indicative of oncoming apoptosis— at a higher frequency than indicated by TUNEL staining, possibly suggesting that this may not be a robust marker of apoptosis in the testis, thus underestimating the levels of apoptosis in mutant testis.

Even more dramatic was the reduction of motile sperm in the mutant. A likely contributing factor was the array of aberrant tail morphologies, including the frequently observed narrowing of the tail between the principal and mid-piece where the electron-dense, ring-like structure known as the annulus resides. This could suggest a defect in the formation of the annulus in mutant sperm, which is thought to provide a barrier against the mixing of specific protein populations in the different tail compartments. Indeed, deletion of a component of the annulus, *Sept4*, results in immotile sperm (Kissel et al., 2005). Two-tailed sperm were also seen and could arise from the observed diploid spermatids owing to the increase in the number of centrioles in these cells from which

the tail will form. These and other abnormalities that are frequently seen in reports of spermiogenesis mutants (Adham et al., 2001; Cho et al., 2001; Giorgini et al., 2002; Kotaja, 2004; Martianov et al., 2005; Roest et al., 1996; Sapiro et al., 2002; Wu et al., 2000; Xiao et al., 2009b; Zhong et al., 1999) included folding of sperm heads against the tail and coiling of the tail, which could indicate a defect in structural components of the tail that lead to its reduced rigidity in these mutants. In all likelihood, these phenotypic commonalities between spermiogenesis mutants indicate that upstream disruptions in the highly-ordered assembly line production of sperm can lead to diverse downstream consequences. A range of sperm head shapes was also seen in the mutant, which may simply reflect the shape of the head at a time when development of that particular sperm halted or could indicate a defect in compaction of the DNA, which is one factor thought to influence sperm head shaping (Kierszenbaum et al., 2007).

Another observation was the presence of multi-nucleated cells in mutant testis. As this is another common phenomenon in spermiogenesis mutants (Crimmins et al., 2009; Wu et al., 2000), it is again likely that a slight disruption in the progression or order of the sperm developmental program is the culprit. As mentioned, spermatogenesis occurs in a syncytium, with the Sertoli cells aiding in the forward movement of cells from the basal to the luminal compartments of the tubule as development progresses. Opening of any given syncytia and trapping of multiple nuclei within a single cytoplasm might be expected if the junctions maintaining these opening are sensitive to changes in the speed or timing of basal to luminal progression. Sperm with multiple heads were never observed and so it is likely that these multi-nucleate cells are eliminated by some means in the earlier steps of spermiogenesis.

The presence of diploid spermatids is perplexing. If these cells had simply skipped meiosis II, they should only contain either the X or Y chromosome, which segregate at the end of meiosis I; however, FISH analysis revealed one round spermatid

with both sex chromosomes. The presence of two autosome signals suggests these cells did not simply skip both meiotic divisions as such cells would be tetraploid and expected to contain four autosome signals in addition to both sex chromosomes. One possibility is that a population of mutant spermatocytes fail to properly segregate specifically the X and Y at the end of meiosis I and then skip meiosis II or that cells skip the end of meiosis I. Moreover, the observation of two-tailed sperm suggests that diploid cells, which are also expected to forego the reduction of centrioles from which tails arise, are able to progress to relatively late stages of spermiogenesis without being eliminated.

As abnormal wild-type sperm are not infrequent, it is tempting to speculate that the robustness of sperm development relies on mechanisms ensuring quantity over quality, thus making this developmental program particularly sensitive to any disturbance that further reduces sperm quality. Though the question still remains, in the absence of *Baz1a*, what is that disturbance?

3. *Baz1a* is not essential for spermatogenesis associated chromatin dynamics.

As detailed in the introduction, the chromatin undergoes a dramatic makeover during spermatogenesis including the incorporation of histone variants, which are subsequently replaced by the protamines to allow for tight compaction of the genome into the relatively small sperm head. Despite BAZ1A having known roles in chromatin assembly *in vitro*, this process appeared to occur normally in the mutant as expression of a large number of histone variants, and the transition proteins and protamines could be detected bound to chromatin, although a disruption in the proper spacing of these factors cannot be ruled out. Another untested possibility is that the ~2% of histones that are retained in mature spermatozoa (Pittoggi et al., 1999) actively require *Baz1a* for their retention and if precociously ejected in its absence, leads to the observed defects during spermiogenesis. Loci at which histones are retained have not been exhaustively

characterized but to my knowledge, there is not a correlation between any genes misregulated in the absence of *Baz1a* and loci at which histones are retained.

The observation that the mature form of PRM2 but not its precursors is reduced in mutant spermatids raises the possibility that *Baz1a* is somehow required for proper processing of the precursors. However, it is also possible that this observation reflects the step of spermiogenesis at which a large number of mutant cells are eliminated, coincidentally occurring after pPRM2 expression but prior to processing. Interestingly, a reduction in the levels of mature PRM2 is common among other spermiogenesis mutants (Cho et al., 2001; Lee et al., 1995; Zhao et al., 2001).

4. *Baz1a* acts as a transcriptional regulator during spermiogenesis.

The expression profiling of mutant and wild-type spermatocytes and spermatids did not provide any obvious candidates for specific misregulated factors with known roles during spermatogenesis that would directly explain the phenotype. However, it should be mentioned that caveats in the methodology used in the analysis could be underestimating the real changes. This owes to the fact that the defined protocol for collection of enriched population of cells from dissociated testis relies on the size and DNA content of cells. It is therefore likely that the observed multi-nucleate and diploid spermatids in the mutant, which may represent the most defective populations of cells, were excluded from the analysis as they would no longer be expected to co-localize with the haploid spermatid populations in the FACS profile that were collected for the analysis. Additionally, a purity assessment of the sorted populations used in the expression profiling indicated that spermatocyte populations contained between 10-20% spermatids or cells of unknown origin while the spermatid populations were always of 95-100% purity. This contamination was quite consistent across genotypes however and therefore should not greatly affect a comparison of wild-type and mutant cells.

86

That being said, upon closer examination of candidate genes, there did appear to be an increase of spermatid specific genes in the mutant spermatocytes that was confirmed by qPCR, namely *Prm1, Hils1, Tnp1* and *Tnp2.* As all of these factors are known to possess DNA condensing abilities and transgenic mice that prematurely express PRM1 (Lee et al., 1995) display almost identical sperm defects as *Baz1a* mutant mice, including reduction in the levels of mature PRM2, it is likely that misregulation of these factors contributes to the observed mutant phenotype.

One of the more interesting aspects of the analysis came from the observation that of those genes that were most highly up-regulated in mutant spermatids, a large proportion were multicopy genes or were located in or near genomic loci where other multicopy genes are encoded. As several reports have implicated *Baz1a* in transcriptional repression (Ewing et al., 2007; Liu et al., 2008; Yasui et al., 2002), it is not difficult to imagine that it might play a specific role in the repression of multicopy genes, as others have speculated that multicopy genes may have evolved as such to ensure their expression (Cocquet et al., 2009). The majority of up-regulated multicopy genes in the mutant spermatids perform ubiquitous 'house-keeping' functions in the cell. However, as spermiogenesis progresses, cells will shed their cytoplasm and repurpose various organelles to essentially form an egg-seeking missile with a DNA payload. Perhaps BAZ1A creates a repressive chromatin state at multicopy gene loci during spermatogenesis to prevent the expression of genes whose house-keeping functions will not be required during spermiogenesis and whose expression may even interfere with the retooling of the cell to become a sleeked down delivery vessel. This hypothesis could potentially be explored by PCR amplifying candidate multicopy genes from a BAZ1A ChIP of FACS sorted spermatids to ask if BAZ1A binds these multicopy loci directly and/or to map nucleosome occupancy at candidate multicopy loci in spermatids to investigate whether the chromatin structures at these sites are indicative of repression.

5. Were BAZ1A localization patterns simply a red herring?

As described in chapter 1, BAZ1A localizes to the pericentromeric heterochromatin and the sex body in primary spermatocytes and the heterochromatic chromocenter of round spermatids before becoming undetectable in elongating spermatids and then detected again in condensing spermatids just before the end of the spermiogenic program. However, the formation of heterochromatin in $Baz1a^{-/-}$ spermatocytes is unperturbed as is the formation and function of the sex body. Moreover, the repression of pericentromeric repetitive elements and the formation of the chromocenter in round spermatids appeared normal in the absence of $Baz1a$. It would therefore appear that the localization pattern of BAZ1A that draws one's eye, the enrichment at pericentromeric heterochromatin in spermatocytes reminiscent of a disco ball, is not indicative of its function. In contrast, it would appear that the not-so-interesting pattern of localization, the diffuse accumulation of BAZ1A on chromatin throughout the nucleus beginning in pachynema, was more informative of its function during spermatogenesis: transcriptional regulation.

Of course, it is formally possible that $Baz1a$ serves multiple functions during spermatogenesis but that deletion results in defects in transcription that preclude observation of roles in the pericentromeric heterochromatin or sex body that make more sense in terms of its localization pattern. Accumulation in the heterochromatin might also play a regulatory role, acting as a sink for BAZ1A, which was shown to target the other components of the CHRAC complex (SNF2H and CHRAC17) to this locale, thus possibly modulating CHRAC function on the rest of the chromatin.

CHAPTER 3. BAZ1A IS DISPENSABLE FOR THE DEVELOPMENT OF CELLS THAT EXPERIENCE PROGRAMMED DNA DOUBLE-STRAND BREAKS.

I. Summary

This chapter reports on the development of several cell populations in $Baz1a^{-/-}$ mice that experience programmed double-strand breaks (DSBs) during the course of their developmental programs. In the absence of $Baz1a$, T cells and B cells developed normally. Moreover, meiotic DSBs were repaired normally in spermatocytes although they may form at slightly higher levels as measured by DMC1 foci counts, which in turn may lead to the increase in MLH1 foci—a marker of crossovers—that was also observed.

II. Background

Events that generate DSBs, be they from exogenous or endogenous sources, trigger a repair response that recruits a host of proteins to the damage site. Many of these factors will directly bind to the DNA to facilitate the processing of broken strands for repair by homologous recombination (HR) from an available template or by alternate, more error-prone mechanisms like non-homologous end-joining (NHEJ). Because nucleosomes positioned around the damaged site will occlude docking of repair proteins, chromatin remodeling at the site is required to eject histones and subsequently to assemble nascent histones onto the newly repaired DNA strand (Costelloe et al., 2006; Lukas et al., 2011).

Reducing BAZ1A levels by RNA interference (RNAi) in cultured human and mouse cells suggests that $Baz1a$ may be essential for proper repair by both HR and NHEJ and for a robust G2/M damage checkpoint (Lan et al., 2010; Sánchez-Molina et al., 2011).

<u>**III. Results**</u>

To ask whether the development of cells that experience programmed DSBs is disrupted in *Baz1a* mutant mice, the three cell populations where this process is known to occur— spermatocytes (meiotic recombination), T-cells (V(D)J recombination) and B-cells (V(D)J and class switch recombination (CSR))—were investigated.

1. *Baz1a*$^{-/-}$ spermatocytes repair meiotic DSBs and progress normally through meiosis.

Meiotic recombination is initiated by the formation of DSBs by SPO11 during the leptotene stage of prophase I (Keeney, 2008). These break sites are decorated by phosphorylated histone H2AX (γH2AX) (Hunter et al., 2001; Mahadevaiah et al., 2001), which dissipates as breaks are repaired during pachynema. Squash preparations of primary spermatocyte nuclei from wild-type and mutant were stained with an anti-γH2AX antibody and substaged using the axial element component SYCP3 (Figure 3.1A&B). γH2AX staining appears and disappears in the mutant in sync with comparable stages of wild-type nuclei. Note that persistent staining on the X and Y is part of the meiotic sex-chromatin inactivation (MSCI) that occurs during this time (Handel, 2004; Turner, 2007). Moreover, DMC1 foci (a marker of DSBs) form and resolve in concert in both wild-type and *Baz1a*$^{-/-}$ spermatocytes as meiosis progresses, providing additional evidence that DSBs are repaired normally in the mutant (Figure 3.1C). It should be noted that in the mutant, DSBs form with a slightly increased frequency in early zygotene spermatocytes which is when DSB formation peaks. Additionally, MLH1 foci, which mark sites where breaks have repaired as crossover exchange products, also form normally (Figure 3.1D), but also with a slightly increased frequency (Figure 3.1E). Moreover, the presence of post-meiotic cell populations indicates that meiotic DSBs
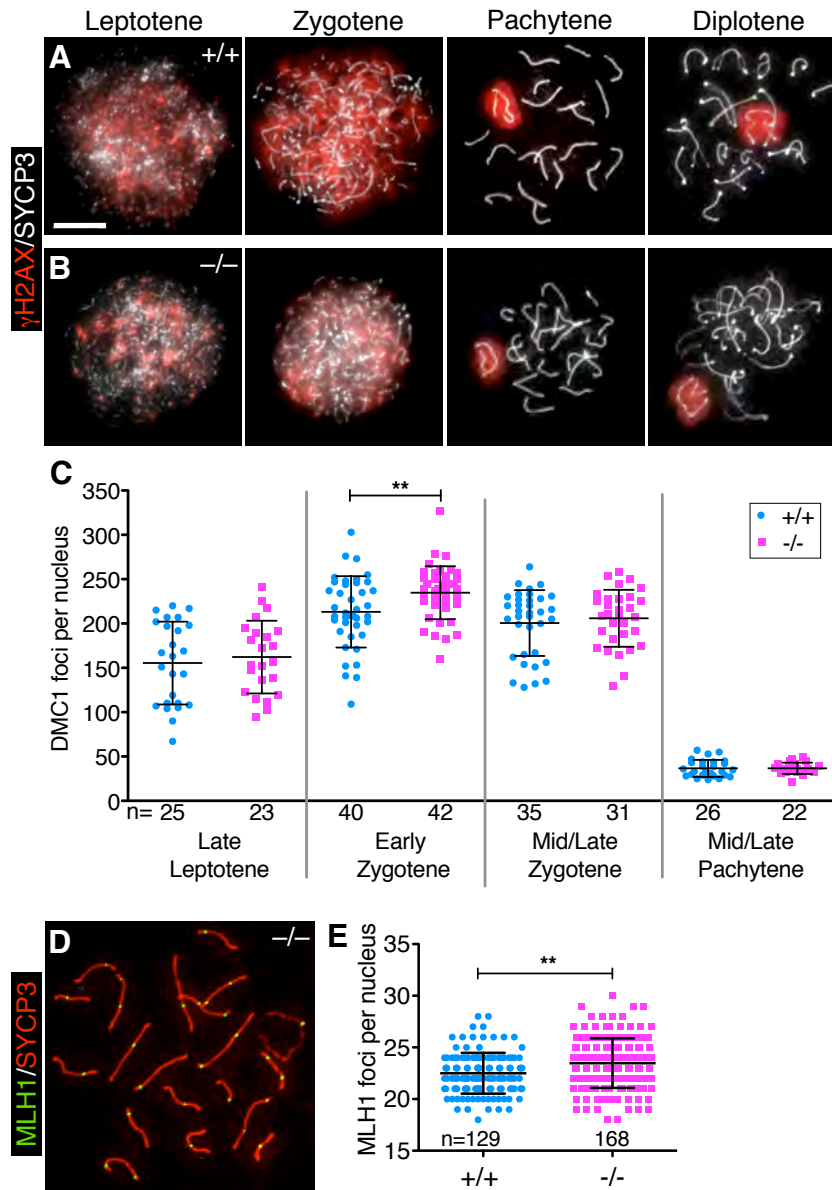
Figure 3.1. *Baz1a* is not required for the repair of meiotic DNA double-strand breaks. (**A**&**B**) Squash preparations of spermatocyte nuclei from wild-type (**A**) and mutant (**B**) showing the accumulation of γH2AX at sites of meiotic DSBs and its disappearance on autosomes as breaks are repaired. Bar = 10 μm. (**C**) DMC1 foci per spread primary spermatocyte nuclei at various stages of prophase I pooled from two sets of wild-type and mutant mice. Nuclei were staged by co-staining spreads with an antibody against the axial element protein SYCP3 (**P=0.007, t-test). (**D**) Chromosome spread of mutant pachytene spermatocyte nuclei showing the accumulation of MLH1 foci. (**E**) Autosomal MLH1 foci per spermatocyte nucleus pooled from two sets of wild-type and mutant mice (**P=0.0002, t-test). Bars, mean ± s.d.

repair normally as a number of mutants defective in repair arrest at the pachytene stage (see discussion for examples).

2. T cells develop normally in the absence of *Baz1a*.

During T cell development, RAG recombinases create DSBs to induce V(D)J recombination (rearrangement of the variable (V), diversity (D) and joining (J) gene segments of the T cell receptor (TCR) locus flanked by conserved recombination signal (RS) sequences) to generate cells with a diverse TCR repertoire (Bassing et al., 2002). Following DSB formation, V, D and J segments with flanking RSs are joined—which results in inversion or deletion of the intervening sequences—by the actions of the nonhomologous eng-joining (NHEJ) proteins. T cells with functionally stable TCRs express both CD4 and CD8 co-receptors, which will eventually give rise to CD4 or CD8 single-positive populations depending on which class of major histocompatibility complex (MHC) molecule they encounter during maturation. FACS analysis of T cells stained with anti-CD4 or CD8 antibodies indicates that T cells with functionally stable TCRs develop in the absence of *Baz1a,* as double- and single-positive populations were present at numbers comparable to wild-type in the thymus and spleen (Figure 3.2A&B). Although this assay is not a direct readout of DSB repair and may not be sensitive enough to detect subtle perturbations, defects like those seen in mice nullizygous for NHEJ components were not seen (see discussion for examples).

3. *Baz1a* is not required for B cell development or CSR in cultured B cells

The exons which encode the immunoglobulin (Ig) variable regions are assembled from V, D and J gene segments of the immunoglobulin locus by the same mechanisms involved in assembly of the TCR variable regions (Bassing et al., 2002). A failure in this process will result in apoptosis of maturing B cells by a mechanism known as clonal
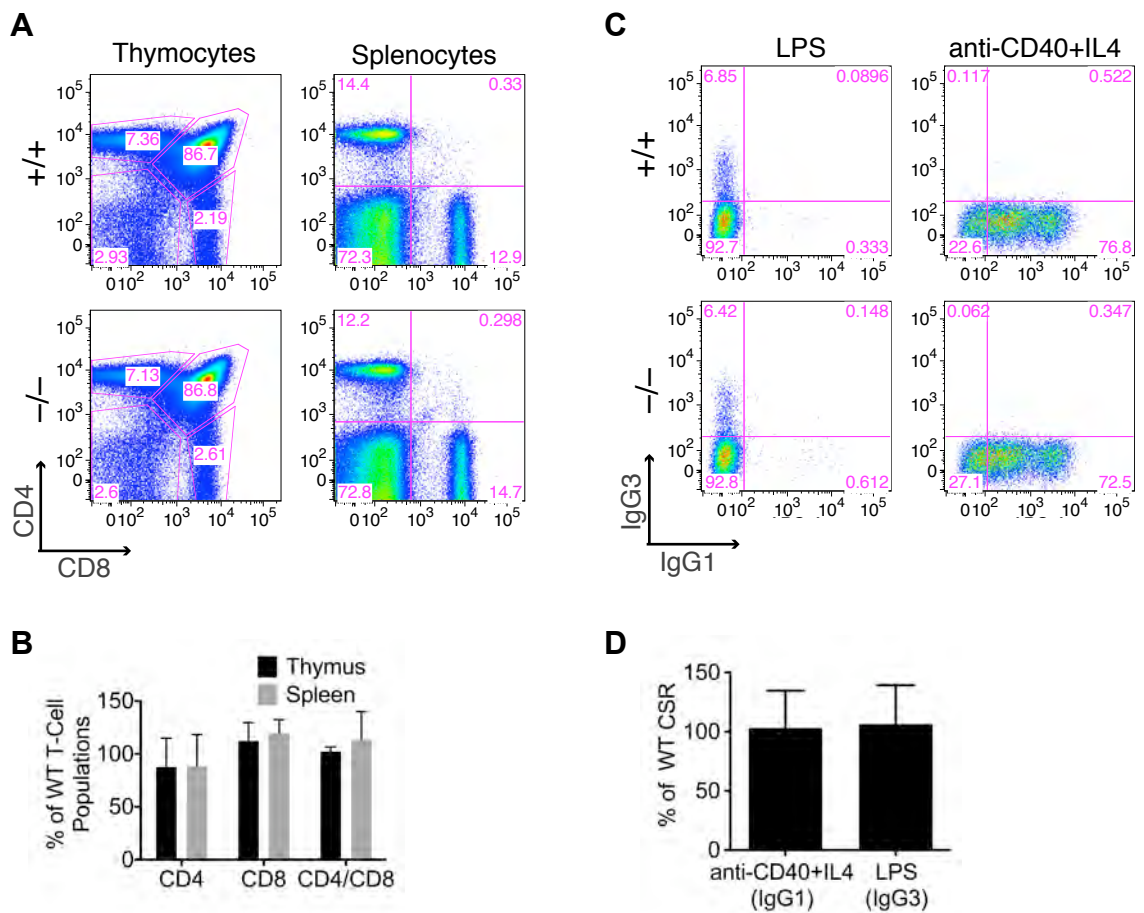
Figure 3.2. T and B cells develop normally in the absence of *Baz1a.* (A&C) Representative fluorescence activated cell sorting (FACS) plots of dissociated thymocytes and splenocytes that have naturally undergone V(D)J recombination to stably express CD4 and CD8 co-receptor molecules (**A**) and cultured B cells stimulated to undergo class-switch recombination (CSR) to IgG1 or IgG3 (**C**). (**B&D**) Quantification of average T cell populations (**B**) and CSR (**D**) in the mutant as a percentage of wild-type from three sets of mice. Bars, mean ± s.d.

deletion. The presence of mature B cells in *Baz1a* mutant mice, and therefore confirmation of proper V(D)J recombination, was confirmed by purifying splenocytes by negative selection using anti-CD43 magnetic beads to remove the immature progenitor B cells that express this marker and culturing the remaining cells for use in the CSR experiments described below (data not shown). Although the presence of B cells may not provide a sensitive measure for subtle repair defects, *Baz1a* is likely not essential for repair as B cells in NHEJ mutants like *Artemis*-deficient mice display a developmental arrest at the CD43$^+$ progenitor stage (Li et al., 2005).

In B cells, CSR is also initiated by the formation of DSBs in the Ig heavy-chain gene locus by activation-induced deaminase (AID) and other enzymes, which repair by components of the NHEJ machinery to induce activated, mature B cells to switch the class of antibody that they produce (Manis et al., 2002). Wild-type and *Baz1a*-deficient mature B cells were stimulated in culture to undergo CSR by treating with lipopolysaccharide (LPS) alone to induce a switch to IgG3, or anti-CD40 antibody + interleukin 4 (IL4) to induce a switch to IgG1. FACS analysis indicated that CSR occurs at levels comparable to wild-type in the absence of *Baz1a* as populations of B cells expressing immunoglobulins with the expected change in their constant region were similar in numbers (Figure 3.2C&D). Although this provides a more direct assay of DSB repair than measuring the numbers of T or B cells, it may not be sensitive enough to detect subtle DNA repair defects. However, if *Baz1a* were essential for DSB repair during CSR, mutants would be expected to look more like mutants of the NHEJ machinery (see discussion for examples).

One possibility to explain the differences in DSB repair requirements observed *in vitro* in human cells versus *in vivo* in mice could be species specific differences in the expression of BAZ1A. To test this, levels of BAZ1A were compared in extracts from two human cell lines (U2OS and HeLa) and two mouse cell lines (B16 and ear fibroblasts

94

(EFs) generated from *Baz1a* wild-type and mutant mice) by immunoblot. Higher expression was seen in HeLa cells but otherwise, expression levels were equivalent in human versus mouse cells (Figure 1.2B, top panel). However, one caveat to this simple interpretation is that the polyclonal antibody used was raised against a 135 amino acid epitope of human BAZ1A which only shares 85% peptide sequence similarity with mouse BAZ1A and so the antibody affinity may vary, making a comparison of mouse and human protein levels difficult. Levels of BAZ1A's binding partner (SNF2H) and paralog (BAZ1B) were also comparable (Figure 1.2B, middle panels).

III. Discussion

The reports implicating a role for BAZ1A in DSB repair in cultured human and mouse cells were intriguing (Lan et al., 2010; Sánchez-Molina et al., 2011). However, the observed effects were subtle, often only on the order of 2-fold depending on what was being measured. Moreover, the use of RNAi in these experiments reflects what happens when BAZ1A levels are reduced but not completely ablated and proper controls to exclude the possibility of off-target effects of the RNAi were not used. An additional caveat is that the majority of cell lines used in these studies were derived from cancerous tissues which harbor numerous mutations in other genes, further complicating interpretation of the results.

Investigating the repair of developmentally-programmed DSBs in *Baz1a*^{-/-} mice provides a genetically cleaner experimental system by which to analyze the role of this factor in DSB repair. Although unable to report on subtle changes in the efficiency of DSB repair, the development of meiocytes, T cells and B cells was unperturbed in the mutant, suggesting there were not gross defects in DSB repair.

1. Is there an increase in meiotic DSBs in the absence of *Baz1a*?

Although embryonic lethality of a number of HR repair pathway mutants precludes characterization during meiosis, those that have been characterized include $Atm^{-/-}$, $Brca2^{-/-}$ mice containing a BAC transgene of the human *BRCA2* gene and mice that carry an in-frame deletion of *Brca1* exon 11. Spermatogenesis in all of these mice arrests during the zygotene to pachytene transition with induction of apoptosis and disruption in the integrity of the axial elements and a reduction in the accumulation of RAD51 and DMC1 foci also evident (Barlow et al., 1998; Sharan et al., 2004; Xu et al., 2003). Therefore, the mere presence of post-meiotic cells in *Baz1a* mutant mice indicates that it cannot be essential for the repair of meiotic DSBs. Additionally, the timely dissipation of γ-H2AX staining and DMC1 foci from autosomes indicated that breaks are properly repaired.

Interestingly, DMC1 counts indicated that DSBs may be slightly elevated in mutant early-zygotene spermatocytes. The observed 10% increase was statistically significant and a corresponding 10% increase in the number of MLH1 foci (which mark sites of cross-over formation) was also observed. Increasing *Spo11* copy number in mice to raise the number of DSBs during meiosis does not increase the number of MLH1 foci thanks to homeostatic mechanisms (Cole et al., 2012). Therefore, the increase in the DSBs alone in $Baz1a^{-/-}$ mice is not sufficient to explain the increase in MLH1 foci. One possibility is that local changes in chromatin structure accompany *Baz1a* deletion and these alterations make the chromatin more permissible to both DSBs and cross-over formation.

2. *Baz1a*-deficient T cells develop normally.

T cells that undergo proper V(D)J recombination have functionally stable TCRs and will express the CD4 and CD8 co-receptors in the spleen and will eventually give rise to CD4

or CD8 single-positive populations in the thymus depending on which MHC molecule they encounter. Populations of these cells were normal in the mutant; however, these cells expand from clonal progenitors and therefore cannot report on subtle decreases in the efficiency of DNA repair. However, CD4/CD8 T cell populations are dramatically reduced when repair is crippled by deleting essential factors in the NHEJ pathway. This is exemplified by Artemis (*Art*) knock-out mice. *Art*$^{-/-}$ thymocytes revealed early arrest of T cell development, which was reflected by >90% of the thymocytes being arrested at the CD4$^-$CD8$^-$ stage, compared with 5–10% observed in wild-type littermates (Li et al., 2005). Therefore, it is a fair assessment that repair of DSBs during T cell development is robust in the absence of *Baz1a* but it is possible that subtle, undetectable changes in the efficiency of repair exist. The use of assays that more directly measure the fidelity and efficiency of coding and signal junction formation (Raghavan et al., 2001) in *Baz1a*-deficient T cells could test this possibility.

3. CSR is not grossly perturbed in the absence of *Baz1a*.

DSBs also form in the Ig heavy-chain locus to induce CSR and are repaired by the NHEJ machinery. Cultured B cells were induced to switch the class of antibody they produce using various treatments. *Baz1a*$^{-/-}$ cells underwent CSR at comparable levels to wild-type, suggesting that repair is not dramatically affected. As cells were directly assayed for a switch to the production of specific IgG molecules shortly after treatment, this is a more direct measurement of the fidelity and efficiency of DSB repair in individual cells, unlike the less sensitive assay for V(D)J recombination in T cells isolated from mice described above which might also detect the clonal expansion of a small population of cells *in vivo* that have properly completed V(D)J recombination and therefore not report on subtle defects in repair. Only B cells that have matured to produce immunoglobulins will undergo CSR. V(D)J recombination is required for this maturation

97

and as both V(D)J recombination and CSR require the NHEJ machinery, mutations in NHEJ pathway components would preclude observing defects in CSR. To circumvent this problem, investigators have reconstituted B cell compartments with pre-rearranged immunoglobulin gene segments in NHEJ mutant mice. Using this system to observe mutants of the DNA-dependent protein kinase (DNA-PK) subunits Ku70 or Ku80, it was observed that mature B cells fail to complete switch recombination to generate secondary isotypes (Casellas et al., 1998; Manis et al., 1998). Such a severe defect was not observed in *Baz1a* mutants, arguing that CSR is not grossly perturbed in the absence of BAZ1A.

4. *Baz1a* involvement in DSB repair.

As already discussed, one possibility for the discrepancy between the cell culture studies and the *in vivo* analysis provided here is the inability of this study to detect subtle changes. Moreover, the cell culture studies were performed mostly in human cells in the context of BAZ1A overexpression, often with an epitope tag, and with strong, exogenous sources of DSB induction. Some of these points could be addressed by performing similar experiments with fibroblast lines derived from $Baz1a^{-/-}$ and wild-type mice. This system would be 'cleaner' in the sense that BAZ1A is completely absent and not merely depleted and there is no possibility of off target effects of RNAi. Additionally, DSB repair could be assessed in the context of endogenous levels of BAZ1A and in the absence of other mutations like those present in most cancer-derived cell lines.

REFERENCES

Abrams, E., Neigeborn, L., and Carlson, M. (1986). Molecular analysis of SNF2 and SNF5, genes required for expression of glucose-repressible genes in Saccharomyces cerevisiae. Mol Cell Biol *6*, 3643-3651.

Adham, I.M., Nayernia, K., Burkhardt-Gottges, E., Topaloglu, O., Dixkens, C., Holstein, A.F., and Engel, W. (2001). Teratozoospermia in mice lacking the transition protein 2 (Tnp2). Mol Hum Reprod *7*, 513-520.

Akhmanova, A.S., Bindels, P.C., Xu, J., Miedema, K., Kremer, H., and Hennig, W. (1995). Structure and expression of histone H3.3 genes in Drosophila melanogaster and Drosophila hydei. Genome *38*, 586-600.

Alfonso, P.J., and Kistler, W.S. (1993). Immunohistochemical localization of spermatid nuclear transition protein 2 in the testes of rats and mice. Biol Reprod *48*, 522-529.

Aoki, V.W., and Carrell, D.T. (2003). Human protamines and the developing spermatid: their structure, function, expression and relationship with male infertility. Asian J Androl *5*, 315-324.

Aoyagi, S., and Hayes, J.J. (2002). hSWI/SNF-catalyzed nucleosome sliding does not occur solely via a twist-diffusion mechanism. Mol Cell Biol *22*, 7484-7490.

Awe, S., and Renkawitz-Pohl, R. (2010). Histone H4 acetylation is essential to proceed from a histone- to a protamine-based chromatin structure in spermatid nuclei of Drosophila melanogaster. Syst Biol Reprod Med *56*, 44-61.

Baarends, W.M., Hoogerbrugge, J.W., Roest, H.P., Ooms, M., Vreeburg, J., Hoeijmakers, J.H., and Grootegoed, J.A. (1999). Histone ubiquitination and chromatin remodeling in mouse spermatogenesis. Dev Biol *207*, 322-333.

Baarends, W.M., Wassenaar, E., Hoogerbrugge, J.W., Schoenmakers, S., Sun, Z.W., and Grootegoed, J.A. (2007). Increased phosphorylation and dimethylation of XY body histones in the Hr6b-knockout mouse is associated with derepression of the X chromosome. J Cell Sci *120*, 1841-1851.

Baarends, W.M., Wassenaar, E., Hoogerbrugge, J.W., van Cappellen, G., Roest, H.P., Vreeburg, J., Ooms, M., Hoeijmakers, J.H., and Grootegoed, J.A. (2003). Loss of HR6B ubiquitin-conjugating activity results in damaged synaptonemal complex structure and increased crossing-over frequency during the male meiotic prophase. Mol Cell Biol *23*, 1151-1162.

Balhorn, R., Brewer, L., and Corzett, M. (2000). DNA condensation by protamine and arginine-rich peptides: analysis of toroid stability using single DNA molecules. Mol Reprod Dev *56*, 230-234.

Balhorn, R., Weston, S., Thomas, C., and Wyrobek, A.J. (1984). DNA packaging in mouse spermatids. Synthesis of protamine variants and four transition proteins. Exp Cell Res *150*, 298-308.

Banting, G.S., Barak, O., Ames, T.M., Burnham, A.C., Kardel, M.D., Cooch, N.S., Davidson, C.E., Godbout, R., McDermid, H.E., and Shiekhattar, R. (2005). CECR2, a protein involved in neurulation, forms a novel chromatin remodeling complex with SNF2L. Hum Mol Genet *14*, 513-524.

Bao, Y., and Shen, X. (2007). Chromatin remodeling in DNA double-strand break repair. Curr Opin Genet Dev *17*, 126-131.

Barak, O., Lazzaro, M.A., Lane, W.S., Speicher, D.W., Picketts, D.J., and Shiekhattar, R. (2003). Isolation of human NURF: a regulator of Engrailed gene expression. EMBO J *22*, 6089-6100.

Barlow, C., Liyanage, M., Moens, P.B., Tarsounas, M., Nagashima, K., Brown, K., Rottinghaus, S., Jackson, S.P., Tagle, D., Ried, T.*, et al.* (1998). Atm deficiency results in severe meiotic disruption as early as leptonema of prophase I. Development *125*, 4007-4017.

Bassing, C.H., Swat, W., and Alt, F.W. (2002). The mechanism and regulation of chromosomal V(D)J recombination. Cell *109 Suppl*, S45-55.

Bastos, H., Lassalle, B., Chicheportiche, A., Riou, L., Testart, J., Allemand, I., and Fouchet, P. (2005). Flow cytometric characterization of viable meiotic and postmeiotic cells by Hoechst 33342 in mouse spermatogenesis. Cytometry A *65*, 40-49.

Becker, P.B., and Hörz, W. (2002). ATP-dependent nucleosome remodeling. Annu Rev Biochem *71*, 247-273.

Becker, P.B., Tsukiyama, T., and Wu, C. (1994). Chromatin assembly extracts from Drosophila embryos. Methods Cell Biol *44*, 207-223.

Blendy, J.A., Kaestner, K.H., Weinbauer, G.F., Nieschlag, E., and Schutz, G. (1996). Severe impairment of spermatogenesis in mice lacking the CREM gene. Nature *380*, 162-165.

Blosser, T.R., Yang, J.G., Stone, M.D., Narlikar, G.J., and Zhuang, X. (2009). Dynamics of nucleosome remodelling by individual ACF complexes. Nature *462*, 1022-1027.

Bochar, D.A., Savard, J., Wang, W., Lafleur, D.W., Moore, P., Côté, J., and Shiekhattar, R. (2000). A family of chromatin remodeling factors related to Williams syndrome transcription factor. Proc Natl Acad Sci USA *97*, 1038-1043.

Bonaldi, T., Längst, G., Strohner, R., Becker, P.B., and Bianchi, M.E. (2002). The DNA chaperone HMGB1 facilitates ACF/CHRAC-dependent nucleosome sliding. EMBO J *21*, 6865-6873.

Bowman, G.D. (2010). Mechanisms of ATP-dependent nucleosome sliding. Curr Opin Struct Biol *20*, 73-81.

Boyer, L.A., Latek, R.R., and Peterson, C.L. (2004). The SANT domain: a unique histone-tail-binding module? Nat Rev Mol Cell Biol *5*, 158-163.

Bozhenok, L., Wade, P.A., and Varga-Weisz, P. (2002). WSTF-ISWI chromatin remodeling complex targets heterochromatic replication foci. EMBO J *21*, 2231-2241.

Bramlage, B., Kosciessa, U., and Doenecke, D. (1997). Differential expression of the murine histone genes H3.3A and H3.3B. Differentiation *62*, 13-20.

Braun, R.E. (1990). Temporal translational regulation of the protamine 1 gene during mouse spermatogenesis. Enzyme *44*, 120-128.

Braun, R.E., Peschon, J.J., Behringer, R.R., Brinster, R.L., and Palmiter, R.D. (1989). Protamine 3'-untranslated sequences regulate temporal translational control and subcellular localization of growth hormone in spermatids of transgenic mice. Genes Dev *3*, 793-802.

Brower-Toland, B.D., Smith, C.L., Yeh, R.C., Lis, J.T., Peterson, C.L., and Wang, M.D. (2002). Mechanical disruption of individual nucleosomes reveals a reversible multistage release of DNA. Proc Natl Acad Sci U S A *99*, 1960-1965.

Cairns, B.R. (2005). Chromatin remodeling complexes: strength in diversity, precision through specialization. Curr Opin Genet Dev *15*, 185-190.

Carmell, M.A., Girard, A., van de Kant, H.J.G., Bourc'his, D., Bestor, T.H., de Rooij, D.G., and Hannon, G.J. (2007). MIWI2 Is Essential for Spermatogenesis and Repression of Transposons in the Mouse Male Germline. Developmental Cell *12*, 503-514.

Casellas, R., Nussenzweig, A., Wuerffel, R., Pelanda, R., Reichlin, A., Suh, H., Qin, X.F., Besmer, E., Kenter, A., Rajewsky, K.*, et al.* (1998). Ku80 is required for immunoglobulin isotype switching. EMBO J *17*, 2404-2411.

Celeste, A., Petersen, S., Romanienko, P.J., Fernandez-Capetillo, O., Chen, H.T., Sedelnikova, O.A., Reina-San-Martin, B., Coppola, V., Meffre, E., Difilippantonio, M.J.*, et al.* (2002). Genomic instability in mice lacking histone H2AX. Science *296*, 922-927.

Chioda, M., Vengadasalam, S., Kremmer, E., Eberharter, A., and Becker, P.B. (2010). Developmental role for ACF1-containing nucleosome remodellers in chromatin organisation. Development *137*, 3513-3522.

Cho, C., Willis, W.D., Goulding, E.H., Jung-Ha, H., Choi, Y.C., Hecht, N.B., and Eddy, E.M. (2001). Haploinsufficiency of protamine-1 or -2 causes infertility in mice. Nat Genet *28*, 82-86.

Clapier, C.R., and Cairns, B.R. (2009). The biology of chromatin remodeling complexes. Annu Rev Biochem *78*, 273-304.

Clapier, C.R., Langst, G., Corona, D.F., Becker, P.B., and Nightingale, K.P. (2001). Critical role for the histone H4 N terminus in nucleosome remodeling by ISWI. Mol Cell Biol *21*, 875-883.

Cocquet, J., Ellis, P.J.I., Yamauchi, Y., Mahadevaiah, S.K., Affara, N.A., Ward, M.A., and Burgoyne, P.S. (2009). The multicopy gene Sly represses the sex chromosomes in the male mouse germline after meiosis. PLoS Biol *7*, e1000244.

Cole, F., Kauppi, L., Lange, J., Roig, I., Wang, R., Keeney, S., and Jasin, M. (2012). Homeostatic control of recombination is implemented progressively in mouse meiosis. Nat Cell Biol.

Collins, N., Poot, R.A., Kukimoto, I., García-Jiménez, C., Dellaire, G., and Varga-Weisz, P.D. (2002). An ACF1-ISWI chromatin-remodeling complex is required for DNA replication through heterochromatin. Nat Genet *32*, 627-632.

Costelloe, T., Fitzgerald, J., Murphy, N.J., Flaus, A., and Lowndes, N.F. (2006). Chromatin modulation and the DNA damage response. Exp Cell Res *312*, 2677-2686.

Couldrey, C., Carlton, M.B., Nolan, P.M., Colledge, W.H., and Evans, M.J. (1999). A retroviral gene trap insertion into the histone 3.3A gene causes partial neonatal lethality, stunted growth, neuromuscular deficits and male sub-fertility in transgenic mice. Hum Mol Genet *8*, 2489-2495.

Crimmins, S., Sutovsky, M., Chen, P.-C., Huffman, A., Wheeler, C., Swing, D.A., Roth, K., Wilson, J., Sutovsky, P., and Wilson, S. (2009). Transgenic rescue of ataxia mice reveals a male-specific sterility defect. Dev Biol *325*, 33-42.

Dang, W., Kagalwala, M.N., and Bartholomew, B. (2006). Regulation of ISW2 by concerted action of histone H4 tail and extranucleosomal DNA. Mol Cell Biol *26*, 7388-7396.

de Boer, P., Searle, A.G., van der Hoeven, F.A., de Rooij, D.G., and Beechey, C.V. (1986). Male pachytene pairing in single and double translocation heterozygotes and spermatogenic impairment in the mouse. Chromosoma *93*, 326-336.

De Lucia, F., Faraone-Mennella, M.R., D'Erme, M., Quesada, P., Caiafa, P., and Farina, B. (1994). Histone-induced condensation of rat testis chromatin: testis-specific H1t versus somatic H1 variants. Biochem Biophys Res Commun *198*, 32-39.

Deuring, R., Fanti, L., Armstrong, J.A., Sarte, M., Papoulas, O., Prestel, M., Daubresse, G., Verardo, M., Moseley, S.L., Berloco, M.*, et al.* (2000). The ISWI chromatin-remodeling protein is required for gene expression and the maintenance of higher order chromatin structure in vivo. Mol Cell *5*, 355-365.

Dickinson, L.A., Joh, T., Kohwi, Y., and Kohwi-Shigematsu, T. (1992). A tissue-specific MAR/SAR DNA-binding protein with unusual binding site recognition. Cell *70*, 631-645.

Doerks, T., Copley, R., and Bork, P. (2001). DDT -- a novel domain in different transcription and chromosome remodeling factors. Trends Biochem Sci *26*, 145-146.

Doyen, C.M., An, W., Angelov, D., Bondarenko, V., Mietton, F., Studitsky, V.M., Hamiche, A., Roeder, R.G., Bouvet, P., and Dimitrov, S. (2006). Mechanism of polymerase II transcription repression by the histone variant macroH2A. Mol Cell Biol *26*, 1156-1164.

Drabent, B., Bode, C., Bramlage, B., and Doenecke, D. (1996). Expression of the mouse testicular histone gene H1t during spermatogenesis. Histochem Cell Biol *106*, 247-251.

Drabent, B., Saftig, P., Bode, C., and Doenecke, D. (2000). Spermatogenesis proceeds normally in mice without linker histone H1t. Histochem Cell Biol *113*, 433-442.

Eberharter, A., Ferrari, S., Längst, G., Straub, T., Imhof, A., Varga-Weisz, P., Wilm, M., and Becker, P.B. (2001). Acf1, the largest subunit of CHRAC, regulates ISWI-induced nucleosome remodelling. EMBO J *20*, 3781-3788.

Eisen, J.A., Sweder, K.S., and Hanawalt, P.C. (1995). Evolution of the SNF2 family of proteins: subfamilies with distinct sequences and functions. Nucleic Acids Res *23*, 2715-2723.

Elliott, D.J., and Grellscheid, S.N. (2006). Alternative RNA splicing regulation in the testis. Reproduction *132*, 811-819.

Engel, W., Keime, S., Kremling, H., Hameister, H., and Schluter, G. (1992). The genes for protamine 1 and 2 (PRM1 and PRM2) and transition protein 2 (TNP2) are closely linked in the mammalian genome. Cytogenet Cell Genet *61*, 158-159.

Erdel, F., and Rippe, K. (2011). Chromatin remodeling in mammalian cells by ISWI type complexes - where, when and why? The FEBS journal.

Eskeland, R., Eberharter, A., and Imhof, A. (2007). HP1 binding to chromatin methylated at H3K9 is enhanced by auxiliary factors. Mol Cell Biol *27*, 453-465.

Ewing, A.K., Attner, M., and Chakravarti, D. (2007). Novel regulatory role for human Acf1 in transcriptional repression of vitamin D3 receptor-regulated genes. Mol Endocrinol *21*, 1791-1806.

Fantz, D.A., Hatfield, W.R., Horvath, G., Kistler, M.K., and Kistler, W.S. (2001). Mice with a targeted disruption of the H1t gene are fertile and undergo normal changes in structural chromosomal proteins during spermiogenesis. Biol Reprod *64*, 425-431.

Flaus, A., Martin, D.M.A., Barton, G.J., and Owen-Hughes, T. (2006). Identification of multiple distinct Snf2 subfamilies with conserved structural motifs. Nucleic Acids Res *34*, 2887-2905.

Flaus, A., and Owen-Hughes, T. (2011). Mechanisms for ATP-dependent chromatin remodelling: the means to the end. The FEBS journal *278*, 3579-3595.

Flaus, A., Rencurel, C., Ferreira, H., Wiechens, N., and Owen-Hughes, T. (2004). Sin mutations alter inherent nucleosome mobility. EMBO J *23*, 343-353.

Frank, D., Doenecke, D., and Albig, W. (2003). Differential expression of human replacement and cell cycle dependent H3 histone genes. Gene *312*, 135-143.

Fyodorov, D.V., Blower, M.D., Karpen, G.H., and Kadonaga, J.T. (2004). Acf1 confers unique activities to ACF/CHRAC and promotes the formation rather than disruption of chromatin in vivo. Genes Dev *18*, 170-183.

Fyodorov, D.V., and Kadonaga, J.T. (2002). Binding of Acf1 to DNA involves a WAC motif and is important for ACF-mediated chromatin assembly. Mol Cell Biol *22*, 6344-6353.

Gangaraju, V.K., and Bartholomew, B. (2007). Mechanisms of ATP dependent chromatin remodeling. Mutat Res *618*, 3-17.

Gaucher, J., Reynoird, N., Montellier, E., Boussouar, F., Rousseaux, S., and Khochbin, S. (2010). From meiosis to postmeiotic events: the secrets of histone disappearance. The FEBS journal *277*, 599-604.

Gavrieli, Y., Sherman, Y., and Ben-Sasson, S.A. (1992). Identification of programmed cell death in situ via specific labeling of nuclear DNA fragmentation. J Cell Biol *119*, 493-501.

Giorgini, F., Davies, H.G., and Braun, R.E. (2002). Translational repression by MSY4 inhibits spermatid differentiation in mice. Development *129*, 3669-3679.

Girard, A., Sachidanandam, R., Hannon, G.J., and Carmell, M.A. (2006). A germline-specific class of small RNAs binds mammalian Piwi proteins. Nature *442*, 199-202.

Goetz, P., Chandley, A.C., and Speed, R.M. (1984). Morphological and temporal sequence of meiotic prophase development at puberty in the male mouse. J Cell Sci *65*, 249-263.

Goldman, J.A., Garlick, J.D., and Kingston, R.E. (2010). Chromatin remodeling by imitation switch (ISWI) class ATP-dependent remodelers is stimulated by histone variant H2A.Z. J Biol Chem *285*, 4645-4651.

Gonzalez-Romero, R., Mendez, J., Ausio, J., and Eirin-Lopez, J.M. (2008). Quickly evolving histones, nucleosome stability and chromatin folding: all about histone H2A.Bbd. Gene *413*, 1-7.

Govin, J., Caron, C., Lestrat, C., Rousseaux, S., and Khochbin, S. (2004). The role of histones in chromatin remodelling during mammalian spermiogenesis. Eur J Biochem *271*, 3459-3469.

Govin, J., Escoffier, E., Rousseaux, S., Kuhn, L., Ferro, M., Thévenon, J., Catena, R., Davidson, I., Garin, J., Khochbin, S.*, et al.* (2007). Pericentric heterochromatin reprogramming by new histone variants during mouse spermiogenesis. J Cell Biol *176*, 283-294.

Greaves, I.K., Rangasamy, D., Devoy, M., Marshall Graves, J.A., and Tremethick, D.J. (2006). The X and Y chromosomes assemble into H2A.Z-containing facultative heterochromatin following meiosis. Mol Cell Biol *26*, 5394-5405.

Grimes, S.R., Jr., Platz, R.D., Meistrich, M.L., and Hnilica, L.S. (1975). Partial characterization of a new basic nuclear protein from rat testis elongated spermatids. Biochem Biophys Res Commun *67*, 182-189.

Grune, T., Brzeski, J., Eberharter, A., Clapier, C.R., Corona, D.F., Becker, P.B., and Muller, C.W. (2003). Crystal structure and functional analysis of a nucleosome recognition module of the remodeling factor ISWI. Mol Cell *12*, 449-460.

Hall, M.A., Shundrovsky, A., Bai, L., Fulbright, R.M., Lis, J.T., and Wang, M.D. (2009). High-resolution dynamic mapping of histone-DNA interactions in a nucleosome. Nat Struct Mol Biol *16*, 124-129.

Hanai, K., Furuhashi, H., Yamamoto, T., Akasaka, K., and Hirose, S. (2008). RSF governs silent chromatin formation via histone H2Av replacement. PLoS Genet *4*, e1000011.

Handel, M.A. (2004). The XY body: a specialized meiotic chromatin domain. Exp Cell Res *296*, 57-63.

Hartlepp, K.F., Fernández-Tornero, C., Eberharter, A., Grüne, T., Müller, C.W., and Becker, P.B. (2005). The histone fold subunits of Drosophila CHRAC facilitate nucleosome sliding through dynamic DNA interactions. Mol Cell Biol *25*, 9886-9896.

Haushalter, K.A., and Kadonaga, J.T. (2003). Chromatin assembly by DNA-translocating motors. Nat Rev Mol Cell Biol *4*, 613-620.

Hazzouri, M., Pivot-Pajot, C., Faure, A.K., Usson, Y., Pelletier, R., Sele, B., Khochbin, S., and Rousseaux, S. (2000). Regulated hyperacetylation of core histones during mouse spermatogenesis: involvement of histone deacetylases. Eur J Cell Biol *79*, 950-960.

Hota, S.K., and Bartholomew, B. (2011). Diversity of operation in ATP-dependent chromatin remodelers. Biochim Biophys Acta *1809*, 476-487.

Hoyer-Fender, S., Costanzi, C., and Pehrson, J.R. (2000). Histone macroH2A1.2 is concentrated in the XY-body by the early pachytene stage of spermatogenesis. Exp Cell Res *258*, 254-260.

Hunter, N., Borner, G.V., Lichten, M., and Kleckner, N. (2001). Gamma-H2AX illuminates meiosis. Nat Genet *27*, 236-238.

Ito, T., Bulger, M., Pazin, M.J., Kobayashi, R., and Kadonaga, J.T. (1997). ACF, an ISWI-containing and ATP-utilizing chromatin assembly and remodeling factor. Cell *90*, 145-155.

Ito, T., Levenstein, M.E., Fyodorov, D.V., Kutach, A.K., Kobayashi, R., and Kadonaga, J.T. (1999). ACF consists of two subunits, Acf1 and ISWI, that function cooperatively in the ATP-dependent catalysis of chromatin assembly. Genes Dev *13*, 1529-1539.

Jones, M.H., Hamana, N., Nezu, J.i., and Shimane, M. (2000). A novel family of bromodomain genes. Genomics *63*, 40-45.

Kamma, H., Portman, D.S., and Dreyfuss, G. (1995). Cell type-specific expression of hnRNP proteins. Exp Cell Res *221*, 187-196.

Kauppi, L., Barchi, M., Baudat, F., Romanienko, P.J., Keeney, S., and Jasin, M. (2011). Distinct Properties of the XY Pseudoautosomal Region Crucial for Male Meiosis. Science *331*, 916-920.

Keeney, S. (2008). Spo11 and the Formation of DNA Double-Strand Breaks in Meiosis. Genome Dyn Stab *2*, 81-123.

Kennedy, B.P., and Davies, P.L. (1980). Acid-soluble nuclear proteins of the testis during spermatogenesis in the winter flounder. Loss of the high mobility group proteins. J Biol Chem *255*, 2533-2539.

Kennedy, B.P., and Davies, P.L. (1981). Phosphorylation of a group of high molecular weight basic nuclear proteins during spermatogenesis in the winter flounder. J Biol Chem *256*, 9254-9259.

Khadake, J.R., and Rao, M.R. (1995). DNA- and chromatin-condensing properties of rat testes H1a and H1t compared to those of rat liver H1bdec; H1t is a poor condenser of chromatin. Biochemistry *34*, 15792-15801.

Kierszenbaum, A.L., Rivkin, E., and Tres, L.L. (2007). Molecular biology of sperm head shaping. Soc Reprod Fertil Suppl *65*, 33-43.

Kissel, H., Georgescu, M.M., Larisch, S., Manova, K., Hunnicutt, G.R., and Steller, H. (2005). The Sept4 septin locus is required for sperm terminal differentiation in mice. Dev Cell *8*, 353-364.

Kistler, W.S., Noyes, C., Hsu, R., and Heinrikson, R.L. (1975). The amino acid sequence of a testis-specific basic protein that is associated with spermatogenesis. J Biol Chem *250*, 1847-1853.

Kleene, K.C., Distel, R.J., and Hecht, N.B. (1984). Translational regulation and deadenylation of a protamine mRNA during spermiogenesis in the mouse. Dev Biol *105*, 71-79.

Kotaja, N. (2004). Abnormal sperm in mice with targeted deletion of the act (activator of cAMP-responsive element modulator in testis) gene. Proceedings of the National Academy of Sciences *101*, 10620-10625.

Kremling, H., Luerssen, H., Adham, I.M., Klemm, U., Tsaousidou, S., and Engel, W. (1989). Nucleotide sequences and expression of cDNA clones for boar and bull transition protein 1 and its evolutionary conservation in mammals. Differentiation *40*, 184-190.

Kruger, W., Peterson, C.L., Sil, A., Coburn, C., Arents, G., Moudrianakis, E.N., and Herskowitz, I. (1995). Amino acid substitutions in the structured domains of histones H3 and H4 partially relieve the requirement of the yeast SWI/SNF complex for transcription. Genes Dev *9*, 2770-2779.

Kukimoto, I., Elderkin, S., Grimaldi, M., Oelgeschläger, T., and Varga-Weisz, P.D. (2004). The histone-fold protein complex CHRAC-15/17 enhances nucleosome sliding and assembly mediated by ACF. Molecular Cell *13*, 265-277.

Lan, L., Ui, A., Nakajima, S., Hatakeyama, K., Hoshi, M., Watanabe, R., Janicki, S.M., Ogiwara, H., Kohno, T., Kanno, S.-I.*, et al.* (2010). The ACF1 Complex Is Required for DNA Double-Strand Break Repair in Human Cells. Molecular Cell *40*, 976-987.

Langst, G., and Becker, P.B. (2001). ISWI induces nucleosome sliding on nicked DNA. Mol Cell *8*, 1085-1092.

Lee, K., Haugen, H.S., Clegg, C.H., and Braun, R.E. (1995). Premature translation of protamine 1 mRNA causes precocious nuclear condensation and arrests spermatid differentiation in mice. Proc Natl Acad Sci USA *92*, 12451-12455.

LeRoy, G., Loyola, A., Lane, W.S., and Reinberg, D. (2000). Purification and characterization of a human factor that assembles and remodels chromatin. J Biol Chem *275*, 14787-14790.

LeRoy, G., Orphanides, G., Lane, W.S., and Reinberg, D. (1998). Requirement of RSF and FACT for transcription of chromatin templates in vitro. Science *282*, 1900-1904.

Li, L., Salido, E., Zhou, Y., Bhattacharyya, S., Yannone, S.M., Dunn, E., Meneses, J., Feeney, A.J., and Cowan, M.J. (2005). Targeted disruption of the Artemis murine counterpart results in SCID and defective V(D)J recombination that is partially corrected with bone marrow transplantation. J Immunol *174*, 2420-2428.

Lin, Q., Sirotkin, A., and Skoultchi, A.I. (2000). Normal spermatogenesis in mice lacking the testis-specific linker histone H1t. Mol Cell Biol *20*, 2122-2128.

Liu, Y.I., Chang, M.V., Li, H.E., Barolo, S., Chang, J.L., Blauwkamp, T.A., and Cadigan, K.M. (2008). The chromatin remodelers ISWI and ACF1 directly repress Wingless transcriptional targets. Dev Biol *323*, 41-52.

Loyola, A., Huang, J.Y., LeRoy, G., Hu, S., Wang, Y.H., Donnelly, R.J., Lane, W.S., Lee, S.C., and Reinberg, D. (2003). Functional analysis of the subunits of the chromatin assembly factor RSF. Mol Cell Biol *23*, 6759-6768.

Luger, K., Mäder, A.W., Richmond, R.K., Sargent, D.F., and Richmond, T.J. (1997). Crystal structure of the nucleosome core particle at 2.8 A resolution. Nature *389*, 251-260.

Luger, K., and Richmond, T.J. (1998). DNA binding within the nucleosome core. Curr Opin Struct Biol *8*, 33-40.

Lukas, J., Lukas, C., and Bartek, J. (2011). More than just a focus: The chromatin response to DNA damage and its role in genome integrity maintenance. Nat Cell Biol *13*, 1161-1169.

Lusser, A., and Kadonaga, J.T. (2003). Chromatin remodeling by ATP-dependent molecular machines. Bioessays *25*, 1192-1200.

Mahadevaiah, S.K., Turner, J.M., Baudat, F., Rogakou, E.P., de Boer, P., Blanco-Rodriguez, J., Jasin, M., Keeney, S., Bonner, W.M., and Burgoyne, P.S. (2001). Recombinational DNA double-strand breaks in mice precede synapsis. Nat Genet *27*, 271-276.

Mali, P., Kaipia, A., Kangasniemi, M., Toppari, J., Sandberg, M., Hecht, N.B., and Parvinen, M. (1989). Stage-specific expression of nucleoprotein mRNAs during rat and mouse spermiogenesis. Reprod Fertil Dev *1*, 369-382.

Malik, H.S., and Henikoff, S. (2003). Phylogenomics of the nucleosome. Nat Struct Biol *10*, 882-891.

Manis, J.P., Gu, Y., Lansford, R., Sonoda, E., Ferrini, R., Davidson, L., Rajewsky, K., and Alt, F.W. (1998). Ku70 is required for late B cell development and immunoglobulin heavy chain class switching. J Exp Med *187*, 2081-2089.

Manis, J.P., Tian, M., and Alt, F.W. (2002). Mechanism and control of class-switch recombination. Trends Immunol *23*, 31-39.

Martianov, I., Brancorsini, S., Catena, R., Gansmuller, A., Kotaja, N., Parvinen, M., Sassone-Corsi, P., and Davidson, I. (2005). Polar nuclear localization of H1T2, a histone H1 variant, required for spermatid elongation and DNA condensation during spermiogenesis. Proc Natl Acad Sci USA *102*, 2808-2813.

Meistrich, M.L., Bucci, L.R., Trostle-Weige, P.K., and Brock, W.A. (1985). Histone variants in rat spermatogonia and primary spermatocytes. Dev Biol *112*, 230-240.

Mendez, J., and Stillman, B. (2000). Chromatin association of human origin recognition complex, cdc6, and minichromosome maintenance proteins during the cell cycle: assembly of prereplication complexes in late mitosis. Mol Cell Biol *20*, 8602-8612.

Mihardja, S., Spakowitz, A.J., Zhang, Y., and Bustamante, C. (2006). Effect of force on mononucleosomal dynamics. Proc Natl Acad Sci U S A *103*, 15871-15876.

Mulugeta Achame, E., Wassenaar, E., Hoogerbrugge, J.W., Sleddens-Linkels, E., Ooms, M., Sun, Z.W., van, I.W.F., Grootegoed, J.A., and Baarends, W.M. (2010). The ubiquitin-conjugating enzyme HR6B is required for maintenance of X chromosome silencing in mouse spermatocytes and spermatids. BMC Genomics *11*, 367.

Muthurajan, U.M., Bao, Y., Forsberg, L.J., Edayathumangalam, R.S., Dyer, P.N., White, C.L., and Luger, K. (2004). Crystal structures of histone Sin mutant nucleosomes reveal altered protein-DNA interactions. EMBO J *23*, 260-271.

Nantel, F., Monaco, L., Foulkes, N.S., Masquilier, D., LeMeur, M., Henriksen, K., Dierich, A., Parvinen, M., and Sassone-Corsi, P. (1996). Spermiogenesis deficiency and germ-cell apoptosis in CREM-mutant mice. Nature *380*, 159-162.

Narlikar, G.J. (2010). A proposal for kinetic proof reading by ISWI family chromatin remodeling motors. Curr Opin Chem Biol *14*, 660-665.

Nasmyth, K., Stillman, D., and Kipling, D. (1987). Both positive and negative regulators of HO transcription are required for mother-cell-specific mating-type switching in yeast. Cell *48*, 579-587.

Neigeborn, L., and Carlson, M. (1984). Genes affecting the regulation of SUC2 gene expression by glucose repression in Saccharomyces cerevisiae. Genetics *108*, 845-858.

Oliva, R., Bazett-Jones, D., Mezquita, C., and Dixon, G.H. (1987). Factors affecting nucleosome disassembly by protamines in vitro. Histone hyperacetylation and chromatin structure, time dependence, and the size of the sperm nuclear proteins. J Biol Chem *262*, 17016-17025.

Oliva, R., and Dixon, G.H. (1991). Vertebrate protamine genes and the histone-to-protamine replacement reaction. Prog Nucleic Acid Res Mol Biol *40*, 25-94.

Oliva, R., and Mezquita, C. (1986). Marked differences in the ability of distinct protamines to disassemble nucleosomal core particles in vitro. Biochemistry *25*, 6508-6511.

Page, J., Suja, J.A., Santos, J.L., and Rufas, J.S. (1998). Squash procedure for protein immunolocalization in meiotic cells. Chromosome Res *6*, 639-642.

Palmer, D.K., O'Day, K., and Margolis, R.L. (1990). The centromere specific histone CENP-A is selectively retained in discrete foci in mammalian sperm nuclei. Chromosoma *100*, 32-36.

Peters, A.H., Plug, A.W., van Vugt, M.J., and de Boer, P. (1997). A drying-down technique for the spreading of mammalian meiocytes from the male and female germline. Chromosome Res *5*, 66-68.

Platz, R.D., Meistrich, M.L., and Grimes, S.R., Jr. (1977). Low-molecular-weight basic proteins in spermatids. Methods Cell Biol *16*, 297-316.

Poot, R.A., Dellaire, G., Hülsmann, B.B., Grimaldi, M.A., Corona, D.F., Becker, P.B., Bickmore, W.A., and Varga-Weisz, P.D. (2000). HuCHRAC, a human ISWI chromatin remodelling complex contains hACF1 and two novel histone-fold proteins. EMBO J *19*, 3377-3387.

Precht, P., Wurster, A.L., and Pazin, M.J. (2010). The SNF2H chromatin remodeling enzyme has opposing effects on cytokine gene expression. Mol Immunol *47*, 2038-2046.

Racki, L.R., Yang, J.G., Naber, N., Partensky, P.D., Acevedo, A., Purcell, T.J., Cooke, R., Cheng, Y., and Narlikar, G.J. (2009). The chromatin remodeller ACF acts as a dimeric motor to space nucleosomes. Nature *462*, 1016-1021.

Raghavan, S.C., Kirsch, I.R., and Lieber, M.R. (2001). Analysis of the V(D)J recombination efficiency at lymphoid chromosomal translocation breakpoints. J Biol Chem *276*, 29126-29133.

Rao, B.J., Brahmachari, S.K., and Rao, M.R. (1983). Structural organization of the meiotic prophase chromatin in the rat testis. J Biol Chem *258*, 13478-13485.

Rattner, B.P., Yusufzai, T., and Kadonaga, J.T. (2009). HMGN proteins act in opposition to ATP-dependent chromatin remodeling factors to restrict nucleosome mobility. Molecular Cell *34*, 620-626.

Rippe, K., Schrader, A., Riede, P., Strohner, R., Lehmann, E., and Langst, G. (2007). DNA sequence- and conformation-directed positioning of nucleosomes by chromatin-remodeling complexes. Proc Natl Acad Sci U S A *104*, 15635-15640.

Robzyk, K., Recht, J., and Osley, M.A. (2000). Rad6-dependent ubiquitination of histone H2B in yeast. Science *287*, 501-504.

Roest, H.P., van Klaveren, J., de Wit, J., van Gurp, C.G., Koken, M.H., Vermey, M., van Roijen, J.H., Hoogerbrugge, J.W., Vreeburg, J.T., Baarends, W.M.*, et al.* (1996). Inactivation of the HR6B ubiquitin-conjugating DNA repair enzyme in mice causes male sterility associated with chromatin modification. Cell *86*, 799-810.

Ryan, D.P., and Owen-Hughes, T. (2011). Snf2-family proteins: chromatin remodellers for any occasion. Curr Opin Chem Biol *15*, 649-656.

Sadate-Ngatchou, P.I., Payne, C.J., Dearth, A.T., and Braun, R.E. (2008). Cre recombinase activity specific to postnatal, premeiotic male germ cells in transgenic mice. Genesis *46*, 738-742.

Saha, A., Wittmeyer, J., and Cairns, B.R. (2005). Chromatin remodeling through directional DNA translocation from an internal nucleosomal site. Nat Struct Mol Biol *12*, 747-755.

Sanchez-Molina, S., Mortusewicz, O., Bieber, B., Auer, S., Eckey, M., Leonhardt, H., Friedl, A.A., and Becker, P.B. (2011). Role for hACF1 in the G2/M damage checkpoint. Nucleic Acids Research *39*, 8445-8456.

Sánchez-Molina, S., Mortusewicz, O., Bieber, B., Auer, S., Eckey, M., Leonhardt, H., Friedl, A.A., and Becker, P.B. (2011). Role for hACF1 in the G2/M damage checkpoint. Nucleic Acids Res.

Sapiro, R., Kostetskii, I., Olds-Clarke, P., Gerton, G.L., Radice, G.L., and Strauss III, J.F. (2002). Male infertility, impaired sperm motility, and hydrocephalus in mice deficient in sperm-associated antigen 6. Mol Cell Biol *22*, 6298-6305.

Schwanbeck, R., Xiao, H., and Wu, C. (2004). Spatial contacts and nucleosome step movements induced by the NURF chromatin remodeling complex. J Biol Chem *279*, 39933-39941.

Sharan, S.K., Pyle, A., Coppola, V., Babus, J., Swaminathan, S., Benedict, J., Swing, D., Martin, B.K., Tessarollo, L., Evans, J.P.*, et al.* (2004). BRCA2 deficiency in mice leads to meiotic impairment and infertility. Development *131*, 131-142.

Shirley, C.R., Hayashi, S., Mounsey, S., Yanagimachi, R., and Meistrich, M.L. (2004). Abnormalities and reduced reproductive potential of sperm from Tnp1- and Tnp2-null double mutant mice. Biol Reprod *71*, 1220-1229.

Shore, D., Langowski, J., and Baldwin, R.L. (1981). DNA flexibility studied by covalent closure of short fragments into circles. Proc Natl Acad Sci U S A *78*, 4833-4837.

Smith, M.M. (2002). Centromeres and variant histones: what, where, when and why? Curr Opin Cell Biol *14*, 279-285.

Steilmann, C., Cavalcanti, M.C.O., Bergmann, M., Kliesch, S., Weidner, W., and Steger, K. (2010). Aberrant mRNA expression of chromatin remodelling factors in round spermatid maturation arrest compared with normal human spermatogenesis. Mol Hum Reprod *16*, 726-733.

Stern, M., Jensen, R., and Herskowitz, I. (1984). Five SWI genes are required for expression of the HO gene in yeast. J Mol Biol *178*, 853-868.

Stopka, T., and Skoultchi, A.I. (2003). The ISWI ATPase Snf2h is required for early mouse development. Proc Natl Acad Sci USA *100*, 14097-14102.

Strahl, B.D., and Allis, C.D. (2000). The language of covalent histone modifications. Nature *403*, 41-45.

Strohner, R., Nemeth, A., Jansa, P., Hofmann-Rohrer, U., Santoro, R., Langst, G., and Grummt, I. (2001). NoRC--a novel member of mammalian ISWI-containing chromatin remodeling machines. EMBO J *20*, 4892-4900.

Strohner, R., Wachsmuth, M., Dachauer, K., Mazurkiewicz, J., Hochstatter, J., Rippe, K., and Längst, G. (2005). A 'loop recapture' mechanism for ACF-dependent nucleosome remodeling. Nat Struct Mol Biol *12*, 683-690.

Tate, P., Lee, M., Tweedie, S., Skarnes, W.C., and Bickmore, W.A. (1998). Capturing novel mouse genes encoding chromosomal and other nuclear proteins. J Cell Sci *111 (Pt 17)*, 2575-2585.

Thompson, P.J., Norton, K.A., Niri, F.H., Dawe, C.E., and McDermid, H.E. (2012). CECR2 is involved in spermatogenesis and forms a complex with SNF2H in the testis. J Mol Biol *415*, 793-806.

Torigoe, S.E., Urwin, D.L., Ishii, H., Smith, D.E., and Kadonaga, J.T. (2011). Identification of a rapidly formed nonnucleosomal histone-DNA intermediate that is converted into chromatin by ACF. Molecular Cell *43*, 638-648.

Tsukiyama, T., Daniel, C., Tamkun, J., and Wu, C. (1995). ISWI, a member of the SWI2/SNF2 ATPase family, encodes the 140 kDa subunit of the nucleosome remodeling factor. Cell *83*, 1021-1026.

Tsukiyama, T., and Wu, C. (1995). Purification and properties of an ATP-dependent nucleosome remodeling factor. Cell *83*, 1011-1020.

Turner, J.M. (2007). Meiotic sex chromosome inactivation. Development *134*, 1823-1831.

Turner, J.M., Burgoyne, P.S., and Singh, P.B. (2001). M31 and macroH2A1.2 colocalise at the pseudoautosomal region during mouse meiosis. J Cell Sci *114*, 3367-3375.

van der Heijden, G.W., Derijck, A.A., Posfai, E., Giele, M., Pelczar, P., Ramos, L., Wansink, D.G., van der Vlag, J., Peters, A.H., and de Boer, P. (2007). Chromosome-wide nucleosome replacement and H3.3 incorporation during mammalian meiotic sex chromosome inactivation. Nat Genet *39*, 251-258.

van Roijen, H.J., Ooms, M.P., Spaargaren, M.C., Baarends, W.M., Weber, R.F., Grootegoed, J.A., and Vreeburg, J.T. (1998). Immunoexpression of testis-specific histone 2B in human spermatozoa and testis tissue. Hum Reprod *13*, 1559-1566.

Varga-Weisz, P.D., Wilm, M., Bonte, E., Dumas, K., Mann, M., and Becker, P.B. (1997). Chromatin-remodelling factor CHRAC contains the ATPases ISWI and topoisomerase II. Nature *388*, 598-602.

Ward, W.S., and Coffey, D.S. (1991). DNA packaging and organization in mammalian spermatozoa: comparison with somatic cells. Biol Reprod *44*, 569-574.

Widom, J. (2001). Role of DNA sequence in nucleosome stability and dynamics. Q Rev Biophys *34*, 269-324.

Wu, J.Y., Ribar, T.J., Cummings, D.E., Burton, K.A., McKnight, G.S., and Means, A.R. (2000). Spermiogenesis and exchange of basic nuclear proteins are impaired in male germ cells lacking Camk4. Nat Genet *25*, 448-452.

Xiao, A., Li, H., Shechter, D., Ahn, S.H., Fabrizio, L.A., Erdjument-Bromage, H., Ishibe-Murakami, S., Wang, B., Tempst, P., Hofmann, K., *et al.* (2009a). WSTF regulates the H2A.X DNA damage response via a novel tyrosine kinase activity. Nature *457*, 57-62.

Xiao, N., Kam, C., Shen, C., Jin, W., Wang, J., Lee, K.M., Jiang, L., and Xia, J. (2009b). PICK1 deficiency causes male infertility in mice by disrupting acrosome formation. J Clin Invest *119*, 802-812.

Xu, X., Aprelikova, O., Moens, P., Deng, C.X., and Furth, P.A. (2003). Impaired meiotic DNA-damage repair and lack of crossing-over during spermatogenesis in BRCA1 full-length isoform deficient mice. Development *130*, 2001-2012.

Yabuta, Y., Ohta, H., Abe, T., Kurimoto, K., Chuma, S., and Saitou, M. (2011). TDRD5 is required for retrotransposon silencing, chromatoid body assembly, and spermiogenesis in mice. J Cell Biol *192*, 781-795.

Yan, W., Ma, L., Burns, K.H., and Matzuk, M.M. (2003). HILS1 is a spermatid-specific linker histone H1-like protein implicated in chromatin remodeling during mammalian spermiogenesis. Proc Natl Acad Sci USA *100*, 10546-10551.

Yang, J.G., Madrid, T.S., Sevastopoulos, E., and Narlikar, G.J. (2006). The chromatin-remodeling enzyme ACF is an ATP-dependent DNA length sensor that regulates nucleosome spacing. Nat Struct Mol Biol *13*, 1078-1083.

Yasui, D., Miyano, M., Cai, S., Varga-Weisz, P., and Kohwi-Shigematsu, T. (2002). SATB1 targets chromatin remodelling to regulate genes over long distances. Nature *419*, 641-645.

Yoshimura, K., Kitagawa, H., Fujiki, R., Tanabe, M., Takezawa, S., Takada, I., Yamaoka, I., Yonezawa, M., Kondo, T., Furutani, Y.*, et al.* (2009). Distinct function of 2 chromatin remodeling complexes that share a common subunit, Williams syndrome transcription factor (WSTF). Proc Natl Acad Sci USA *106*, 9280-9285.

Yu, Y.E., Zhang, Y., Unni, E., Shirley, C.R., Deng, J.M., Russell, L.D., Weil, M.M., Behringer, R.R., and Meistrich, M.L. (2000). Abnormal spermatogenesis and reduced fertility in transition nuclear protein 1-deficient mice. Proc Natl Acad Sci U S A *97*, 4683-4688.

Zhao, M., Shirley, C.R., Yu, Y.E., Mohapatra, B., Zhang, Y., Unni, E., Deng, J.M., Arango, N.A., Terry, N.H., Weil, M.M.*, et al.* (2001). Targeted disruption of the transition protein 2 gene affects sperm chromatin structure and reduces fertility in mice. Mol Cell Biol *21*, 7243-7255.

Zhong, J., Peters, A.H., Lee, K., and Braun, R.E. (1999). A double-stranded RNA binding protein required for activation of repressed messages in mammalian germ cells. Nat Genet *22*, 171-174.

Zofall, M., Persinger, J., Kassabov, S.R., and Bartholomew, B. (2006). Chromatin remodeling by ISW2 and SWI/SNF requires DNA translocation inside the nucleosome. Nat Struct Mol Biol *13*, 339-346.